Universität Duisburg-Essen
Fakultät für Chemie

Development of hyphenated techniques for the analysis of complex mixtures

Dissertation

zur Erlangung des akademischen Grades eines
Doktors der Naturwissenschaften
- Dr. rer. nat. -

vorgelegt von

Alessandro Vetere

aus Dissen am Teutoburger Wald

2017

Der experimentelle Teil der vorliegenden Arbeit wurde im Zeitraum von Januar 2013 bis Februar 2017 im Arbeitskreis von Prof. Dr. Wolfgang Schrader am Max-Planck-Institut für Kohlenforschung in Mülheim an der Ruhr durchgeführt.

Tag der Disputation: 13. Juli 2017

Gutachter:	Prof. Dr. Wolfgang Schrader
	PD Dr. Ursula Telgheder
	Prof. Dr. Jan Andersson
Vorsitzender:	Prof. Dr. Mathias Ulbricht

Erklärung

Hiermit versichere ich, dass ich die vorliegende Arbeit mit dem Titel

„Development of hyphenated techniques for the analysis of complex mixtures”

selbst verfasst und keine außer den angegebenen Hilfsmitteln und Quellen benutzt habe, und dass die Arbeit in dieser oder ähnlicher Form noch bei keiner anderen Universität eingereicht wurde.

Essen, im April 2017

Omnes qui crediderunt in me

dederuntque mihi potestatem viam meam ire.

ἀρχὰς εἶναι τῶν ὅλων ἀτόμους καὶ κενόν, τὰ δ' ἄλλα πάντα νενομίσθαι [δοξάζεσθαι]·

Nothing exists except atoms and empty space; everything else is opinion.

Democritus of Abdera

Kurzfassung

Erdöl als wichtigster Teil unserer Energieversorgung ist eine der wichtigsten Ressourcen für unsere technologisierte Gesellschaft. Obwohl enorme Anstrengungen unternommen werden, Energie aus erneuerbaren Quellen zu gewinnen, wird Erdöl auch über die nächsten Jahrzehnte als Grundstoff für Treibstoffe, als Rohstoff für die chemische Industrie und für etliche weitere Anwendungen benötigt werden. Die jeweiligen Produkte müssen gleichbleibend umweltfreundlich sowie auch ökonomisch produziert werden, obwohl die Rohstoffe sich kontinuierlich ändern. Die analytische Chemie ist hierbei von zentraler Bedeutung, da eine eingehende Analyse helfen kann, ungewollte Phänomene im Zuge der Produktion zu verstehen. Die genaue Analyse von Erdöl ist allerdings eine problematische Aufgabe. Im Laufe der letzten Jahre wurde gezeigt, dass es keine einzelne analytische Methode gibt, die eine vollständige Charakterisierung von Erdöl erlaubt. Allerdings hat sich die ultrahoch auflösende Fourier-Transformations-Massenspektrometrie (FTMS) zur Methode der Wahl entwickelt, um molekulare Informationen zu gewinnen. Ein Hauptproblem ist die Komplexität der Probe, die zu Unterdrückungseffekten bei der Ionisation und allgemein zu Empfindlichkeitsproblemen führt. Erdöl „sabotiert“ damit praktisch seine eigene Analyse.

Ziel dieser Arbeit war die Entwicklung von Methoden zur Probenvereinfachung, um durch die Vermeidung von Diskriminierungseffekten die Detektion einzelner Analyten zu erleichtern. Dies wurde durch die Kopplung von FTMS mit Ionenmobilitätsspektrometrie (FAIMS) bzw. Ligandenaustauschchromatographie (LEC) erreicht. Ein neuer Quellenblock zur 1- und 2-Photonen Ionisation mit FAIMS-FTMS wurde für die Analyse unpolarer Analyten entwickelt. Details über die strukturelle Beschaffenheit einzelner Komponenten konnten gewonnen werden, indem Strukturmotive verschiedener isomerer Verbindungen untersucht wurden.

Die Entwicklung einer LEC-Methode mit einer Pd-basierten stationären Phase erlaubte die gruppenselektive Analyse schwefelhaltiger Verbindungen. Die Methode löst eines der drängendsten Probleme der Erdölforschung: Die quantitative Analyse einzelner Verbindungen innerhalb einer komplexen Erdölprobe. Wegen unterschiedlicher Ansprechverhalten war dies bislang nicht möglich. Das Problem wurde mit ICP-MS/MS umgangen, die eine selektive Detektion mit einheitlichem Ansprechverhalten bietet. Die Kombination von gruppenselektiver Trennung mit einer qualitativen Analyse schwefelhaltiger Verbindungen durch LEC-FTMS und mit der Quantifizierung per LEC-ICP-MS/MS erlaubte zum ersten Mal die Quantifizierung verschiedener Typen von Schwefelverbindungen in Erdöl.

Abstract

Being the most important part in the energy supply chain, crude oil is one of the most important resources for our technology-driven society. Although strong efforts are undertaken to gain energy out of renewable resources, it is certain that crude oil will be needed at least for the next couple of decades as feedstock for transportation fuels, as raw material for the chemical industry and for a number of other different applications. The respective products need to be produced constantly in an environmentally friendly and economical way, even though feedstocks are continuously changing. Analytical chemistry is of particular importance here, as a detailed analysis can help understanding numerous adverse effects during production. The comprehensive analysis of crude oil, however, is a problematic task. Over the last years it has been shown that no single analytical technique exists that allows a complete description of a crude oil. However, ultra-high resolving Fourier transform mass spectrometry (FTMS) has developed into the method of choice to gain information on a molecular level. One major problem is the complexity of the sample which leads to suppression effects during ionization and overall sensitivity issues. Crude oil is thus "sabotaging" its own analysis.

Aim of this work was the development of methods that allow a simplification of the sample and thus help analyte detection by reducing discrimination and suppression effects. This has been achieved by hyphenating FTMS to separation techniques such as ion mobility spectrometry (FAIMS) and ligand exchange chromatography (LEC). A new source block for 1- and 2-photon ionization with FAIMS-FTMS was developed that allows also the studying of non-polar analytes. Details of the structural composition of individual components in very complex crude oil samples were investigated by detecting structural motifs in different isomeric compounds.

A group-selective analysis of sulfur containing compounds was offered through the development of a LEC separation method on a Pd-based stationary phase. The application of this method solves one of the most glaring problems in petroleum research: The quantitative analysis of individual compounds within a complex crude oil sample. This had not been possible before due to unresolved response issues. This problem was addressed by selective detection with uniform response using ICP-MS/MS. The combination of class selective separation and qualitative analysis of sulfur containing compounds by LEC-FTMS with quantitative analysis by LEC-ICP-MS/MS allowed the quantitative analysis of different sulfur containing compounds in crude oil for the first time.

Table of Contents

1. Introduction

The history of human civilization and technological progress have from ancient times been connected with the usage of crude oil and its relatives tar and bitumen. Archaeological evidences reveal that composite tools like arrows were constructed by gluing flint stone heads to wooden shafts with bitumen as early as 40,000 BC.[1] It is not unexpected that the oldest narrations of people using what is today known to be a crude oil product originate in the middle-east region. Among various mentions in biblical texts, one of the oldest written testimonies is given in the annals of the Assyrian king Tukulti-Ninurta II. (890 to 884 BC) where it says:[1]

»In front of Hit, by the bitumen springs, the place of the Usmeta stone, in which the gods speak, I spent the night.«

At that time bitumen and asphalt were used as waterproofing for ships, as mortar in the construction of buildings, as pavement for ceremonial roads and for various similar purposes.

Modern usage of crude oil can be dated back to the middle of the nineteenth century with the foundation of Abraham P. Gesner's "*Kerosene Gaslight Company*" and Edwin Drake's first drilling of a commercial oil well near Titusville, Pennsylvania in 1859.[2] While (refined) crude oil was initially only interesting as replacement for whale oil in lamps, other possibilities were soon discovered. Today crude oil is mainly used for four purposes:

- as feedstock for the chemical industry and to gain compounds such as lubricants and other chemicals on which the whole industry is based
- as fuel in heating units to generate heat
- as fuel in power plants to generate electricity and
- as fuel in combustion engines to operate ships, aircrafts or land-based vehicles.

The most relevant sector with more than 64 % of the overall consumption in 2014 was the transportation sector.[3] Recently, efforts have been increased to gain electric energy from so-called "renewable resources" like wind, sunlight or fast growing crops. Also, the automotive industry is seeking ways to move from fossil fuel driven cars to vehicles operated purely by electric energy or by hybrid engines that combine both fossil fuel burning and electric engines. This approach, however, is to date only feasible for small personal vehicles and/or in urban centers where a supply of electricity for recharging is easily available. For heavy goods

transportation by trucks, the operation of ships and aviation reliable alternatives to fossil fuel driven engines have still to be found.

Despite the ongoing efforts to replace fossil fuels, crude oil is expected to be the major source of transportation fuels for the next couple of decades. However, sources of commercially and technically interesting light and sweet - so-called conventional - oils that are easily exploited are mostly depleted. Over the past years the focus had to be shifted to alternative sources that had not been commercially interesting before. These non-conventional sources include heavy and very heavy oils, oil shale, sour (sulfur rich) oils and bituminous oil sands. All these feedstocks share the common feature that an increased technological effort is necessary to convert these raw materials into high-quality petroleum products.

1.1 Crude oil composition and processing

1.1.1 Origin and composition

Up until the late 1970s a purely inorganic origin of crude oil or petroleum has been discussed, especially among the Russian community.[4] Nowadays it is commonly accepted that fossil materials like petroleum and coal are of organic origin. Precursors of crude oil are mostly marine organisms like algae, phyto- and zooplankton that have been submerged into the sedimentary regime.[5]

These materials – mostly lipids, proteins, carbohydrates and biopolymers – undergo a series of transformation processes, depending on the depth of burial and related to this the surrounding temperature. In shallow depths transformations are mostly microbial degradation, hydrolysis of biopolymers (e.g. proteins and sugars) and, along with this, recombination reactions that may lead to polymerization e.g. of olefins and the formation of humic acids. During this stage – the so-called *diagenesis* – bio-relevant components such as amines or hydrocarbons might be lost due to microbial uptake. Also, most nitrogen is commonly lost in the form of ammonia. In later stages, thermal cracking of the substances created during *diagenesis* – the so-called *kerogen* – is initiated. The following processes, grouped under the term *catagenesis*, usually start with oxygen being released in the form of water or carbon dioxide. The atomic O/C ratio of the remaining *kerogen* is sharply decreased (see also Figure 1-1). With increasing depth and temperature thermal cracking of the carbon backbones becomes more likely, resulting in smaller, more soluble hydrocarbons being released. The processes involved here can be classified as hydrogen rearrangements or disproportionations. The hydrocarbons released from

the *kerogen* are relatively rich in hydrogen, leaving a more and more carbonaceous, hydrogen deficient *kerogen* behind. Part of this hydrogen transfer are also cyclization and aromatization reactions, leading to naphthenic and aromatic compounds. These processes take place over geological timescales of several millions of years and eventually result in methane as the main product.[6-8]

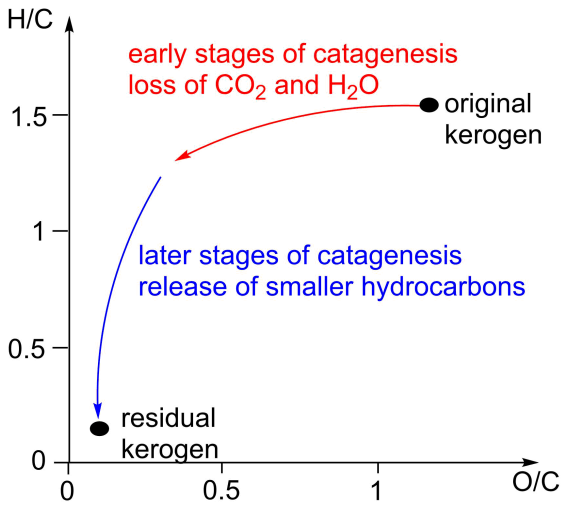

Figure 1-1: Van-Krevelen diagram showing the two principal stages of *catagenesis*. First, mainly CO_2 and H_2O are lost, leading to a decrease in O/C ratio (red). Later, smaller hydrocarbons are released by hydrogen rearrangement, leading to a decrease in H/C ratio (blue). Reproduced after [8].

The result of these petroleum generating processes is a rather complex mixture that contains mostly aliphatic and naphthenic hydrocarbons and to a lesser extent aromatic species of different size. The molecular sizes of the compounds and thus their boiling points range from small gaseous alkanes (methane to butane) up to high molecular weight asphaltic components with a molecular weight of 2,000 Da and above. Reactive sites like hydroxyl groups or isolated π-bonds that were initially present or have been generated during the thermal cracking process were transformed over time and are uncommon functional groups in crude oils.

Table 1-1: Typical composition of crude oil and biogenic precursor substances. Values are average wt.-%, reproduced after [7].

compound type	avg. wt.-% of element				
	C	H	N	O	S
carbohydrates	44	6	-	50	-
proteins	53	7	17	22	1
lipids	76	12	-	12	-
petroleum	80-90	10-15	0-2	0-2	0-10

Regarding the elemental composition, crude oil mainly consists of carbon (~85 %) and hydrogen (~12 %) with minor and varying amounts of sulfur (0-10 %), oxygen and nitrogen (0-2 % each). Traces of metals like vanadium, nickel or iron are also commonly found, often in complexes with porphyrinic residues of the original organic matter. A comparison given in Table 1-1 shows that crude oil is relatively rich in carbon and hydrogen but mostly depleted in nitrogen and oxygen. Especially sour crudes can contain amounts of sulfur that exceed the content of living matter by far with reports showing values of up to 14 wt.-%.[9] This can be attributed to the thermochemical reduction of sulfate (from seawater or sediment minerals) by hydrocarbons. Such reactions lead to the formation of reduced sulfur species like elemental sulfur or H_2S. In sediments that are void of iron (such that pyrite cannot be formed) these can, in turn be incorporated into hydrocarbon structures to form sulfides and thiophenes. Example reactions are shown in Scheme 1-1.

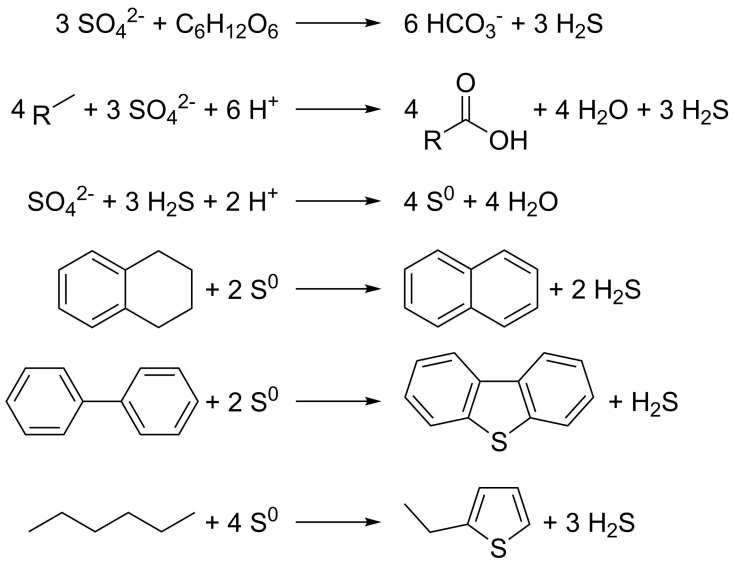

Scheme 1-1: Reactions involved in the reduction of sulfate by organic matter (top rows), symproportionation of sulfate and sulfide (third row), aromatization of hydrocarbons (fourth row) and generation of thiophenic compounds (bottom rows).

1.1.2 Refinery processes

During refining crude oil is first desalted and then submitted to an atmospheric distillation. Here a set of different temperature cuts are obtained that can be finally transferred into the main fuel types. Higher boiling residues are further submitted to a vacuum distillation with a temperature equivalent of ~570 °C. These high boiling fractions are usually transferred to a cracking unit where the compounds are fragmented to lighter subunits. These fractions and the remaining residue can be used as heavy ship diesel or heating oil. Some parts of the highly bituminous

residuals are used for asphalt production. Figure 1-2 shows a simplified scheme of such a process.[10]

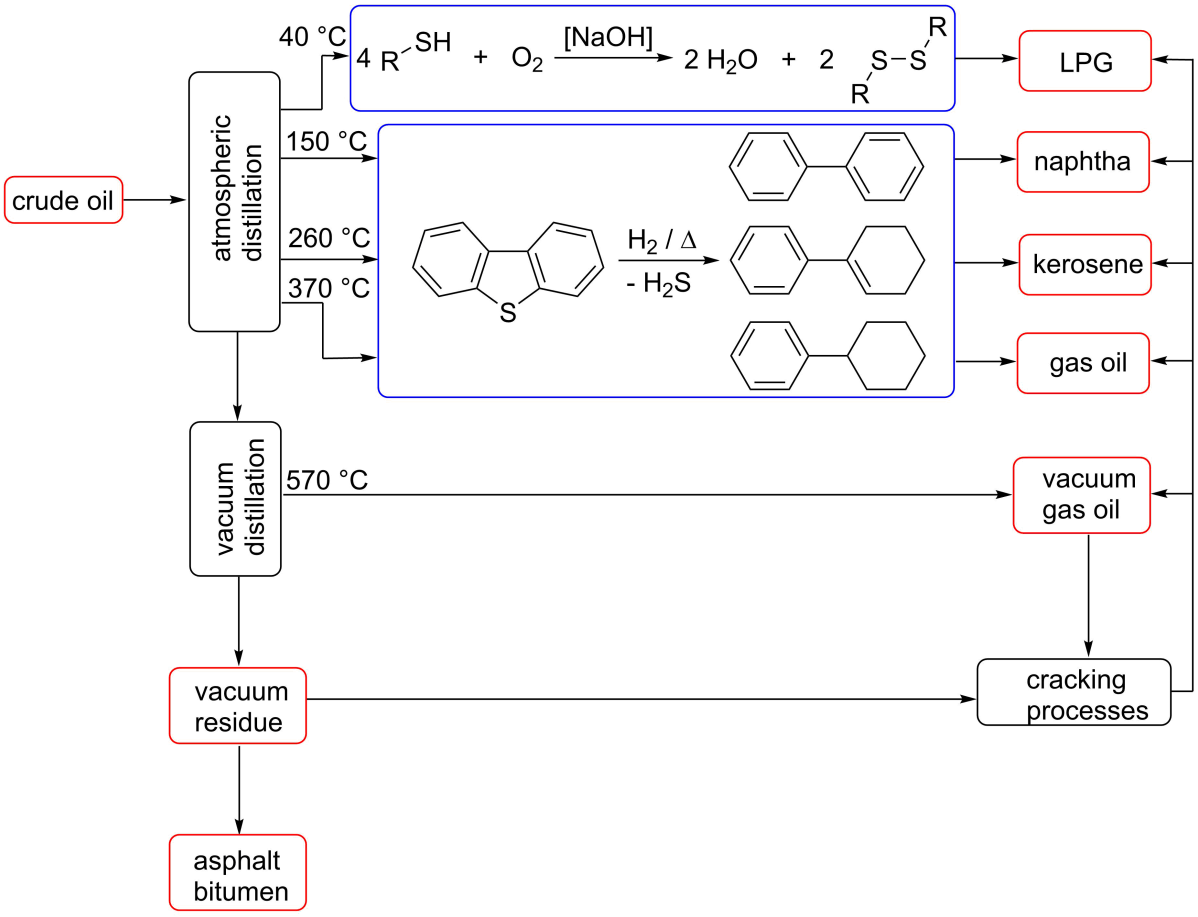

Figure 1-2: Simplified crude oil refinery workflow. Various distillation cuts are upgraded to main fuel types after desulfurization steps (blue). Heavy components are submitted to different cracking processes to yield more valuable products. Remaining residues can be used for production of bitumen, asphalt or lubricants. Reproduced after [10].

The heteroatomic content of a crude oil - especially nitrogen and sulfur - is held responsible for adverse effects like catalyst poisoning, acid rain (SO_2 and NO_x) or air pollution (NO_x). During combustion of heteroatom-rich fuels sulfur and nitrogen oxides (SO_x and NO_x) are formed that easily hydrolyze to their corresponding acids. Therefore, strong legal requirements must be met to reduce heteroatom content in final products down to a few parts per million. Within the European Union the sulfur content of fuels is limited to a maximum of 10 $mg \cdot kg^{-1}$ by directive 98/70/EG.[11] Thus, any of the aforementioned distillation cuts need to be treated to remove these heteroatoms. Desulfurization is commonly done by treatment with hydrogen at elevated temperatures and pressures using a heterogenous catalyst. During this process the material will get partly hydrogenated and heteroatoms such as sulfur as well as nitrogen are removed in the

form of H_2S or NH_3, respectively. This process is exemplarily shown for the desulfurization of mercaptans or dibenzothiophene in Figure 1-2 (blue boxes).

1.2 State of the Art in crude oil analysis

For the assessment of what is state of the art in crude oil analysis one has to acknowledge the unmatched complexity of the material with more than 1,000,000 distinct compounds estimated within a single sample.[12] While this is an unmatched amount of analytes, this also means that a crude oil sample is a very complex matrix that cannot be removed or simulated. As a result, there is not one single technique that yields a comprehensive set of data. In many cases the analysis of a crude oil sample will focus on one feature at a time. This might be one physical property or the overall amount of a certain type of compounds. Such features are often addressed by methods that give bulk properties of the whole sample assembly. Important features for oil refineries include overall properties like the API gravity and/or viscosity of the sample. A molecular weight distribution is typically assessed by a simulated distillation curve.[13, 14]

1.2.1 Spectroscopic methods

An important key figure for oil processing is the ratio of aliphatic to aromatic compounds. This is typically estimated by ^{1}H- and ^{13}C-NMR.[15-18] Additionally, FTIR spectroscopy can be used to estimate the naphthenic acid number[19] of a sample or generally to shed light onto the distribution of oxygen containing functional groups, be it in *kerogens*, oil shale or crude oil.[15] Naphthalene hydrocarbons in fuels have been determined by UV-spectrophotometry.[20] Heteroatom and especially sulfur content is evaluated by traditional elemental analysis. Quantitation and/or oxidation state speciation of sulfur containing compounds is also available using X-ray techniques such as WDXRF or XANES.[21, 22]

Whenever a more detailed view, i.e. on a molecular level, on either a group of compounds or the whole sample is needed, different techniques need to be employed. These include any type of separation techniques, a mass spectrometric analysis or, ideally, a combination of both.

1.2.2 Gas chromatography

Gas chromatography (GC) and especially comprehensive GC×GC separations have been successfully used for the analysis of certain groups of compounds like aliphatic and polyaromatic hydrocarbons or for the fingerprinting of crude oil samples.[23-25] Thiophenes and sulfides have been analyzed separately by GC-MS after a multistep reaction and separation cascade.[26] Also naphthenic acids have been successfully analyzed by GC-MS after a multistep reduction to their corresponding naphthenes.[27] While gas chromatography is a very powerful separation technique with high resolving power, it is still limited to the analysis of volatile compounds. With the increased usage of heavier crudes, a comprehensive analysis of the entire sample by GC techniques becomes more and more unfavorable.

1.2.3 Liquid chromatography

Liquid phase separations do not suffer from this limitation but typically lack the separation power of a GC approach. Many investigations on crude oil rely on a so-called SARA fractionation (Saturates, Aromatics, Resins, Asphaltenes) followed by further analyses.

A SARA fractionation is a two-step separation process. First, *n*-alkane (pentane to heptane) insoluble material, the asphaltenes, are precipitated. The filtrate, containing the soluble material – the maltenes, is then subjected to a polarity-driven normal phase (NP) chromatography, mostly run as open tubular chromatography. While no uniform procedure exists, typically three fractions are collected with increasing elution strength of the solvent:[28-32]

- Saturates (mostly aliphatic and naphthenic hydrocarbons)
- Aromatics (mostly polycyclic aromatic hydrocarbons (PAH) and unpolar polycyclic aromatic heterocycles (PAXH) like thiophenes, furanes or indole type PANH) and
- Resins (mostly polar PAXH like pyridinic PANH, acids and generally highly condensed polyaromatic structures.

For HPLC separations of either whole crudes or fractions obtained by a SARA pre-separation more or less broad groups of compounds are expected to be eluted, rather than single compounds. Reversed phase separations have been used in conjunction with mass spectrometric analysis. However, this has only been reported for an offline, multistep analysis using fraction collection over a series of HPLC runs, followed by MS analysis of the resulting fractions.[33] Interestingly the separation does not seem to be related to heteroatom functional groups, but

rather to the degree of unsaturation (DBE) and molecular size. Much more common is the use of normal phase chromatography both on- and offline with a mass spectrometric detection. Here results have been reported based on polarity-type separations, e.g. on aminocyano phases.[29, 34, 35] Ligand exchange chromatography (LEC) on a metal impregnated stationary phase or a metal organic framework (MOF) have been extensively used in offline pre-separations, followed by a GC or GC-MS analysis or a purely (high resolving) mass spectrometric analysis. Separations have been performed according to the type of sulfur[36-40] or nitrogen[41] compounds present. A separation based on the size of the π-system was achieved on an Ag(I) containing phase.[42]

1.2.4 Mass spectrometry

The analysis of alkylated mono- and polycyclic aromatic hydrocarbons (PAH) has long been a major interest in crude oil analysis. These relatively volatile compounds have commonly been addressed by GC and GC-MS methods.[43-47] Also the studying of sulfur containing PASH[38, 39, 48] or crude oil fingerprinting with the help of biomarkers[27, 49, 50] is performed by (GC×)GC-MS approaches. Mass spectrometry in this case allows the benefit of a mass-selective detection. Thus, compounds within the complex mixture that are not fully separated by the chromatographic step can still be analyzed (given they are not isobars or isomers). However, most of these studies rely on the use of low resolving quadrupole mass analyzers or double-focusing sector field instruments held at relatively low resolution of $R \approx 1{,}000$ ($R = m \cdot \Delta m^{-1}$, 10% valley). Additionally, GC-MS approaches typically involve electron ionization (EI) at 70 eV. Often only unspecific fragment ions are generated from unresolved chromatographic peaks and molecular ions are often suppressed due to heavy fragmentation of the parent ions. The absence of often both specific fragment ions and molecular ions renders an identification of single compounds impossible.

Better mass resolution can be achieved by using time-of-flight (TOF) mass spectrometers. This includes hyphenations to gas or liquid chromatography,[24, 51, 52] or the implementation of ion mobility spectrometry,[53-56] often involving atmospheric pressure ionization (API) methods that yield molecular ions with no to little fragmentation. However, due to a limitation in resolving power of usually not exceeding $R \approx 40{,}000$ the technique is only suitable for pre-separated or relatively low-weight compounds if important isobaric species are to be distinguished.

Gold standard for the direct analysis of crude oil and related samples is Fourier transform ion cyclotron resonance mass spectrometry (FT-ICR MS).[25, 28, 31, 35, 37, 40, 57-70] Due to the ultra-high

mass resolving power of $R \approx 10^5$ - 10^6 most relevant isobaric species, including isotopologs, can be distinguished even without a pre-separation step.

Over the last decade the newly developed FT Orbitrap has been continuously employed in crude oil analysis.[66, 71-74] Commercial instruments reach resolving powers in the medium 10^5 range, sufficient for many issues. Beneficial in comparison to FT-ICR MS is a relatively fast acquisition rate and a high sensitivity, especially in the low mass range. A general problem of any mass spectrometric analysis, however, remains the distinction of isomeric species.

1.2.5 Ion mobility spectrometry

A somewhat newer approach in the field of crude oil analysis is the implementation of an ion mobility (ion mobility spectrometry, IMS) separation into the mass spectrometric scheme. The technique allows the determination of collisional cross sections (CCS) and by their different structure and shape the separation of isomeric compounds. The method has been used successfully to follow up on homologous series within a group of analytes, to increase the peak capacity of a mass spectrometric measurement and to correct for assignment errors due to limited mass resolving power.[53-56, 75, 76] A direct coupling to mass spectrometers, capable of a mass resolving power higher than obtained by TOF MS is not common. Ultimately, a high resolving IMS separation combined with ultra-high resolving mass spectrometry would have the potential to allow a very deep view onto the molecular composition of crude oils.

1.3 Analytical techniques used in the course of this work

1.3.1 Ultra-high resolution mass spectrometry

The complexity of crude oil renders the acquisition of insightful yet comprehensive mass spectrometric data difficult. This complexity covers several aspects, one being a broad range of analyte polarities ranging from fully unpolar hydrocarbons up to acids and bases. Considering that electron ionization is not the optimal approach, this results in the need for a set of adequate ionization techniques. Another factor is a broad range of molecular weights, leading to the need for mass analyzers of a high dynamic range. Finally, an unmatched range of elemental compositions is found in a single sample resulting in very crowded mass spectra. Therefore, an ultra-high mass resolving power $R = m \cdot \Delta m^{-1}$ (with Δm the full peak width at half maximum height (FWHM)) is mandatory as well as a high mass accuracy, typically better than ±1 ppm.

When analyzing crude oil, one has to deal with certain isobaric compositions that raise the need for mass resolving power. Figure 1-3 shows theoretical spectra of seven isobaric compositions that have been found in crude oil, calculated for different resolution settings. Among the most crucial mass splits that need to be distinguished are the mass differences between C_5 and N_2O_2 (4.0 mDa) and between C_3 and SH_4 (3.4 mDa). Even at the low *m/z* values shown here a resolving power of $R \geq 200{,}000$ is needed for baseline resolution of all signals. This needed resolving power will linearly increase with analyte mass, as Δm is constant for a given mass split to be covered.

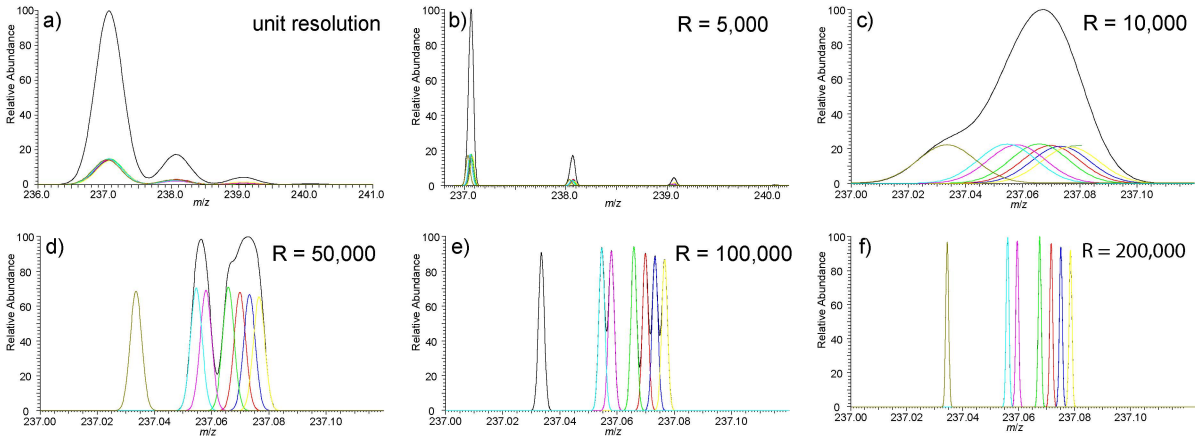

Figure 1-3: Effect of mass resolving power *R* on mass spectrometric peaks of a mixture of compounds potentially found in crude oil (theoretical spectra simulated in XCalibur 2.1). Resolution settings are based on capabilities of a) Quadrupole mass analyzers, b-d) (double focusing) sector field instruments, d) high-end TOF MS, e-f) FTMS. For panels c-f) only the monoisotopic peaks are shown. The black line represents the mass spectrum obtained at the resolving power given. Contributions of the single compound ions are shown as follows: dark yellow: $[C_{18}H_4O+H]^+$, cyan: $[C_{15}H_8O_3+H]^+$, magenta: $[C_{12}H_{13}O_3S+H]^+$, green: $[C_{14}H_8O_2N_2+H]^+$, red: $[C_{19}H_8+H]^+$, blue: $[C_{16}H_{12}S+H]^+$, yellow: $[C_{13}H_{16}S_2+H]^+$.

The mass spectrometric analysis of crude oil therefore requires mass analyzers that are capable of reaching a mass resolving power of $R \approx 10^5$ - 10^6 throughout the whole mass range, while allowing a sub-ppm mass accuracy. To reach these requirements, to date only two types of mass spectrometers are available:

- Fourier transform ion cyclotron resonance mass spectrometers (FT-ICR MS) and
- Fourier transform Orbitrap mass spectrometers (FT Orbitrap MS)

Both instrument types store the ions for the course of the measurement in either a Penning trap (FT-ICR) or an Orbitrap cell. Both approaches share the common feature that a time dependent image current is recorded that originates from ions periodically passing by a set of detection

electrodes. The period (and thus the frequency of passing by the detector electrodes) is – for a given instrumental setup – only dependent on the ions mass-to-charge ratio (*m*/*z*). Ultimately, the time-domain signal (the transient) is Fourier transformed into a frequency spectrum with the frequency *f* directly related to *m*/*z* of an ion. Both instrument types record the signals from all stored ions at the same time. All other types of modern mass spectrometers record signals consecutively as an ion current using an impact detector. One benefit of the FT-based mass analyzers (FTMS) is that the *m*/*z* determination is independent of the ions initial kinetic energy. Resolving power is additionally gained by increased scanning time, thus increasing the number of oscillations that are monitored. For a given instrumental setup the resolving power available on impact-detection instruments is ultimately limited by kinetic energy distributions, while line-width in FT-based instruments is theoretically limited only by Heisenberg uncertainty and measuring time.

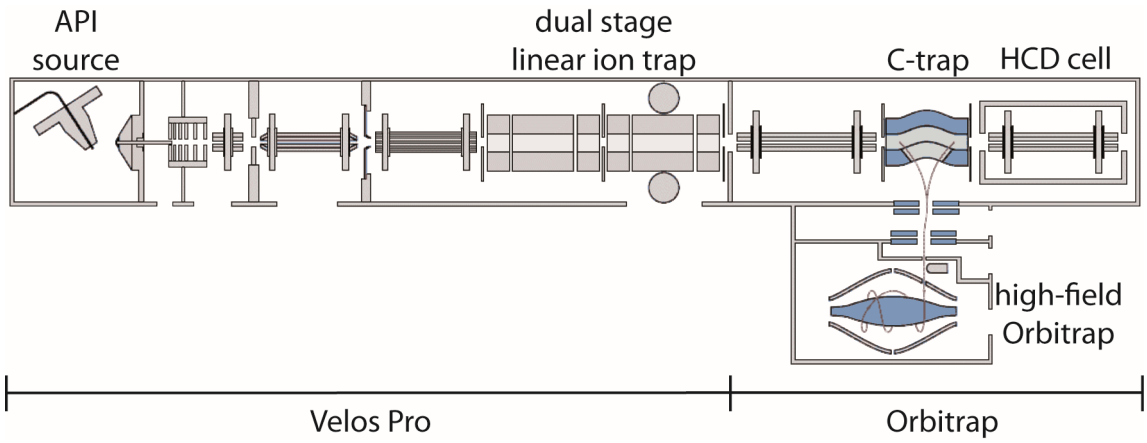

Figure 1-4: Schematic view on an Orbitrap Elite mass spectrometer. Ionization is performed in a variable API type ion source. Ions are first transported into a linear quadrupole iontrap (LTQ) for pre-selection, accumulation and/or MS^n fragmentation experiments. For FTMS measurement, ions are axially ejected into the C-trap, where they are refocused into small ion packets before injection into the Orbitrap analyzer. Here ion oscillations are monitored over a set period of time and the transient signal recorded for FT-processing.

For the course of this work a research-type Orbitrap Elite (Thermo Fisher Scientific, Bremen, Germany) was used either directly or in conjunction with HPLC or IMS hyphenations. Figure 1-4 shows a schematic representation of the instrument. It belongs to the group of hyphenated mass spectrometers, incorporating two mass analyzers, a linear quadrupole ion trap (LTQ, model Velos Pro) and a high-field Orbitrap. The LTQ trap is used for (low resolution) MS^n experiments and for ion pre-selection and accumulation. Rapid pre-scans are used to determine and correct the number of stored ions. This Automated Gain Control (AGC) keeps

the number of ions transmitted into the Orbitrap stable.[77, 78] Thus, a sub-ppm scan-to-scan mass accuracy can be achieved.

The ion motion inside the Orbitrap cell includes a rotational motion around the central electrode (held at constant potential during measurement), depending on the ions initial energy and a back-and-forth motion along the cell axis. The angular frequency ω of this axial motion is recorded by monitoring the image current induced onto the outer electrodes (isolated half-cups forming the endcaps of the trap). This frequency is dependent only on the ions mass-to-charge ratio after $\omega = \sqrt{(kez/m)}$, with k being an instrument specific constant and e the elementary charge.[79]

The instrument used here allows the recording of absorption mode spectra through eFT processing, thus enabling a mass resolving power of $R \geq 480{,}000$ at m/z 400 for a scan rate of 0.65 Hz. This research-type instrument is additionally equipped with an extra-precise Orbitrap cell, allowing a nominal resolving power of $R \geq 960{,}000$ at m/z 400 with the recording of a 3.04 s transient (scan rate 0.33 Hz) enabled.[80]

1.3.1.1 Atmospheric Pressure Ionization (API)

The results of a mass spectrometric analysis will be largely affected by the ionization technique employed.[62, 64] In modern mass spectrometry of liquid samples atmospheric pressure ionization (API) techniques are the most widespread and versatile ionization methods available. These methods include electrospray ionization (ESI) and atmospheric pressure chemical (APCI), photo- (APPI), or laser-ionization (APLI). Beneficial for the analysis of highly complex mixtures is the fact that all of these methods are so-called soft ionization methods, resulting in little to no fragmentation of the initially created ions. This simplifies the determination of the molecular ions and keeps the already crowded spectra free from – often unspecific – fragment ions. All of these techniques exhibit certain characteristics, rendering them useful for the analysis of certain types of analytes, while being discriminating against others.

Electrospray ionization (ESI), while probably the most used method throughout the community, is a rather selective and highly discriminating technique. Although it has been shown that condensed polyaromatic hydrocarbons might be ionized by ESI[81] the technique preferably releases ions in the form of (de-)protonated polar species. Spectra recorded using electrospray

ionization are typically biased towards acidic (negative mode) or basic (positive mode) compounds. In ESI the ionization is undertaken in the liquid phase, while for the other techniques the ionization takes place in the gas phase after thermal evaporation of solvents and analytes that in turn need to be thermally stable. The different ionization mechanisms will determine the versatility and selectivity of these methods.

APCI typically uses a corona discharge to create a low temperature plasma, mostly initiated by the ionization of nitrogen (N_2^+) in positive mode.[82, 83] By further reactions with traces of water this forms protonated water clusters as shown in Scheme 1-2. Additionally, ions like NO^+ and O_2^+ are present. These form a reservoir of reagent ions that indirectly ionize the analyte molecules by either proton or charge transfer or by hydride abstraction (See right side of Scheme 1-2 for example reactions). APCI readily ionizes basic species, the method is, however, extraordinarily useful for the ionization of aliphatic hydrocarbons that are not accessible by other API methods. However, the ionization efficiency and pathways depend to a high extend on the composition of the solvent.

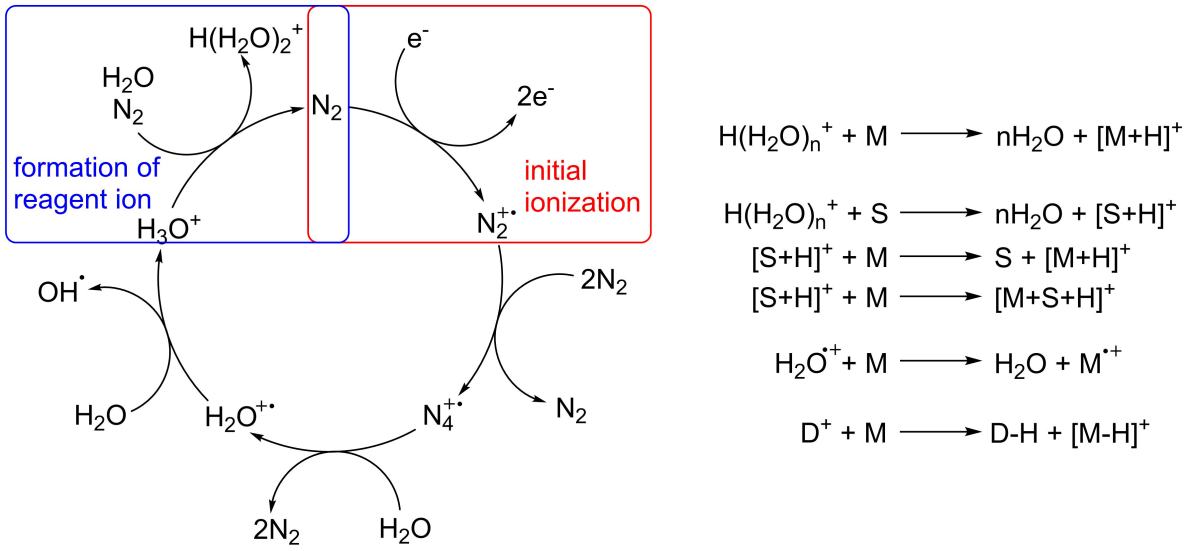

Scheme 1-2: Typical reaction pathways for ionization of an analyte molecule (M) in APCI (positive mode). S denotes a solvent molecule, D denotes an unspecified ion present.[82, 83]

For APPI usually a Krypton VUV lamp is used that emits photons at energies of 10.0 and 10.6 eV. This is comparable to the ionization potential of most organic compounds (typically 8-12 eV). Especially molecules with energetically high HOMOs, i.e. free electron pairs or π-bonds can easily be ionized by direct, photoinduced ejection of an electron. This process leads to the formation of radical cations (see Scheme 1-3).

Atmospheric gases, water and common solvents like methanol, acetonitrile or hexane are not directly ionized due to their high ionization potentials (IP). An initially formed radical cation can undergo secondary reactions with solvent, matrix or other analyte molecules.

These reactions include charge as well as proton transfer reactions in a way that also protonated molecules can be observed. This effect can be deliberately exploited for the ionization of analytes with IP > 10 eV by the addition of a dopant like acetone or toluene. In dopant-assisted APPI the dopant (D) is ionized first to generate a radical dopant ion. This ion can further react with analyte molecules by charge or proton transfer (see Scheme 1-3).[84-86] In an alternative pathway a dopant ion can react with solvent molecules or water within the source region to form protonated water/solvent clusters. These can now in turn lead to the formation of analyte ions by proton transfer.[87, 88] This rather complex reaction cascade enables the ionization of analytes that might not be directly ionized due to an elevated IP, rendering the technique versatile and unselective. A broad range of analytes of varying polarities and molecular weights can be ionized using dopant-assisted APPI. Fully saturated hydrocarbons are among the few compound classes that are not addressable.

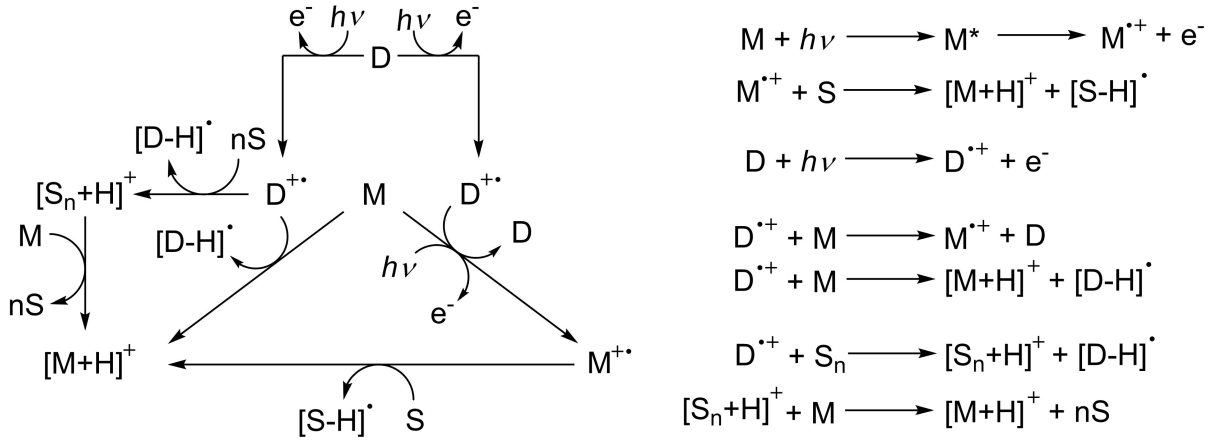

Scheme 1-3: Reaction pathways for ionization of an analyte molecule (M) in APPI (positive mode). S denotes a solvent molecule or water. In case of dopant-assisted APPI, the dopant (D) is ionized first, which leads to further reactions that finally give analyte ions. Single reaction steps are indicated on the right side.[84-86]

APLI also uses photons for the ionization of analytes. While APPI is a 1-photon ionization, APLI or REMPI (Resonance Enhanced MultiPhoton Ionization) is a 2-photon (1+1) ionization method (compare Figure 1-5 for a simplified view of the process). The main instrumental difference between the two techniques is the light source. For APLI a laser with photon energies of around 5 eV is used, typical are a quadrupled Nd:YAG laser (266 nm) or a KrF-Excimer laser (248 nm). Here absorption of a first photon brings the analyte molecule to an excited state. This metastable state needs to be long-lived enough for a second photon to be absorbed, which then

exceeds the molecules ionization potential, resulting in a radical cation (blue portion in Figure 1-5). Limiting factor for the ionizability of a compound are the lifetime and the reaction cross section of a metastable excited state that exists at an adequate energy level. These requirements are met especially for condensed polyaromatic compounds, while most non-aromatic compounds (including most typical solvents and water) are essentially transparent in the UV range used. Thus, APLI is an ionization method that is selective towards analytes with condensed aromatic systems.[89-91]

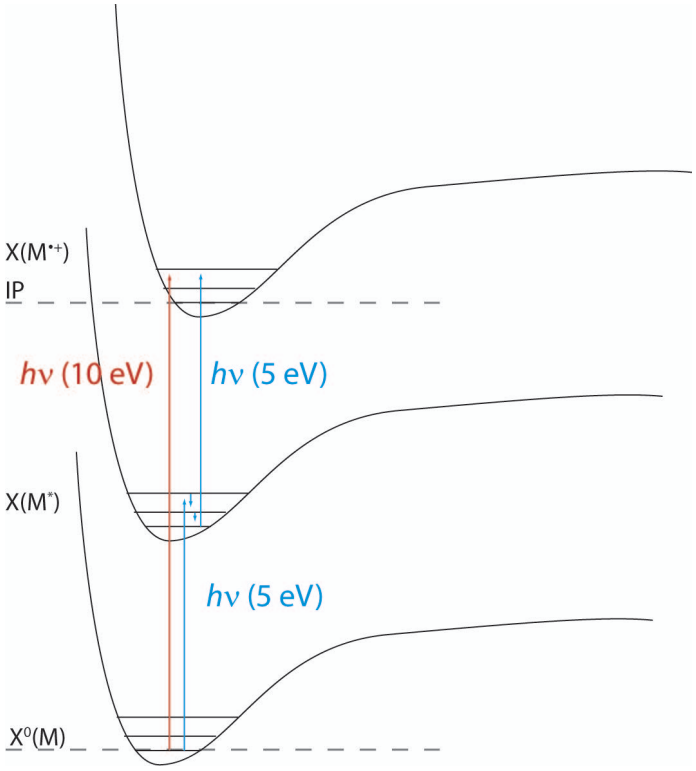

Figure 1-5: Simplified Jablonski diagram showing the photoionization process. For APPI photons with an energy of 10.0 and 10.6 eV are used. These can directly ionize a molecule from its ground state (X^0) as the ionization potential (IP) is typically lower. For APLI a first photon of 5.0 eV brings the molecule to an excited state (X). This needs to be long-lived enough for a second photon to push the excited molecule over the ionization potential. In both ways a radical cation is formed by expulsion of an electron.

1.3.2 Ligand exchange chromatography

While crucial for the simplification of the sample as well as the resulting mass spectra, a chromatographic separation of crude oil is not a trivial task to do. Common reversed phase (RP) HPLC, as typically performed using octadecyl-bonded silica phases (C_{18} or ODS), suffers from poor solubility of crude oil components in aqueous or even polar organic solvents like pure methanol or acetonitrile.

In this work ligand exchange chromatography (LEC) on a Pd(II)-bonded silica phase is used as a NP type separation. As opposed to previous studies, the separation is performed using an online-coupling to mass spectrometric detection using photoionization on samples without prior simplification. The chromatographic approach introduces a group selectivity and allows distinguishing sulfur-free hydrocarbons from thiophenic and in turn from sulfidic compounds.[36-38] On the one hand this allows a deeper insight into the type of sulfur compounds present and on the other hand the separation of sulfur-free from sulfur containing species eases the need for utmost resolving power. The separation relies on the reversible interaction of molecularly bound sulfur with the immobilized Pd ion. Initially retained sulfur containing compounds are successively released by the introduction of a competitive ligand (e.g. isopropanol (^{i}PrOH) or tetrahydrofuran (THF)) into the mobile phase.

1.3.3 Differential ion mobility

While high mass resolving power is crucial to differentiate between isobaric species present in the sample and a chromatographic pre-separation might help to reduce the number of isobars present at one single time (e.g. by separating hydrocarbons from thiophenes), there is still one group of compounds that cannot be told apart this way: Isomers. As isomeric compounds share the same elemental composition they cannot be distinguished by mass spectrometry alone, unless they are ionized exclusively by different ionization techniques. In addition, normal phase chromatographic separations are typically not powerful enough to separate compounds that only differ by their alkylation pattern.

One possibility to separate ions of isomeric species in the gas phase is ion mobility spectrometry (IMS). In classical IMS separations ions formed in an ion source are brought into a drift tube through which they are accelerated by an electric potential.[92, 93] As opposed to mass spectrometry this technique is not performed under vacuum but requires a medium, typically nitrogen and/or helium at or close to atmospheric pressure. This gas phase, typically introduced as a counter-stream of opposite direction, serves as collision partner for the analyte ions. While accelerated by the electric potential they are constantly retarded by low energy collisions with the inert gas. As a result of this constant acceleration and deceleration cycle ions travel at a uniform net speed v that is depending on the field strength E and on the ions collisional cross section (CCS) Ω (see equation 1).[94]

$$v = KE = \frac{3}{16}\sqrt{(2\pi/\mu kT)}\ \frac{ze}{\Omega}\ \frac{E}{N} \qquad (1)$$

Because of the relation between ion mobility *K* and CCS the method can be used for the determination of CCS of known compounds as well as for the separation of structurally different isomers in the gas phase.

Considering the speed at which an ion travels through the flight tube and the differences thereof, an IMS spectrum is typically recorded on the timescale of milliseconds. This is not well compatible with the time domain of FT-based mass spectrometers that record a mass spectrum over the range of seconds. Using classical IMS together with FTMS would therefore require the operation of shutters at the exit of the IMS unit and the accumulation of ions over several IMS runs to gather ions of only one mobility for the subsequent FTMS analysis. While this is generally possible, an alternative approach is to use high-field asymmetric waveform ion mobility spectrometry (FAIMS) which is a differential ion mobility method. Here, ions are transported through the mobility unit by a carrier gas, while the accelerating potentials are applied perpendicular to this direction through a 2-electrode assembly that forms an ion channel.[94-96]

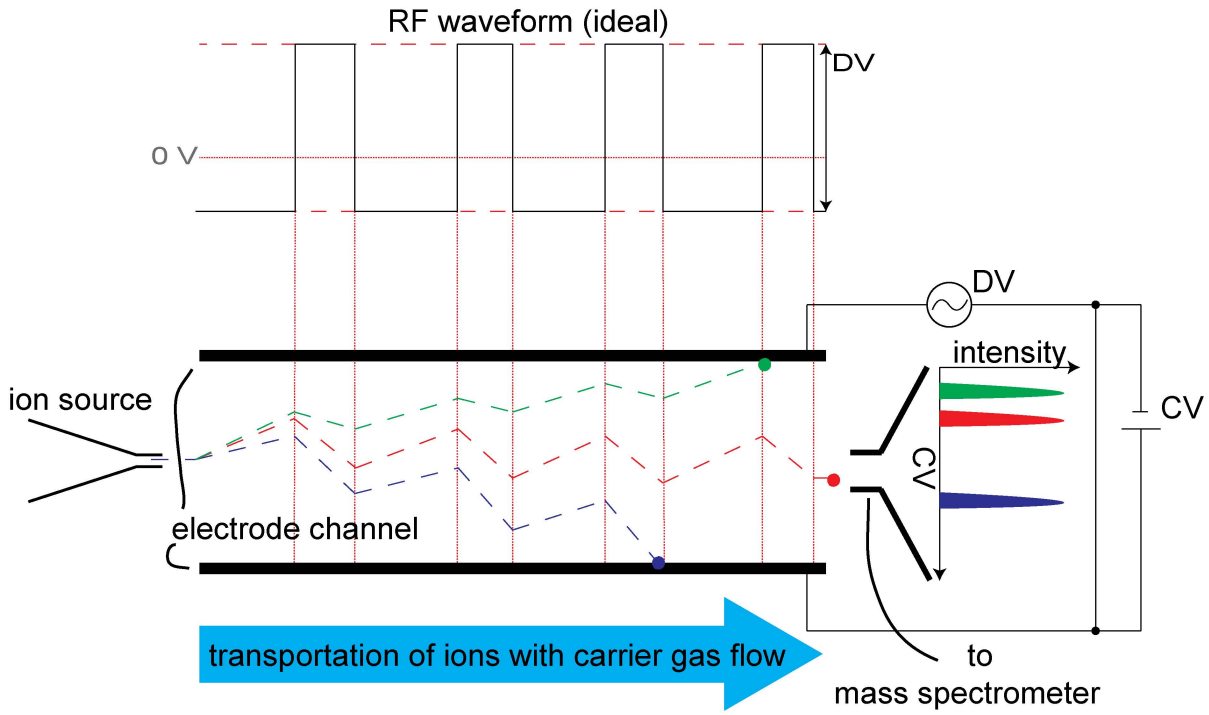

Figure 1-6: Schematics of a FAIMS-MS coupling. Ions generated in the ion source are sprayed into an electrode channel and transported towards the exit (the MS inlet) by a carrier gas flow. The asymmetry of the acceleration potential (DV, see upper part) leads to different ion mobilities during the two wave portions and thus to a net displacement towards one of the electrodes. This displacement is counteracted by application of a compensation voltage (CV) onto one of the electrodes.

In FAIMS the accelerating potential is not uniform as in classical IMS but consists of an asymmetric wave of a high amplitude (A), high frequency (v) portion and a low amplitude, low frequency portion of opposite polarity such that $A/v = const$. (see also upper part in Figure 1-6). During the different portions of the wave an ion is accelerated towards one or the other electrode with ideally no net displacement. Separation is possible because at high electric field strength ion mobilities K of most ions are not constant but become a function of the field strength. As a result, mobilities are different during the high and the low field portion of the wave. This might be caused by structural rearrangements (folding) under the effect of different field strengths or by clustering/declustering of the ions with the carrier gas (typically nitrogen and helium). These different mobilities result in a net displacement of the ion towards one of the electrodes such that it will be neutralized on the electrode surface and effectively filtered out of the ion flux. This net displacement can be gradually counteracted by application of a so-called compensation voltage (CV) on one of the electrodes. This way the separating direction is perpendicular to the ion flow path and a FAIMS unit is effectively operated as a filter. By keeping the CV stable over the course of a mass spectrometric scan, this technique is perfectly suitable for a combination with long scanning FTMS instrumentation.

For the course of this work a Thermo Fisher Scientific FAIMS unit with a cylindrical electrode setup was used. Compared to a planar setup as depicted in Figure 1-6 this approach is supposed to yield a better ion transmission due to ion focusing in the asymmetric field, but at the expense of a lowered resolving power.

1.4 References

1. Connan, J., *Use and trade of bitumen in antiquity and prehistory: molecular archaeology reveals secrets of past civilizations* in: *Philos. Trans. R. Soc. London, Ser. B* **1999**, *354*(1379), 33-50.

2. Beaton, K., *Dr. Gesner's Kerosene: The Start of American Oil Refining* in: *Business History Review* **2012**, *29*(01), 28-53.

3. International Energy Agency, *Key World Energy Statistics 2016*, accessed on 01.11.2016. Available from: https://www.iea.org/publications/freepublications/publication/key-world-energy-statistics.html.

4. Glasby, G. P., *Abiogenic Origin of Hydrocarbons: An Historical Overview* in: *Resour. Geol.* **2006**, *56*(1), 83-96.

5. Durand, B., *A History of Organic Geochemistry* in: *Oil Gas Sci. Technol.* **2003**, *58*(2), 203-231.

6. Bordenave, M. L., *Applied Petroleum Geochemistry* **1993**, Editions Technips, Paris.

7. Hunt, J. M., *Petroleum geochemistry and geology*. A Series of books in geology **1979**, W. H. Freeman, San Francisco.

8. Schobert, H. H., *The chemistry of hydrocarbon fuels* **1990**, Butterworths, London ; Boston.

9. Andersson, J. T., *Schwefel in Erdöl: Ein problematisches Element?* in: *Chem. unserer Zeit* **2005**, *39*(2), 116-120.

10. Eßer, J., *Vom Rohöl zu Energie- und Chemierohstoffen. Erdölverarbeitung in der Mineralölraffinerie* in: *Chem. unserer Zeit* **2011**, *45*(2), 96-120.

11. *E. Parliament Directive 98/70/EC of 13 October 1998 relating to the quality of petrol and diesel fuels and amending Council Directive 93/12/EEC*.

12. Blomberg, J.; Schoenmakers, P. J.; Beens, J. and Tijssen, R., *Compehensive two-dimensional gas chromatography (GC×GC) and its applicability to the characterization of complex (petrochemical) mixtures* in: *J. High. Resolut. Chromatogr.* **1997**, *20*(10), 539-544.

13. Alomair, O.; Jumaa, M.; Alkoriem, A. and Hamed, M., *Heavy oil viscosity and density prediction at normal and elevated temperatures* in: *J. Pet. Explor. Prod. Technol.* **2016**, *6*(2), 253-263.

14. Argirov, G.; Ivanov, S. and Cholakov, G., *Estimation of crude oil TBP from crude viscosity* in: *Fuel* **2012**, *97*, 358-365.

15. Wang, Q.; Ye, J.-b.; Yang, H.-y. and Liu, Q., *Chemical Composition and Structural Characteristics of Oil Shales and Their Kerogens Using Fourier Transform Infrared (FTIR) Spectroscopy and Solid-State13C Nuclear Magnetic Resonance (NMR)* in: *Energy Fuels* **2016**, *30*(8), 6271-6280.

16. Kim, E.; Cho, E.; Moon, C.; Ha, J.; Cho, E.; Ha, J.-H. and Kim, S., *Correlation among Petroleomics Data Obtained with High-Resolution Mass Spectrometry and Elemental and NMR Analyses of Maltene Fractions of Atmospheric Pressure Residues* in: *Energy Fuels* **2016**, *30*(9), 6958-6967.

17. Dutta Majumdar, R.; Bake, K. D.; Ratna, Y.; Pomerantz, A. E.; Mullins, O. C.; Gerken, M. and Hazendonk, P., *Single-Core PAHs in Petroleum- and Coal-Derived Asphaltenes: Size and Distribution from Solid-State NMR Spectroscopy and Optical Absorption Measurements* in: *Energy Fuels* **2016**, *30*(9), 6892-6906.

18. Abdul Jameel, A. G.; Naser, N.; Emwas, A.-H.; Dooley, S. and Sarathy, S. M., *Predicting Fuel Ignition Quality Using1H NMR Spectroscopy and Multiple Linear Regression* in: *Energy Fuels* **2016**, *30*(11), 9819-9835.

19. Chakravarthy, R.; Naik, G. N.; Savalia, A.; Sridharan, U.; Saravanan, C.; Das, A. K. and Gudasi, K. B., *Determination of Naphthenic Acid Number in Petroleum Crude Oils and Their Fractions by Mid-Fourier Transform Infrared Spectroscopy* in: *Energy Fuels* **2016**, *30*(10), 8579-8586.

20. ASTM D1840-07(2013), Standard Test Method for Naphthalene Hydrocarbons in Aviation Turbine Fuels by Ultraviolet Spectrophotometry, ASTM Interational, West Conshohocken, PA, 2013

21. Sugumaran, V.; Biswas, H.; Yadav, A.; Christopher, J.; Kagdiyal, V.; Patel, M. B. and Basu, B., *Molecular-Level Characterization of Refinery Streams by High-Resolution Mass Spectrometry* in: *Energy Fuels* **2015**, *29*(5), 2940-2950.

22. Bolin, T. B.; Birdwell, J. E.; Lewan, M. D.; Hill, R. J.; Grayson, M. B.; Mitra-Kirtley, S.; Bake, K. D.; Craddock, P. R.; Abdallah, W. and Pomerantz, A. E., *Sulfur Species in Source Rock Bitumen before and after Hydrous Pyrolysis Determined by X-ray Absorption Near-Edge Structure* in: *Energy Fuels* **2016**, *30*(8), 6264-6270.

23. Lobodin, V. V.; Maksimova, E. V. and Rodgers, R. P., *Gas Chromatography/Atmospheric Pressure Chemical Ionization Tandem Mass Spectrometry for Fingerprinting the Macondo Oil Spill* in: *Anal. Chem.* **2016**, *88*(13), 6914-6922.

24. Gao, X.; Zhu, S.; Zhang, W.; Li, D.; Dai, W. and He, S., *Analysis of crude oils using gas purge microsyringe extraction coupled to comprehensive two dimensional gas chromatography-time-of-flight mass spectrometry* in: *Fuel* **2016**, *182*, 788-797.

25. Benigni, P.; DeBord, J. D.; Thompson, C. J.; Gardinali, P. and Fernandez-Lima, F., *Increasing Polyaromatic Hydrocarbon (PAH) Molecular Coverage during Fossil Oil Analysis by Combining Gas Chromatography and Atmospheric-Pressure Laser Ionization Fourier Transform Ion Cyclotron Resonance Mass Spectrometry (FT-ICR MS)* in: *Energy Fuels* **2016**, *30*(1), 196-203.

26. Wang, M.; Zhao, S.; Chung, K. H.; Xu, C. and Shi, Q., *Approach for Selective Separation of Thiophenic and Sulfidic Sulfur Compounds from Petroleum by Methylation/Demethylation* in: *Anal. Chem.* **2015**, *87*(2), 1083-1088.

27. Wilde, M. J. and Rowland, S. J., *Structural Identification of Petroleum Acids by Conversion to Hydrocarbons and Multidimensional Gas Chromatography-Mass Spectrometry* in: *Anal. Chem.* **2015**, *87*(16), 8457-8465.

28. Klein, G. C.; Angström, A.; Rodgers, R. P. and Marshall, A. G., *Use of Saturates/Aromatics/Resins/Asphaltenes (SARA) Fractionation To Determine Matrix Effects in Crude Oil Analysis by Electrospray Ionization Fourier Transform Ion Cyclotron Resonance Mass Spectrometry* in: *Energy Fuels* **2006**, *20*(2), 668-672.

29. Bissada, K. K.; Tan, J.; Szymczyk, E.; Darnell, M. and Mei, M., *Group-type characterization of crude oil and bitumen. Part I: Enhanced separation and quantification of saturates, aromatics, resins and asphaltenes (SARA)* in: *Org. Geochem.* **2016**, *95*, 21-28.

30. Hegazi, A. H.; Fathalla, E. M. and Andersson, J. T., *Weathering trend characterization of medium-molecular weight polycyclic aromatic disulfur heterocycles by Fourier transform ion cyclotron resonance mass spectrometry* in: *Chemosphere* **2014**, *111*, 266-271.

31. Hegazi, A. H.; Fathalla, E. M.; Panda, S. K.; Schrader, W. and Andersson, J. T., *High-molecular weight sulfur-containing aromatics refractory to weathering as determined by Fourier transform ion cyclotron resonance mass spectrometry* in: *Chemosphere* **2012**, *89*(3), 205-212.

32. Shi, Q.; Hou, D.; Chung, K. H.; Xu, C.; Zhao, S. and Zhang, Y., *Characterization of Heteroatom Compounds in a Crude Oil and Its Saturates, Aromatics, Resins, and Asphaltenes (SARA) and Non-basic Nitrogen Fractions Analyzed by Negative-Ion Electrospray Ionization Fourier Transform Ion Cyclotron Resonance Mass Spectrometry* in: *Energy Fuels* **2010**, *24*(4), 2545-2553.

33. Sim, A.; Cho, Y.; Kim, D.; Witt, M.; Birdwell, J. E.; Kim, B. J. and Kim, S., *Molecular-level characterization of crude oil compounds combining reversed-phase high-performance liquid chromatography with off-line high-resolution mass spectrometry* in: *Fuel* **2015**, *140*, 717-723.

34. Lababidi, S.; Panda, S. K.; Andersson, J. T. and Schrader, W., *Direct coupling of normal-phase high-performance liquid chromatography to atmospheric pressure laser ionization fourier transform ion cyclotron resonance mass spectrometry for the characterization of crude oil* in: *Anal. Chem.* **2013**, *85*(20), 9478-9485.

35. Lababidi, S. and Schrader, W., *Online normal-phase high-performance liquid chromatography/Fourier transform ion cyclotron resonance mass spectrometry: effects of different ionization methods on the characterization of highly complex crude oil mixtures* in: *Rapid Commun. Mass Spectrom.* **2014**, *28*(12), 1345-1352.

36. Müller, H.; Andersson, J. T. and Schrader, W., *Characterization of high-molecular-weight sulfur-containing aromatics in vacuum residues using Fourier transform ion cyclotron resonance mass spectrometry* in: *Anal. Chem.* **2005**, *77*(8), 2536-2543.

37. Panda, S. K.; Schrader, W. and Andersson, J. T., *Fourier transform ion cyclotron resonance mass spectrometry in the speciation of high molecular weight sulfur heterocycles in vacuum gas oils of different boiling ranges* in: *Anal. Bioanal. Chem.* **2008**, *392*(5), 839-848.

38. Japes, A.; Penassa, M. and Andersson, J. T., *Analysis of Recalcitrant Hexahydrodibenzothiophenes in Petroleum Products Using a Simple Fractionation Process* in: *Energy Fuels* **2009**, *23*(4), 2143-2148.

39. Moustafa, N. E. and Andersson, J. T., *Analysis of polycyclic aromatic sulfur heterocycles in Egyptian petroleum condensate and volatile oils by gas chromatography with atomic emission detection* in: *Fuel Process. Technol.* **2011**, *92*(3), 547-555.

40. Panda, S. K.; Brockmann, K. J.; Benter, T. and Schrader, W., *Atmospheric pressure laser ionization (APLI) coupled with Fourier transform ion cyclotron resonance mass spectrometry applied to petroleum samples analysis: comparison with electrospray ionization and atmospheric pressure photoionization methods* in: *Rapid Commun. Mass Spectrom.* **2011**, *25*(16), 2317-2326.

41. Gole, A. and Andersson, J. T., *Group-Type Separation of Nitrogen Containing Aromatic Compounds in Coal Tar Pitch on a Hafnium Modified Silica HPLC Phase* in: *Polycyclic Aromat. Compd.* **2014**, *35*(1), 129-142.

42. Nocun, M. and Andersson, J. T., *Argentation chromatography for the separation of polycyclic aromatic compounds according to ring number* in: *J. Chromatogr. A* **2012**, *1219*, 47-53.

43. Hartgers, W. A.; Damsté, J. S. S. and de Leeuw, J. W., *Geochemical significance of alkylbenzene distributions in flash pyrolysates of kerogens, coals, and asphaltenes* in: *Geochim. Cosmochim. Acta* **1994**, *58*(7), 1759-1775.

44. Ellis, L.; Singh, R. K.; Alexander, R. and Kagi, R. I., *Geosynthesis of organic compounds: III. Formation of alkyltoluenes and alkylxylenes in sediments* in: *Geochim. Cosmochim. Acta* **1995**, *59*(24), 5133-5140.

45. Ioppolo-Armanios, M.; Alexander, R. and Kagi, R. I., *Geosynthesis of organic compounds: I. Alkylphenols* in: *Geochim. Cosmochim. Acta* **1995**, *59*(14), 3017-3027.

46. Budzinski, H.; Raymond, N.; Nadalig, T.; Gilewicz, M.; Garrigues, P.; Bertrand, J. C. and Caumette, P., *Aerobic biodegradation of alkylated aromatic hydrocarbons by a bacterial community* in: *Org. Geochem.* **1998**, *28*(5), 337-348.

47. Ivanova, I. K.; Chalaya, O. N. and Kashirtsev, V. A., *Normal alkylbenzenes of the composition C12H18-C23H40 in oils from the Nepa-Botuoba oil-and-gas-bearing region and possible mechanism of n-pentadecylbenzene formation* in: *Russ. J. Appl. Chem.* **2007**, *80*(10), 1759-1763.

48. Fathalla, E. M. and Andersson, J. T., *Products of polycyclic aromatic sulfur heterocycles in oil spill photodegradation* in: *Environ. Toxicol. Chem.* **2011**, *30*(9), 2004-2012.

49. Koopmans, M. P.; De Leeuw, J. W. and Damsté, J. S. S., *Novel cyclised and aromatised diagenetic products of β-carotene in the Green River Shale* in: *Org. Geochem.* **1997**, *26*(7), 451-466.

50. Gorchs, R.; Olivella, M. A. and de las Heras, F. X. C., *New aromatic biomarkers in sulfur-rich coal* in: *Org. Geochem.* **2003**, *34*(12), 1627-1633.

51. Furbo, S.; Hansen, A. B.; Skov, T. and Christensen, J. H., *Pixel-Based Analysis of Comprehensive Two-Dimensional Gas Chromatograms (Color Plots) of Petroleum: A Tutorial* in: *Anal. Chem.* **2014**, *86*(15), 7160-7170.

52. Jia, L.; Le Brech, Y.; Mauviel, G.; Qi, F.; Bente-von Frowein, M.; Ehlert, S.; Zimmermann, R. and Dufour, A., *Online Analysis of Biomass Pyrolysis Tar by Photoionization Mass Spectrometry* in: *Energy Fuels* **2016**, *30*(3), 1555-1563.

53. Fernandez-Lima, F. A.; Becker, C.; McKenna, A. M.; Rodgers, R. P.; Marshall, A. G. and Russell, D. H., *Petroleum Crude Oil Characterization by IMS-MS and FTICR MS* in: *Anal. Chem.* **2009**, *81*(24), 9941-9947.

54. Ponthus, J. and Riches, E., *Evaluating the multiple benefits offered by ion mobility-mass spectrometry in oil and petroleum analysis* in: *Int. J. Ion Mobility Spectrom.* **2013**, *16*(2), 95-103.

55. Santos, J. M.; Galaverna, R. d. S.; Pudenzi, M. A.; Schmidt, E. M.; Sanders, N. L.; Kurulugama, R. T.; Mordehai, A.; Stafford, G. C.; Wisniewski, A. and Eberlin, M. N., *Petroleomics by ion mobility mass spectrometry: resolution and characterization of contaminants and additives in crude oils and petrofuels* in: *Anal. Methods* **2015**, *7*(11), 4450-4463.

56. Farenc, M.; Corilo, Y. E.; Lalli, P. M.; Riches, E.; Rodgers, R. P.; Afonso, C. and Giusti, P., *Comparison of Atmospheric Pressure Ionization for the Analysis of Heavy Petroleum Fractions with Ion Mobility-Mass Spectrometry* in: *Energy Fuels* **2016**, *30*(11), 8896-8903.

57. Hughey, C. A.; Rodgers, R. P. and Marshall, A. G., *Resolution of 11,000 compositionally distinct components in a single electrospray ionization Fourier transform ion cyclotron resonance mass spectrum of crude oil* in: *Anal. Chem.* **2002**, *74*(16), 4145-4149.

58. Schrader, W. and Klein, H. W., *Liquid chromatography/Fourier transform ion cyclotron resonance mass spectrometry (LC-FTICR MS): an early overview* in: *Anal. Bioanal. Chem.* **2004**, *379*(7-8), 1013-1024.

59. Panda, S. K.; Schrader, W. and Andersson, J. T., *beta-Cyclodextrin as a stationary phase for the group separation of polycyclic aromatic compounds in normal-phase liquid chromatography* in: *J. Chromatogr. A* **2006**, *1122*(1-2), 88-96.

60. Purcell, J. M.; Rodgers, R. P.; Hendrickson, C. L. and Marshall, A. G., *Speciation of Nitrogen Containing Aromatics by Atmospheric Pressure Photoionization or Electrospray Ionization Fourier Transform Ion Cyclotron Resonance Mass Spectrometry* in: *J. Am. Soc. Mass. Spectrom.* **2007**, *18*(7), 1265-1273.

61. Schrader, W.; Panda, S. K.; Brockmann, K. J. and Benter, T., *Characterization of non-polar aromatic hydrocarbons in crude oil using atmospheric pressure laser ionization and Fourier transform ion cyclotron resonance mass spectrometry (APLI FT-ICR MS)* in: *Analyst* **2008**, *133*(7), 867-869.

62. Panda, S. K.; Andersson, J. T. and Schrader, W., *Characterization of supercomplex crude oil mixtures: what is really in there?* in: *Angew. Chem. Int. Ed.* **2009**, *48*(10), 1788-1791.

63. Gaspar, A. and Schrader, W., *Expanding the data depth for the analysis of complex crude oil samples by Fourier transform ion cyclotron resonance mass spectrometry using the spectral stitching method* in: *Rapid Commun. Mass Spectrom.* **2012**, *26*(9), 1047-1052.

64. Gaspar, A.; Zellermann, E.; Lababidi, S.; Reece, J. and Schrader, W., *Impact of different ionization methods on the molecular assignments of asphaltenes by FT-ICR mass spectrometry* in: *Anal. Chem.* **2012**, *84*(12), 5257-5267.

65. Lababidi, S.; Panda, S. K.; Andersson, J. T. and Schrader, W., *Deep Well Deposits: Effects of Extraction on Mass Spectrometric Results* in: *Energy Fuels* **2013**, *27*(3), 1236-1245.

66. Wang, X. and Schrader, W., *Selective Analysis of Sulfur-Containing Species in a Heavy Crude Oil by Deuterium Labeling Reactions and Ultrahigh Resolution Mass Spectrometry* in: *Int. J. Mol. Sci.* **2015**, *16*(12), 30133-30143.

67. Giraldo-Dávila, D.; Chacón-Patiño, M. L.; Orrego-Ruiz, J. A.; Blanco-Tirado, C. and Combariza, M. Y., *Improving compositional space accessibility in (+) APPI FT-ICR mass spectrometric analysis of crude oils by extrography and column chromatography fractionation* in: *Fuel* **2016**, *185*, 45-58.

68. Orrego-Ruiz, J. A.; Gomez-Escudero, A. and Rojas-Ruiz, F. A., *Combination of Negative Electrospray Ionization and Positive Atmospheric Pressure Photoionization Fourier Transform Ion Cyclotron Resonance Mass Spectrometry as a Quantitative Approach of Acid Species in Crude Oils* in: *Energy Fuels* **2016**, *30*(10), 8209-8215.

69. Pudenzi, M. A. and Eberlin, M. N., *Assessing Relative Electrospray Ionization, Atmospheric Pressure Photoionization, Atmospheric Pressure Chemical Ionization, and Atmospheric Pressure Photo- and Chemical Ionization Efficiencies in Mass Spectrometry Petroleomic Analysis via Pools and Pairs of Selected Polar Compound Standards* in: *Energy Fuels* **2016**, *30*(9), 7125-7133.

70. Rojas-Ruiz, F. A. and Orrego-Ruiz, J. A., *Distribution of Oxygen-Containing Compounds and Its Significance on Total Organic Acid Content in Crude Oils by ESI Negative Ion FT-ICR MS* in: *Energy Fuels* **2016**, *30*(10), 8185-8191.

71. Alhassan, A. and Andersson, J. T., *Ketones in Fossil Materials—A Mass Spectrometric Analysis of a Crude Oil and a Coal Tar* in: *Energy Fuels* **2013**, *27*(10), 5770-5778.

72. Huba, A. K. and Gardinali, P. R., *Characterization of a crude oil weathering series by ultrahigh-resolution mass spectrometry using multiple ionization modes* in: *Sci. Total Environ.* **2016**, *563-564*, 600-610.

73. Romão, W.; Tose, L. V.; Vaz, B. G.; Sama, S. G.; Lobinski, R.; Giusti, P.; Carrier, H. and Bouyssiere, B., *Petroleomics by Direct Analysis in Real Time-Mass Spectrometry* in: *J. Am. Soc. Mass. Spectrom.* **2015**, *27*(1), 182-185.

74. Zhurov, K. O.; Kozhinov, A. N. and Tsybin, Y. O., *Evaluation of High-Field Orbitrap Fourier Transform Mass Spectrometer for Petroleomics* in: *Energy Fuels* **2013**, *27*(6), 2974-2983.

75. Da Costa, C.; Turner, M.; Reynolds, J. C.; Whitmarsh, S.; Lynch, T. and Creaser, C. S., *Direct Analysis of Oil Additives by High-Field Asymmetric Waveform Ion Mobility Spectrometry-Mass Spectrometry Combined with Electrospray Ionization and Desorption Electrospray Ionization* in: *Anal. Chem.* **2016**, *88*(4), 2453-2458.

76. Fasciotti, M.; Lalli, P. M.; Klitzke, C. F.; Corilo, Y. E.; Pudenzi, M. A.; Pereira, R. C. L.; Bastos, W.; Daroda, R. J. and Eberlin, M. N., *Petroleomics by Traveling Wave Ion Mobility–Mass Spectrometry Using CO2as a Drift Gas* in: *Energy Fuels* **2013**, *27*(12), 7277-7286.

77. Makarov, A.; Denisov, E.; Kholomeev, A.; Balschun, W.; Lange, O.; Strupat, K. and Horning, S., *Performance Evaluation of a Hybrid Linear Ion Trap/Orbitrap Mass Spectrometer* in: *Anal. Chem.* **2006**, *78*(7), 2113-2120.

78. Schwartz, J. C. and Kovtoun, V. V., "*Automatic gain control (AGC) method for an ion trap and a temporally non-uniform ion beam*", Patent US 7960690 B2, 14 June 2011.

79. Perry, R. H.; Cooks, R. G. and Noll, R. J., *Orbitrap mass spectrometry: Instrumentation, ion motion and applications* in: *Mass Spectrom. Rev.* **2008**, *27*(6), 661-699.

80. Denisov, E.; Damoc, E.; Lange, O. and Makarov, A., *Orbitrap mass spectrometry with resolving powers above 1,000,000* in: *Int. J. Mass spectrom.* **2012**, *325–327*, 80-85.

81. Molnarne Guricza, L. and Schrader, W., *Electrospray ionization for determination of non-polar polyaromatic hydrocarbons and polyaromatic heterocycles in heavy crude oil asphaltenes* in: *J. Mass Spectrom.* **2015**, *50*(3), 549-557.

82. Horning, E. C.; Carroll, D. I.; Dzidic, I.; Haegele, K. D.; Horning, M. G. and Stillwell, R. N., *Atmospheric Pressure Ionization (API) Mass Spectrometry. Solvent-Mediated Ionization of Samples Introduced in Solution and in a Liquid Chromatograph Effluent Stream* in: *J. Chromatogr. Sci.* **1974**, *12*(11), 725-729.

83. Carroll, D. I.; Dzidic, I.; Stillwell, R. N.; Haegele, K. D. and Horning, E. C., *Atmospheric pressure ionization mass spectrometry. Corona discharge ion source for use in a liquid chromatograph-mass spectrometer-computer analytical system* in: *Anal. Chem.* **1975**, *47*(14), 2369-2373.

84. Kauppila, T. J.; Kuuranne, T.; Meurer, E. C.; Eberlin, M. N.; Kotiaho, T. and Kostiainen, R., *Atmospheric Pressure Photoionization Mass Spectrometry. Ionization Mechanism and the Effect of Solvent on the Ionization of Naphthalenes* in: *Anal. Chem.* **2002**, *74*(21), 5470-5479.

85. Raffaelli, A. and Saba, A., *Atmospheric pressure photoionization mass spectrometry* in: *Mass Spectrom. Rev.* **2003**, *22*(5), 318-331.

86. Vaikkinen, A.; Haapala, M.; Kersten, H.; Benter, T.; Kostiainen, R. and Kauppila, T. J., *Comparison of Direct and Alternating Current Vacuum Ultraviolet Lamps in Atmospheric Pressure Photoionization* in: *Anal. Chem.* **2012**, *84*(3), 1408-1415.

87. Kauppila, T. J.; Kersten, H. and Benter, T., *The Ionization Mechanisms in Direct and Dopant-Assisted Atmospheric Pressure Photoionization and Atmospheric Pressure Laser Ionization* in: *J. Am. Soc. Mass. Spectrom.* **2014**, *25*(11), 1870-1881.

88. Klee, S.; Albrecht, S.; Derpmann, V.; Kersten, H. and Benter, T., *Generation of ion-bound solvent clusters as reactant ions in dopant-assisted APPI and APLI* in: *Anal. Bioanal. Chem.* **2013**, *405*(22), 6933-6951.

89. Constapel, M.; Schellenträger, M.; Schmitz, O. J.; Gäb, S.; Brockmann, K. J.; Giese, R. and Benter, T., *Atmospheric-pressure laser ionization: a novel ionization method for liquid chromatography/mass spectrometry* in: *Rapid Commun. Mass Spectrom.* **2005**, *19*(3), 326–336.

90. Lorenz, M.; Schiewek, R.; Brockmann, K. J.; Schmitz, O. J.; Gäb, S. and Benter, T., *The distribution of ion acceptance in atmospheric pressure ion sources: Spatially resolved APLI measurements* in: *J. Am. Soc. Mass. Spectrom.* **2008**, *19*(3), 400-410.

91. Schiewek, R.; Schellenträger, M.; Mönnikes, R.; Lorenz, M.; Giese, R.; Brockmann, K. J.; Gäb, S.; Benter, T. and Schmitz, O. J., *Ultrasensitive Determination of Polycyclic Aromatic Compounds with Atmospheric-Pressure Laser Ionization as an Interface for GC/MS* in: *Anal. Chem.* **2007**, *79*(11), 4135-4140.

92. Laakia, J.; Adamov, A.; Jussila, M.; Pedersen, C. S.; Sysoev, A. A. and Kotiaho, T., *Separation of different ion structures in atmospheric pressure photoionization-ion mobility spectrometry-mass spectrometry (APPI-IMS-MS)* in: *J. Am. Soc. Mass. Spectrom.* **2010**, *21*(9), 1565–1572.

93. Laakia, J.; Kauppila, T. J.; Adamov, A.; Sysoev, A. A. and Kotiaho, T., *Separation of isomeric amines with ion mobility spectrometry* in: *Talanta* **2015**, *132*, 889–893.

94. Shvartsburg, A. A., *Differential ion mobility spectrometry : nonlinear ion transport and fundamentals of FAIMS* **2009**, CRC Press, Boca Raton.

95. Guevremont, R., *High-field asymmetric waveform ion mobility spectrometry: A new tool for mass spectrometry* in: *J. Chromatogr. A* **2004**, *1058*(1-2), 3–19.

96. Isenberg, S. L.; Armistead, P. M. and Glish, G. L., *Optimization of peptide separations by differential ion mobility spectrometry* in: *J. Am. Soc. Mass. Spectrom.* **2014**, *25*(9), 1592–1599.

2. Scope of the work

The comprehensive mass spectrometric analysis of crude oil is biased by a number of factors. One is the overwhelming number of different compounds present in the mixture which leads to very crowded mass spectra. This is especially true for elevated *m*/*z* values > 900 where a larger variety of elemental compositions can be expected due to a generally increased number of heteroatoms per molecule. Additionally, the impact of isotopolog peaks, especially ^{13}C and with increasing molecular size also $^{13}C_2$, becomes relevant. Other factors are a broad variety of functional groups and polarities of compounds, ranging from fully unpolar hydrocarbons to very polar (naphthenic) acids and (pyridinic) bases. All these different groups and for that matter all members among one compound group will show a largely different response factor for every single ionization technique that can possibly be used. Discriminating effects of the sample itself play another important role. Typical problems during any analysis are matrix effects that suppress or even eliminate the signal of the desired analyte. In the case of crude oil, the sample is at the same time matrix and analyte, such that matrix effects are omnipresent.

These problems could be lessened if the sample entering the mass spectrometer at any given time during the analysis was simplified, i.e. removed from the majority of the accompanying co-analytes. This can be achieved prior to mass spectrometric analyses during offline separation (e.g. by a SARA fractionation) and fraction collection. Scope of this work is the development and improvement of methods that can be used for online hyphenations of a separating step with high resolving mass spectrometry. Two different approaches, ion mobility spectrometry (IMS) and ligand exchange chromatography (LEC), are investigated in detail and further discussed in the subsequent chapters:

First, in chapter 3, a general overview on data analysis of high resolving mass spectra of crude oil is given. A major concern is the transformation of detected *m*/*z* values into elemental compositions of the corresponding analytes and an adequate representation thereof. For the hyphenation of separation methods with mass spectrometry new procedures needed to be developed to enable the time-resolved interpretation of the acquired data.

Chapter 4 introduces a research type Orbitrap Elite mass spectrometer that allows the recording of a 3 s transient, thus enabling a mass resolving power of nearly one million (FWHM at *m*/*z* 400). The instrument is tested against the coverage of compositional space of crude oil. The

combination of high sensitivity and resolving power with fast scan rates sets the ground for the following hyphenation approaches.

In chapter 5 the hyphenation of differential ion mobility (FAIMS) and FTMS is evaluated for the analysis of a whole crude oil. For this purpose, a new ion source is introduced that allows 1- and 2-photon ionization (APPI and APLI) together with the ion mobility unit used. The introduction of an isomer-discriminating method (FAIMS) between ion source and mass spectrometer also proves the necessity for multiple ionization techniques.

Based on the results from chapter 5, modifications of the source design and electrode setup are introduced in chapter 6. These changes address signal transmission and resolving power of the ion mobility unit. The adapted setup is used to gain further insight into the structural variety of selected compounds by fragmentation experiments using collision-induced dissociation.

A different separation approach is discussed chapter 7. Here, an online coupling of liquid chromatography to high resolving mass spectrometry is shown. The method relies on a ligand exchange mechanism on immobilized Pd ions and is used for the separation of sulfur containing species. After adaption and optimization of the method it is used for the group-selective quantification of sulfur containing species in a relatively light whole crude oil by means of ICP-MS/MS.

In chapter 8 the method is used for the group-selective quantification of sulfur containing compounds in a heavy, bituminous crude oil and its fractions obtained by a modified SARA procedure.

Finally, in chapter 9 the results of this work are summarized.

3. Data analysis and data representation

Complex samples will unavoidably result in equally complex mass spectra, especially as – a certain signal abundance given – every organic species will give multiple mass spectrometric signals resulting from isotopologs. When analyzing crude oil, mass spectra with up to > 150,000 distinct peaks need to be evaluated; each, if possible, assigned with the molecular formula of the corresponding ion. This can hardly be done manually but with the help of specialized software algorithms. During the course of this work different software solutions have been developed that help to interpret and visualize the analysis results gained during this first assignment step.

3.1 Peak assignment for elemental composition determination

Mass spectra discussed here were usually evaluated with the help of the software package Composer (Sierra Analytics, Modesto, CA, USA, versions 1.0.5 to 1.5.0). The package includes the possibility to internally recalibrate a mass spectrum based either on a predefined mass list or according to homologous series of compounds found within the spectrum. The peak assignment is based on user defined restrictions, e.g. on elemental composition restrictions and a maximum allowed mass accuracy error. Instead of calculating a molecular formula for each given *m/z* by brute force a more elegant approach is followed that takes advantage of the fact that typically broad distributions of homologous series of compounds are present in a crude oil sample as can be seen from an example spectrum shown in Figure 3-1.

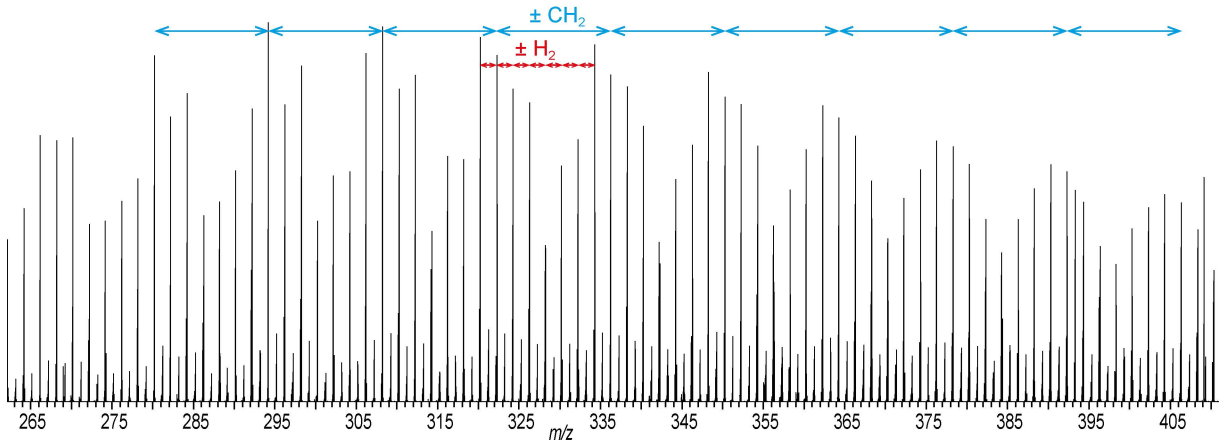

Figure 3-1: Example mass spectrum of a crude oil (positive ESI) showing nested homologous series present. For a given heteroatom content (here N_1) homologous series are present with repeating units of methylene groups (CH_2) and for a given amount of carbon atoms as difference in degree unsaturation (repeating unit H_2).

Briefly, an abundant signal is assigned with an elemental composition and then members of the same homologous series (repeating unit: CH_2) are identified. Afterwards adjacent series differing by the repeating unit H_2 are searched for. This procedure is continued until no more initial matches are found.

Finding starting points for this homologous series search, especially the determination of heteroatom content, is facilitated by conversion of the mass scale into the so-called Kendrick mass scale and determination of the associated Kendrick mass defect.

3.1.1 Kendrick mass scale and Kendrick plots

Visualization of mass spectrometric data from complex mixtures is often difficult to achieve. In the case of natural organic matter or crude oil a whole range of compound classes (i.e. compounds with the same number of heteroatoms per molecule) is usually present in the form of homologous series of certain repeating units. In the case of hydrocarbons and related classes this repeating unit is the methylene group (CH_2). In the case of polyethylene glycols the repeating unit would be C_2H_4O.

An overview of all detected compositions of a whole compound class (e.g. hydrocarbons) is gained when plotting the nominal mass of a species against its mass defect (i.e. the difference between the exact mass and the rounded nominal mass, see equation 2). For convenience, the mass defect is usually given in milli mass units by a multiplication with 1,000.

$$m_{defect} = (m_{nominal} - m_{exact}) \cdot 1000 \qquad (2)$$

When plotting the mass defect against the nominal mass discrete diagonal lines of signals are obtained for related compound series. Figure 3-2 (left side) shows such a plot for homologous series of hydrocarbons (alkanes and olefins) with different degrees of unsaturation (double bond equivalents, DBE). Within a series with increasing mass (i.e. increasing number of CH_2-units) the mass defect decreases. This is due to the mass defect of hydrogen (m_{defect}(H) = -7.825 mDa). Series with higher DBE (loss of 2 hydrogen atoms) are therefore shifted to higher (more positive) mass defect values. While a whole range of compounds with different degrees of unsaturation can be easily plotted into such a diagram, these are hardly readable due to the diagonality of the distinct homologous series.

This can be circumvented by altering the mass scale. The base unit of the mass system is transferred from ^{12}C (exactly 12 mass units) to $^{12}CH_2$ which is now defined with a mass of exactly 14 mass units in the so-called Kendrick mass scale. This is done by a simple multiplication of the real mass by a conversion factor $f(CH_2) = 14 / m(CH_2)$ as seen from equation 3.

$$KM = m_{exact} \cdot f(CH_2) = m_{exact} \cdot \frac{14.00000}{14.01565} \quad (3)$$

Now Kendrick nominal mass (*KNM*) and Kendrick mass defect (*KMD*) can be calculated from this Kendrick mass (*KM*) as in equation 4.

$$KMD = (KNM - KM) \cdot 1000 \quad (4)$$

Because the Kendrick mass of a methylene group is exactly 14, the addition of more methylene groups to a molecule (increasing its degree of alkylation) does not change its Kendrick mass defect. Therefore, a homologous series gives a horizontal line. Differences in the number of heteroatoms or the degree of unsaturation will also produce horizontal lines that are set off by a certain, constant value because of the mass defect of heteroatoms or hydrogens relative to a methylene group (see Figure 3-2, right side).

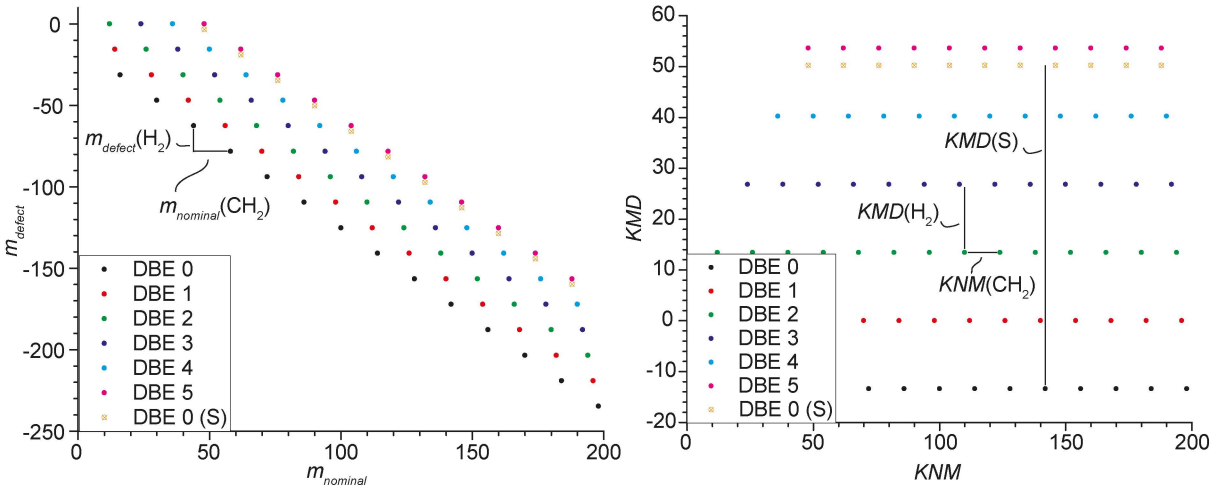

Figure 3-2: Plot of mass defect vs nominal mass (left) and Kendrick mass defect vs Kendrick nominal mass (right) of homologous series of hydrocarbons of different DBE (full dots). The series of hollow dots additionally shows a series of sulfur containing compounds of DBE 0.

As for each number of heteroatoms present the base *KMD* of the saturated species is known (e.g. -13.4 mmu for hydrocarbons, +50.2 mmu for S_1-compounds) and differences in DBE always lead to a difference in *KMD* of 13.4 mmu, the *KMD*-scale can easily be converted to a

DBE-scale. The conversion of the mass scale to the Kendrick scale thus eases up the assignment of a heteroatom class to a mass spectrometric peak and equally the finding of additional members of a given homologous series.

3.1.2 Transformation of assignment results into user-readable data

Simple lists of assigned peaks are not useful for an insightful discussion of the results. The results of a measurement need to be visualized graphically using plots with different degrees of grouping. For a fast and reproducible conversion of the assignment results gained during the first step of data interpretation (data present in XML format) into data that can be easily handled and visualized a portable desktop application – Composer2Excel – was written in C#. It uses an XSLT2.0 processor (Saxon-HE, v9.5.1.3, Saxonica, Berkshire, UK) and self-designed XSLT stylesheets to convert the assignment data into an MS Excel workbook.

Ordering and grouping of the assignments is done hierarchically as follows:

- Each heteroatom class (defined by the number and type of heteroatoms present) is handled individually on a separate worksheet.
- A separate worksheet is used for different types of ions (odd-electron radical ions or even-electron adduct ions).
- Within each worksheet/class assignments are ordered by:
    - Degree of unsaturation (DBE) or hydrogen deficiency (z-number)
    - Amount of carbon (molecular weight).

For each assignment a variety of associated values is computed and stored into separate columns, the most important being:

- Observed *m*/*z*
- Observed signal intensity
- Assigned elemental composition
- Theoretical *m*/*z*
- Degree of unsaturation (DBE, z-number)
- Mass accuracy error (absolute and in ppm)
- Atomic ratios H/C, O/C, N/C and S/C where applicable
- Kendrick mass data (KM, KNM, KMD) and
- Type of isotopologs detected (can be used as means of verification of assignment).

For each class (heteroatom content plus type of ion) a set of commonly needed graphs is automatically generated, including Kendrick plots, DBE distributions (intensity as well as population based) and error distributions (mass accuracy error vs *m*/*z*). An example of such plots is given in Figure 3-3.

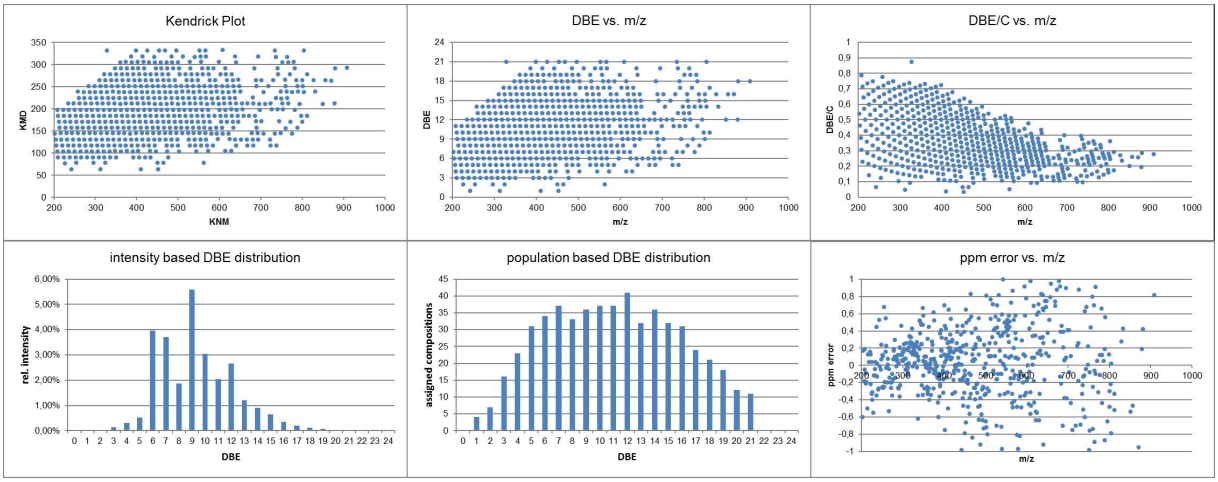

Figure 3-3: Examples for typical plots, automatically generated inside the Excel workbook. Kendrick plots (top left) are translated to DBE vs *m*/*z* plots (top center) and, together with the assigned number of carbon atoms, to DBE/C vs *m*/*z* plots (top right). A grouped overview of a heteroatom class is gained using cumulative DBE distributions either based on signal intensity (bottom left) or number of assigned compositions (bottom center). An assessment of data quality is possible using a mass resolved plot of the mass accuracy error for the assignments (bottom right).

Additionally, an overview sheet is generated that holds some overall data like the total amount of elemental compositions found and sums of signal intensity and population (i.e. amount of detected compositions, irrelevant of signal intensity) for each class, grouped by double bond equivalent. This data is in turn used to generate overview graphs to show class distributions found in the sample as well as a simplified, centroid mass spectrum of all assignments.

For comparison of different samples or measurements an additional stylesheet was implemented that checks the corresponding datasets for common or uniquely present assignments. In comparison mode (see graphical interface on the left side in Figure 3-4) three workbooks are created for each input file:

- One containing the complete results (as above)
- One only containing those assignments that are common between at least two compared datasets and

- One only containing those assignments that are uniquely present in the corresponding dataset.

For data postprocessing inside an Excel workbook a VBA script was written that offers the possibility to correct assignments that are known to be wrong (see Figure 3-4, right side) or to delete assignments considered not trustworthy.

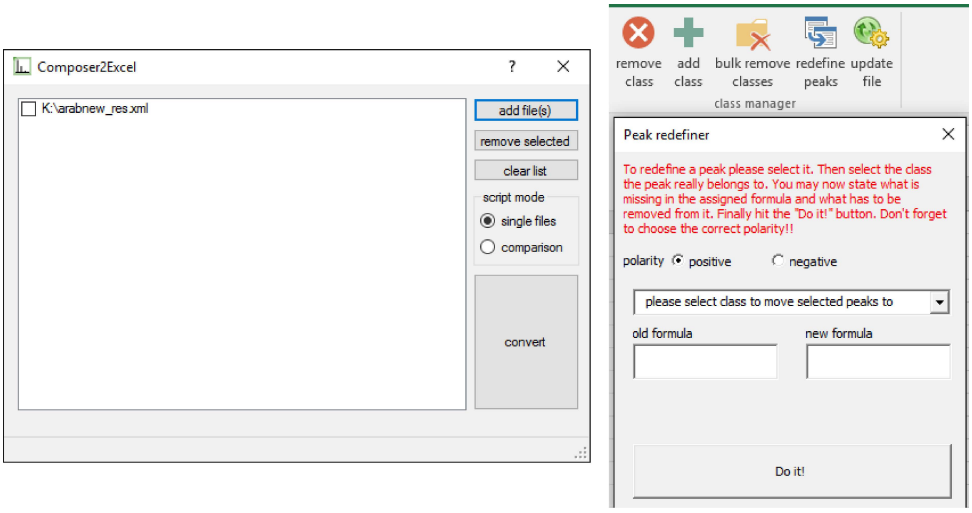

Figure 3-4: Left: User interface of self-written Composer2Excel package. Right: Excel VBA-script for peak reassignment showing the redefine interface.

Tsybin and co-workers have introduced a hexagonal plot for an overview of class distributions.[1] This idea was further elaborated to allow an easy production of such plots in vector (SVG) format. For this an HTML5/JavaScript application was written that automatically creates a plot based on class distribution data given in the aforementioned Excel workbooks. With the current script a direct comparison of up to six individual datasets is possible. Color coding for signal abundance is based on a 330° HSL color coding with selectable scaling (either base 2 or base 10 logarithmic or linear). Figure 3-5 shows an example of such a plot with results from a single measurement. The three axes represent the amount of (freely definable) heteroatoms per molecule with pure hydrocarbons in the center. Each addition of a set heteroatom (here N, O and S) moves the representing hexagon of the class by one unit along the corresponding axis. Each hexagon is (based on data input) automatically split into a maximum of six subunits, each representing a distinct dataset. These might include results from different measurements and/or, as shown here, different types of ions detected, e.g. radical ions (right half) or protonated molecules (left half).

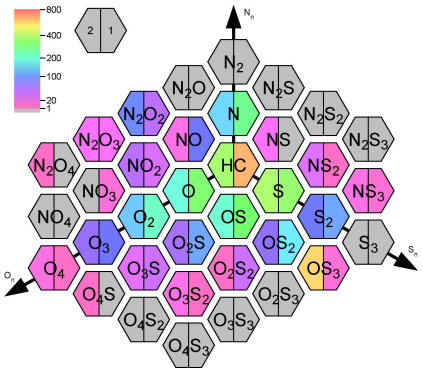

Figure 3-5: Hexagonal representation of class distribution developed from [1]. Each hexagonal box represents one heteroatom class with pure hydrocarbons (HC) at the center. Each addition of one heteroatom to the molecular formula shifts the corresponding hexagon one unit along the respective axis. Each hexagon can be split into up to six slices, thus enabling the easy comparison of different measurements or, as in this case different ion types. Here the right half (1) represents radical cations, while the left half (2) represents protonated molecules (assigned in the same measurement). Color coding of the boxes represents the overall signal intensity or, here, the amount of assigned compositions.

3.1.3 Database for storage and visualization of 3-dimensional data

A major problem during the present studies was that at this time no software package was available that can perform the steps described in the previous sections for 3-dimensional, i.e. time-resolved, data. The procedure described earlier is optimized on the handling of one single spectrum per measurement (which may well be an averaged spectrum, summed over several hundred distinct scans). Main topic of this work, however, was the hyphenation of liquid chromatography and ion mobility to high resolving mass spectrometry. Thus, handling of time-resolved data is necessary.

As a meantime solution to this problem an intermediate way was used. Time-resolved data from chromatographic runs were interpreted in bins of adequate time scales. For example, mass spectra were averaged over the course of one minute. In case of ion mobility separations several mass spectra were recorded and averaged using distinct CV settings of a predefined spacing. This reduction in retention time or CV resolution was necessary as all of these bins needed to be analyzed and interpreted individually. Thus, for every separation measurement a still manageable amount of 40-100 single mass spectra ware interpreted as stated above.

In order to recombine the resulting single, standalone datasets and therefore to be able to monitor the fate of single compounds or groups of compounds over the course of the separation a MySQL database was designed to store the resulting data. As a template for the database the same depth of information as present in the aforementioned MS Excel workbooks was used.

Additionally, the database can store detailed data also for isotopolog peaks that is removed for simple Excel workbooks and additional comments, e.g. regarding sample preparation that is not directly available from the assignment results. A feature to store signals that have not been assigned yet, possibly due to too rigid composition restraints, also exists. Figure 3-6 shows a graphical representation of the database. Accompanying PHP scripts were written that allow the filling of the database, data re-evaluation (e.g. (de-)activation of assignments or redefining of assignments known to be wrong. From this database storage queries can be handled that combine results from different single spectra evaluations throughout a chromatographic run to create Excel workbooks that contain time-resolved data either covering all assignments found throughout the entire measurement or selecting distinct compositions or groups to be monitored.

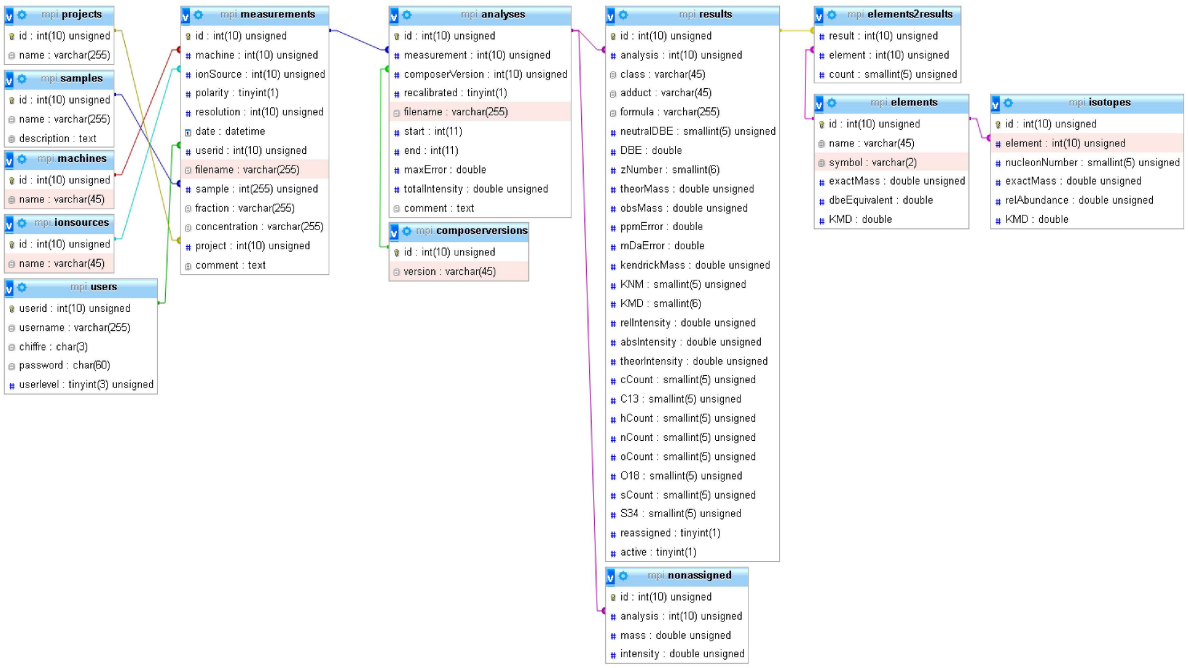

Figure 3-6: Graphical representation of the database structure used for storage of 3-dimensional FTMS data. Table relations are indicated by colored connections.

For a quick graphical overview reconstructed ion chromatograms can be created on the fly that allow the monitoring of either all ions of a specific class (e.g. radical cations of hydrocarbons) split into the distinct DBE series or single DBE series split into single compounds. An example for this is shown in Figure 3-7. Also comparisons across measurements, i.e. regarding different measurements of the same sample, measurements using different ionization techniques or measurements of different samples can be easily compared using adequate database queries, regardless of the original analysis being time-resolved or not.

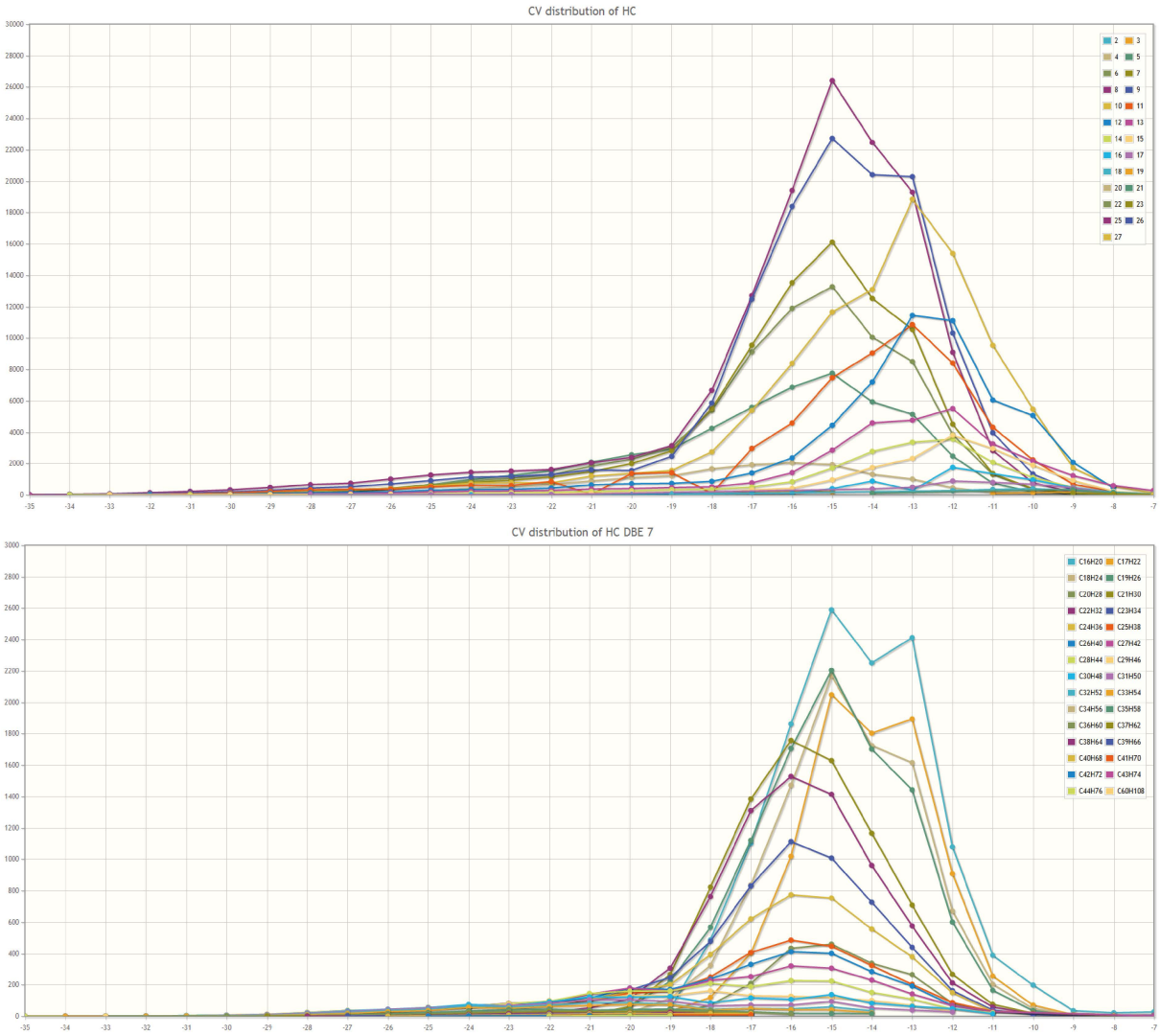

Figure 3-7: Overview graphs for reconstructed ion chromatograms. Data from the distinct analyses are directly drawn from the underlying MySQL database. Shown here is the behavior of hydrocarbons (radical cations) throughout an ion mobility separation (variation of compensation voltage) either as cumulative sums over distinct DBE series (top) or detailed for a given DBE series (bottom).

3.2 References

1. Zhurov, K. O.; Kozhinov, A. N. and Tsybin, Y. O., *Hexagonal Class Representation for Fingerprinting and Facile Comparison of Petroleomic Samples* in: *Anal. Chem.* **2013**, *85*(11), 5311-5315.

4. Mass Spectrometric Coverage of Complex Mixtures: Exploring the Carbon Space of Crude Oil

Adapted with permission from:
Vetere, A. and Schrader, W., *Mass Spectrometric Coverage of Complex Mixtures: Exploring the Carbon Space of Crude Oil* in: *ChemistrySelect* **2017**, *2*, 849-853.

4.1 Abstract

Mass spectrometry is a powerful tool to investigate complex reactions in complex matrices such as crude oils. However, certain requirements have to be met. Apart from a good instrument sensitivity and mass measurement accuracy, especially a certain minimum mass resolving power of above 500,000 at *m/z* 1,000 needs to be reached to resolve critical peak pairs. If the desired parameters are met, a good coverage of the full compositional space or "carbon space" can be achieved to allow a comprehensive picture of the sample at hand. Here, the performance of a newly introduced High-field Fourier transform Orbitrap setup with nominal resolving power of 960,000 at *m/z* 400 is tested against the demands.

4.2 Introduction

With the fast development of sophisticated analytical techniques more complex problems can be approached. Among the most challenging analytical tasks are tracing and monitoring of so called "emerging contaminants" including source identification and elucidation of metabolization and degradation pathways. Thus, the ability to thoroughly analyze complex, widely unknown mixtures and chemical changes within those mixtures is getting into the focus of interest.[1-8] Studies on emerging contaminants commonly cover the anthropogenic groups of healthcare products, pharmaceuticals or pesticides, but other pollutants such as crude oil spills – natural or man-made – are mostly neglected. Studies on emerging contaminants are often focusing on the quantification of certain target analytes before or after attempts of removal but disregard the question of their fate considering naturally occurring weathering or metabolization processes.[9, 10] This characterization of previously unknown contaminants and the monitoring of unknown reactions can only involve a non-targeted analytical approach that requires a wide coverage of the sample's constituents down to a molecular level. Common techniques that provide bulk information such as NMR or IR spectroscopy are therefore only of limited value.[11, 12] The method of choice for the analysis of natural samples is mass spectrometry. Here, apart from sensitivity, mass resolving power ($R = m \cdot \Delta m^{-1}$, with Δm being the full peak width at half maximum height (FWHM)) is a crucial instrument parameter that defines whether isobaric species, exhibiting close-by masses, can be distinguished from each other. Ultra-high resolution mass spectrometry, such as Fourier transform ion cyclotron resonance MS (FT-ICR MS) or Fourier transform Orbitrap MS, with soft ionization techniques have been shown to be a key tool for the investigation of complex systems.[1-3, 13-16]

However, it has been shown that very complex mixtures suffer from effects by the analytes themselves that sabotage their analysis. Such effects include ion suppression, discrimination and poor sensitivity of low concentrated compounds, leading to the necessity to use multiple methods for their characterization.[17-20] Still, one of the major questions addressed here is: How far can one analytical method alone represent the compositional or carbon space?[21]

Is a good coverage of a given complex system obtained, then the method can also be used to monitor changes within this system, i.e. the progression of complex reactions.

In this regard the carbon space coverage of crude oils is a challenging benchmark. Crude oil is arguably the most complex natural mixture in the world, reports estimating more than 10^6 distinct chemical compounds of varying abundance.[14, 22] Although the range of elements is

limited – only carbon, hydrogen, sulfur, oxygen and nitrogen are considerably abundant – a broad structural variety can be observed. Hydrocarbons range from (branched) alkanes and (condensed) naphthenes over mono- and polyaromatic structures up to highly condensed polycyclic aromatic hydrocarbons (PAH) such as benzoperylenes. Additionally, all of these subunits are combined into molecular species that may contain one or more N, O and/or S heteroatoms (for examples of core structures see Figure 4-7 in section 4.6.1). Excluding isomeric variety, inaccessible by mass spectrometry alone, this spans a wide compositional space – or carbon space – to be explored. Within a typically addressed mass range of 200 to 1,200 Da a theoretical maximum of 4,308 hydrocarbon compositions (from fully saturated alkanes to black carbon) can possibly be found. Similar values are calculated for heteroatom containing species (see also Table 4-1 in section 4.6.4). For this study photoionization (APPI) was chosen as a rather unselective technique that covers a broad polarity range of analytes, and is especially suitable for the ionization of non-polar hydrocarbon and sulfur species.[17, 23]

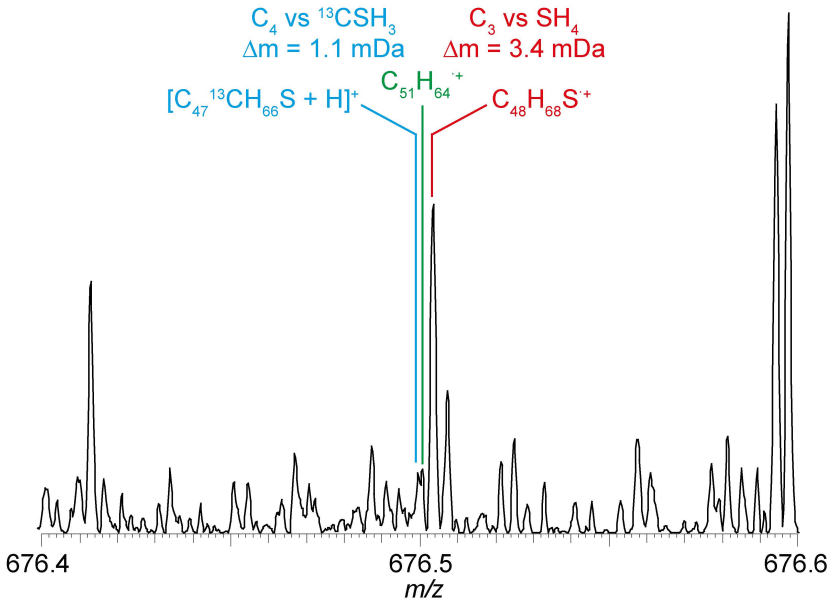

Figure 4-1: Zoom into *m/z* 676.5 of a mass spectrum of crude oil after photoionization. The spectrum was recorded at a transient length of 3.04 s using spectral stitching. Highlighted are examples for important mass splits that occur throughout the spectrum.

The limiting factors of a full elucidation of the entire carbon space by mass spectrometry are instrument sensitivity, mass resolving power and mass measurement error.

Regarding mass resolving power, the requirements to instrumentation are set by the narrowest mass splits expected for the compositional variety given. Most notably a mass split of 3.4 mDa needs to be resolved.[24, 25] This corresponds to the mass difference between C_3 and SH_4 (see

Figure 4-1). Thus, the ability to distinguish between the corresponding peaks can be used as a benchmark for the capabilities of the system. Another mass split is that of 1.1 mDa, corresponding to the difference between C_4 and $^{13}CSH_3$, which is of lesser importance, because it includes the additional isotopic signal. This mass split occurs when using ionization techniques that yield even and odd electron ions (such as APPI) and is mainly relevant for the validation of assignments by the presence of signals from higher isotopologs.

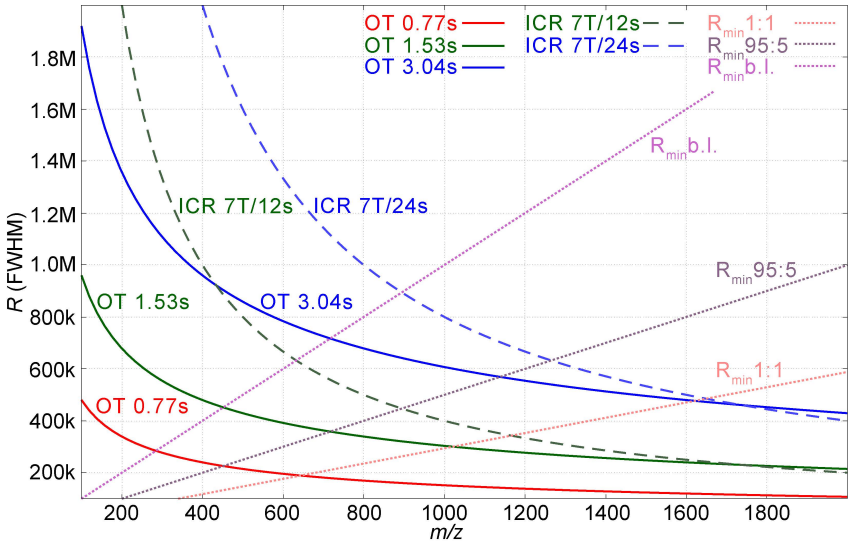

Figure 4-2: Resolving power *R* required to distinguish peaks of different signal ratios that differ by 3.4 mDa (dotted lines, b.l.: baseline resolution). Dashed and solid lines show calculated resolving powers available using benchmarks of a commercial LTQ-FT-ICR MS (Thermo Fisher Scientific, Bremen, Germany) setup (dashed, magnetic field strength/transient length, magnitude mode) and a high-field FT Orbitrap MS at given transient lengths (solid, eFT mode). It has to be noted that approx. a doubling of resolving power can be gained in FT-ICR MS, when absorption mode data processing is being used.

Given a commonly applied mass range of interest of up to 1,200 Da, $R > 400{,}000$ is needed at *m/z* 1,200 to resolve similarly abundant signals (see Figure 4-2, dotted lines). Such high levels of resolving power have so far been reached only by using FT-ICR MS (dashed lines).[24] However, even with this technique long transient lengths (scanning time per single spectrum) of several seconds and/or high magnetic field strengths exceeding 7 T are needed. Both long scanning times and stronger magnets bear the risk of an increasingly poor sensitivity due to loss and dephasing of ion packets or poor ion transmission.[25-28]

An alternate approach is enabled by recent high-field Orbitrap instrumentation. The combination of 2nd generation high-field Orbitrap mass analyzers with enhanced Fourier transform (utilization of absorption mode spectra) and prolonged transient lengths of up to 3.04 s allows a nominal resolving power of $R > 960{,}000$ at *m/z* 400 and above 500,000 at

m/z 1,200 (Figure 4-2, solid lines).[29] The instrument evaluated here allows a mass resolving power beyond the commercially available standard (240,000 at *m/z* 400, transient of 0.768 s) by means of a software patch. Careful choice of an accurately manufactured Orbitrap cell and stable electronic parts allows keeping ion packets stable for up to 3 s, thus leading to a mass resolving power of $R > 960{,}000$ at *m/z* 400. However, a 1.5 s transient leading to a resolving power $R > 480{,}000$ is a commercial option and can be achieved with standard instrumentation.

4.3 Experimental

Heavy crude oil was diluted in toluene to a concentration of 250 $\mu g \cdot ml^{-1}$ and analyzed by mass spectrometry via direct infusion at a flow rate of 10 $\mu L \cdot min^{-1}$. Ionization was performed by atmospheric pressure photoionization (APPI) using a Kr VUV lamp with photon energies of 10.0 and 10.6 eV. The desolvatisation temperature was set to 350 °C. As mass analyzer a research type Orbitrap Elite (Thermo Fisher Scientific, Bremen, Germany) was used that allows an increased transient length of up to 3.04 s. Effects on instrument sensitivity and resolving power were studied by running analyses at the three highest transient time settings (0.768 s, 1.53 s, 3.04 s, resulting in a resolving power of $R > 240{,}000$; $R > 480{,}000$ and $R > 960{,}000$ (FWHM at *m/z* 400), respectively). Additionally, analyses were performed either in full scan mode with $200 \leq m/z \leq 1200$ and by spectral stitching. In the latter case the same mass range was divided into narrow SIM windows of 30 Da with a 5 Da overlap. In each case a total of 250 to 260 scans was recorded in reduced profile mode and summed up before data analysis. Peak assignment was performed using Composer64 (v1.5.0, Sierra Analytics, Modesto, CA, USA) after internal recalibration according to the following constraints: $C_{1\text{-}200}H_{0\text{-}1000}N_{0\text{-}3}O_{0\text{-}4}S_{0\text{-}3}$, $0 \leq DBE \leq 60$. The maximum allowed mass measurement error was ±1.0 ppm, with more than 70 % of the assignments having an accuracy error below 600 ppb as can be seen from Figure 4-3. Additionally, for the 3 s transient about 20,000-25,000 assignments were manually removed from the data set because they did not belong to a larger homologous series, were mostly scattered signals and/or were assigned unreasonable elemental formulas.

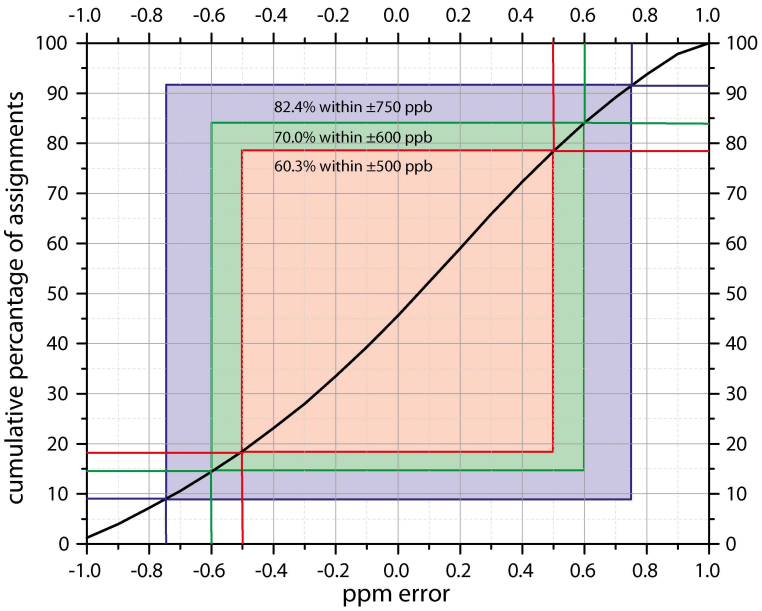

Figure 4-3: Cumulative plot that shows the percentage of assigned signals vs accuracy error. Examples show that 60.3 % of the assignments are obtained within an accuracy error of ±500 ppb (between 18 and 78 %) while 70 % and 82.4 % of the assignments fall within ± 600 ppb and ±750 ppb, respectively.

4.4 Results and Discussion

For the analysis of the crude oil samples presented here, each doubling of transient time and therefore resolving power increased the amount of detected compositions by a factor of 1.2 to 1.8. While using the 0.768 s transient yielded a total of 3,630 assignments, this value increased over 5,472 using the 1.53 s transient up to a total of 6,815 assignments for the 3.04 s transient when measuring in full scan mode (see Figure 4-4). This increase can mostly be attributed to better resolved signals. Signal assignments were allowed up to a mass error of ±1 ppm, with > 70 % of the assignments exhibiting a mass error < 600 ppb.

Given the compositional variety of crude oil a dynamic range of more than 5 orders of magnitude needs to be covered.[14] Mass spectrometers with a trapping analyzer such as the Orbitrap suffer from limited filling rates due to increasing ion-ion interactions. For each scan the maximum number of ions injected into the trap is spread over all ions that are present in the scanned mass range. Therefore, the abundance of lower concentrated ions is statistically limited.

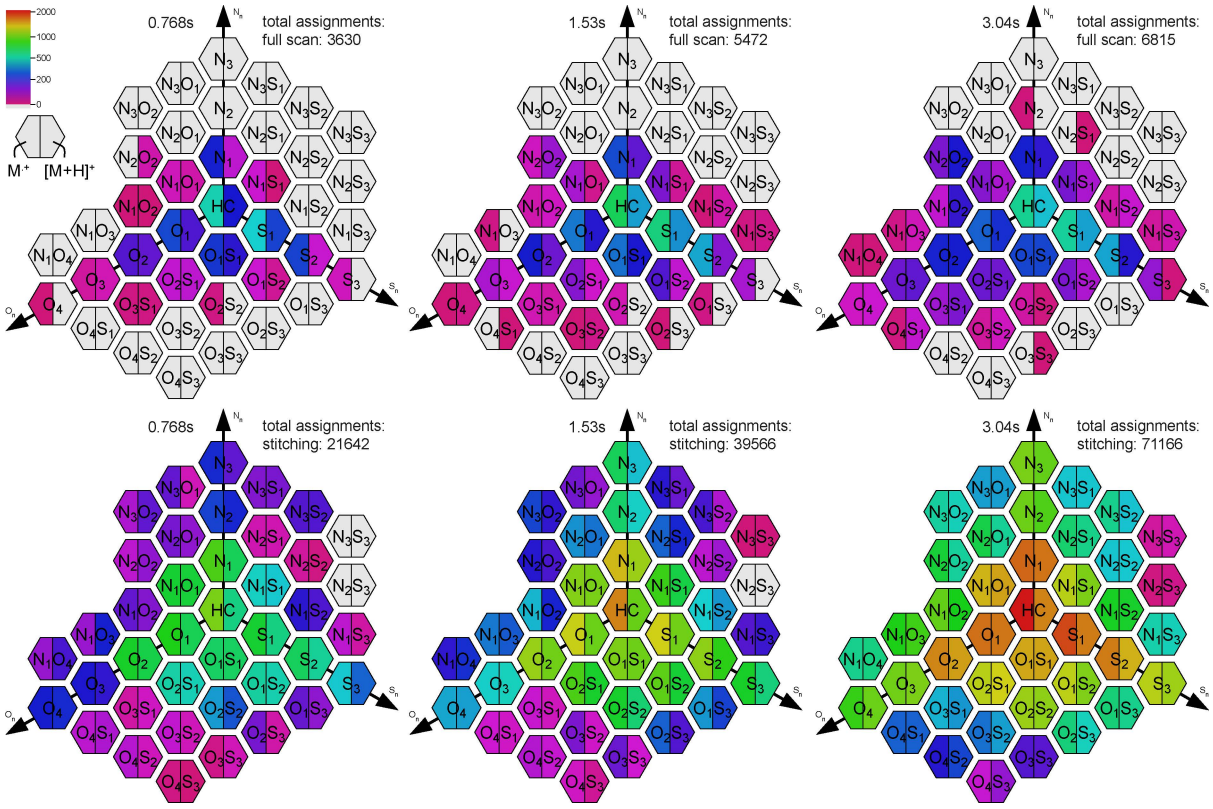

Figure 4-4: Distribution of heteroatom classes found after measurements using different parameters. Hexagon positions on the element axes show amount of that element within the assigned formula. Color filling represents the total amount of compositions assigned to that class. Left half of hexagons depicts population of radical cations, right half corresponds to protonated molecules. Plots from left to right represent increasing transient length/resolving power, top panel for full scan mode, bottom panel for spectral stitching. Total assignments as written at top right corners are sums over all classes and both ion types. Hexagon plots are a further development from work presented by Tsybin and co-workers.[20]

For a good representation of the sample the whole mass range is scanned with often more than 250 scans averaged for statistical depth. The real increase in information depth is achieved when using the spectral stitching mode as can be seen in Figure 4-4.[18] Here the trap is filled only with ions of a smaller scan range of 30 Da. Each set of ions is therefore present at a much higher abundance. Thus, only 5 to 10 scans per window are needed to be averaged to obtain a representative spectrum. After each consecutive 30 Da scan window along the scan range is measured, the whole spectrum is "stitched" together. The stitching results show that the number of assignments is increasing from 21,642 with the lower resolving power up to 71,166 elemental compositions for the highest resolving power setup (3.04 s transient). Overall, analysis times for both scan methods are the same. A more detailed description of the effects is given in section 4.6.2.

Compared to previous studies using FT-ICR MS[18] around double the amount of assignments was achieved for the 0.768 s transient, despite the lower resolution setting (400k vs 240k) and a four-fold lower amount of overall scans (1,000 vs 250) both in full scan and in SIM mode. This leads to the assumption that the sensitivity advantage of the Orbitrap approach is in the region of at least a factor of 5-10. While a similar data depth might still be achievable using FT-ICR MS a much higher number of accumulated scans and therefore analysis time seem to be required.

The benefit of good instrument sensitivity together with increased resolving power is shown in Figure 4-5 around *m/z* 1,070. Standard instrument resolution (0.768 s transient, R > 240,000 at *m/z 400*, blue line) is not sufficient to resolve important mass splits, only enveloped signals are recorded. For a full separation of all underlying peaks the resolving power enabled by the 3.04 s transient (R > 450,000 at *m/z* 1070) is needed. This setting suffices to distinguish the individual signals.

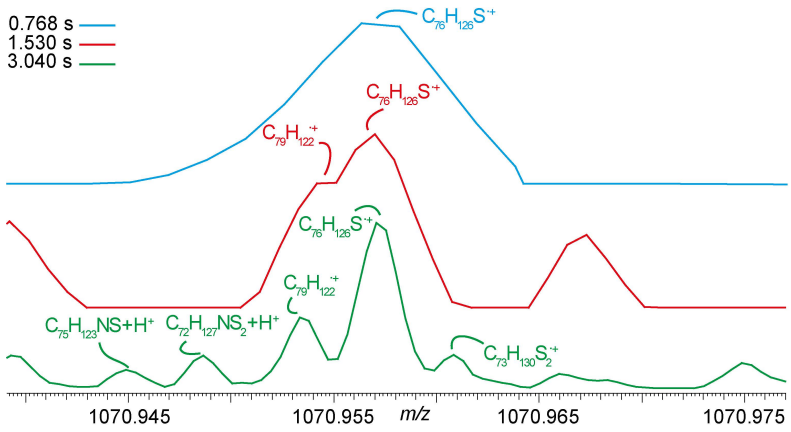

Figure 4-5: Effect of transient length on resolving power shown for *m/z* 1070. Assignments are shown for monoisotopic signals in 3.04 s spectrum (green), for 1.53 s spectrum (red) and for 0.768 s spectrum (blue).

For the full characterization of a complex, unknown mixture a view on all compositions that can theoretically be present is desirable. But how fully can one single analytical method cover the carbon space, still considering that probably not all possible compositions are present in one crude oil sample? To really assess the boundaries of the method the data of the hydrocarbon class obtained from two different stitching scans of 0.768 and 3.04 s are summarized in a Kendrick plot in Figure 4-6.[30]

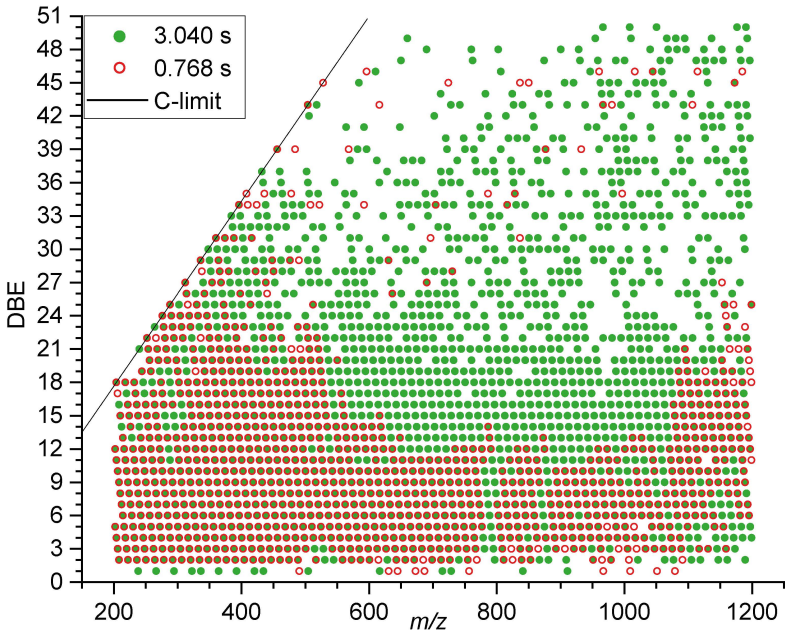

Figure 4-6: Plot of double bond equivalent (DBE) vs *m/z* for compositions of hydrocarbons unambiguously detected with 0.768 s transient (red) and with 3.04 s transient (green). Black line depicts lower mass limit at given DBE.

The red circles representing results from the lower resolving transient show a coverage that is limited especially in the areas where overlapping signals interfere (compare Figure 4-10). The 3.04 s transient with $R > 900{,}000$ at *m/z* 400 (green dots) is capable of separating the important mass splits (see also Figure 4-9) leading to a much better depth of assigned compositions. Within a broad window of DBE (double bond equivalent) values between 4 and 19, 1120 out of 1143 possible hydrocarbon compositions are found, which equals to a 98 % coverage of the compositional space (see Figure 4-10, top). These series can be attributed to (alkylated) PAH ranging from benzene to coronene (see Figure 4-7 for core structures). The coverage in the DBE range below DBE 4 suffers from the fact that the corresponding molecules are hardly ionizable by APPI while the range above 21 is strongly reduced due to lower abundance but also due to absence of the elemental compositions. Overall, out of 3,588 possible compositions within assignment limits (without DBE boundary max. 4,308 compositions are possible) 2,101 hydrocarbon compositions were found as radical cations (see Table 4-1). Additionally, 318 compositions were detected exclusively as protonated molecules. This accounts for a 58.6 % (67.4 %) coverage with a maximum DBE value of 51.

Similarly high coverages are observed for the sulfur containing classes. The sulfur content of this sample, according to elemental analysis, is a little higher than average with a total of 4.6 wt.-%. A relatively high amount of sulfur containing species is therefore expected. For the

S_1-class 1,072 out of 1,128 possible compositions are found for DBE between 6 and 21 (95 %), with the overall coverage being 53.4 %. The coverages of all heteroatom classes are summarized in Table 4-1.

For classes with increased nitrogen and/or oxygen content a low intensity and subsequently a lower coverage is observed. This is in good accordance with results from an elemental analysis of the sample that reveals the nitrogen content to be 0.47 wt.-% and the oxygen content to be < 1 wt.-%. At such low abundances it cannot be expected that all theoretically possible compositions for the corresponding heteroatom classes are found or even present within the mixture. However, the use of complementary ionization techniques, especially ESI in positive and negative mode will enhance the findings of those mostly basic or acidic compounds.

4.5 Conclusion

In summary, our results show that current high-field FT Orbitrap MS provides sufficient mass resolving power and mass measurement accuracy to resolve and assign the critical peak pairs in complex mixtures such as crude oils. By additionally employing the spectral stitching method a sufficient sensitivity is achieved to gain a good coverage of all possible compositions throughout the carbon space. Once this is ensured, the setup can now be used to follow up on unknown, complex reactions like the weathering of oil spills or the investigation of metabolization pathways of the numerous emerging contaminants of interest.

Of course, neither compound class nor structural information is accessible by simple mass spectrometry alone. For more detailed information chromatographic and/or ion mobility separation combined with different ionization techniques and preferably MS^n experiments should be used.[31]

The appendix below discusses the structural variety of compounds in crude oil. The effect of SIM mode analysis on the resulting data and the effect of increased resolving power are shown in detail. Finally, the carbon space coverage achieved, using ultimate resolving power is shown in detail.

4.6 Appendix

4.6.1 Structural variety found in crude oil

Structural motifs of the hydrocarbon backbones found in crude oils are mainly aromatic cores of different sizes, aliphatic, naphthenic rings and branched as well as unbranched alkyl chains. All of these motifs are commonly found to be freely arranged and connected through different sites to build up molecules of varying sizes and degrees of unsaturation. Additionally, one or more heteroatoms of the group oxygen, nitrogen and sulfur can be incorporated into the resulting structures. Thus, usually broad homologous series are found, which exhibit a large isomeric variety. Figure 4-7 shows a group of core structures and motifs commonly found.

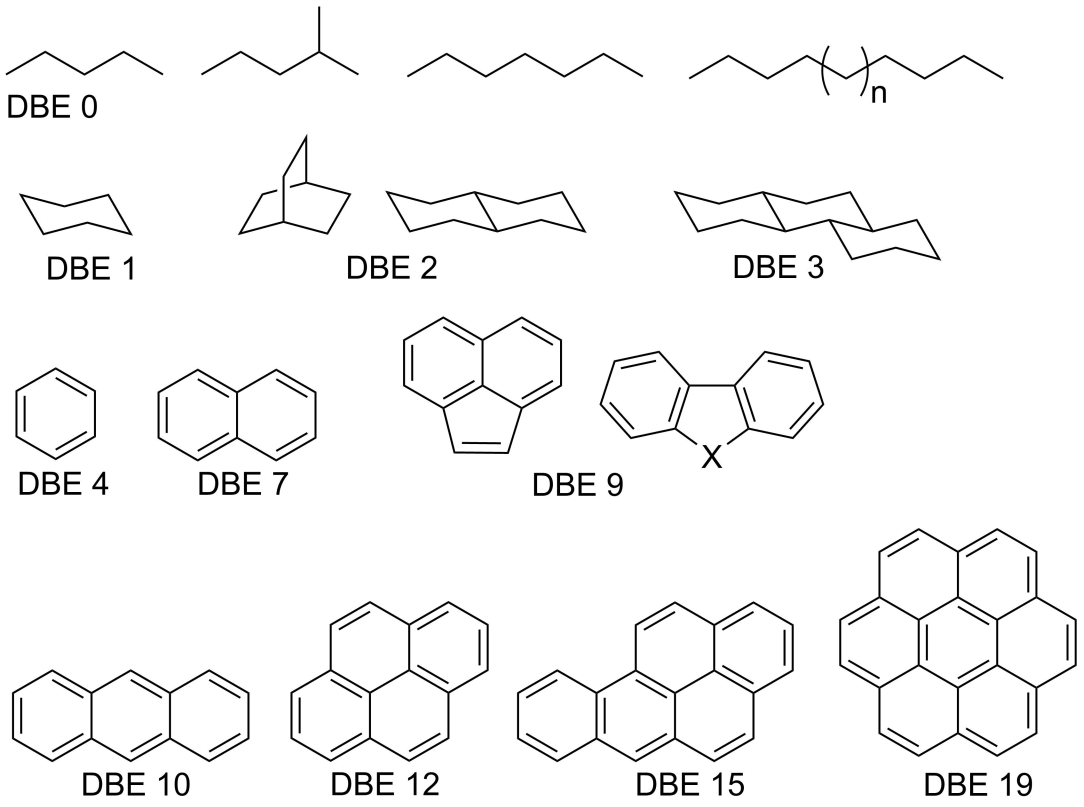

Figure 4-7: Examples for structural motifs found in crude oil.

4.6.2 Effect of spectral stitching on instrument sensitivity

The dynamic range of a single mass spectrum typically spans over 4 to 5 decades. When analyzing complex mixtures, this will arguably not be enough to get a full picture of all present species. A possible solution to this problem is the spectral stitching method. Here, instead of one broad mass range (full scan) a set of small mass windows (single ion monitoring or SIM scans) is used. During this study windows of 30 Da each were used that overlap by 5 Da on

each side. Now, for each of these windows a dynamic range of 4 to 5 decades can be reached. When putting the spectra from the single scan windows together (stitching) now a much richer total spectrum is gained, although the number of individual scans for each window is relatively low. Here a total number of 250 to 260 single scans was recorded, thus, when using spectral stitching, for each mass range only an average of 7 scans is used as opposed to a total of 250 scans over the whole mass range in case of full range scanning. From Figure 4-8 it can be seen that especially in higher mass regions, where overall intensity is quite low, a dramatic increase in signal can be obtained. The increase in signal – and therefore sensitivity - finally leads to a plus of assigned peaks, i.e. detected compositions, by a factor of 6 to 10 (see Figure 4-4).

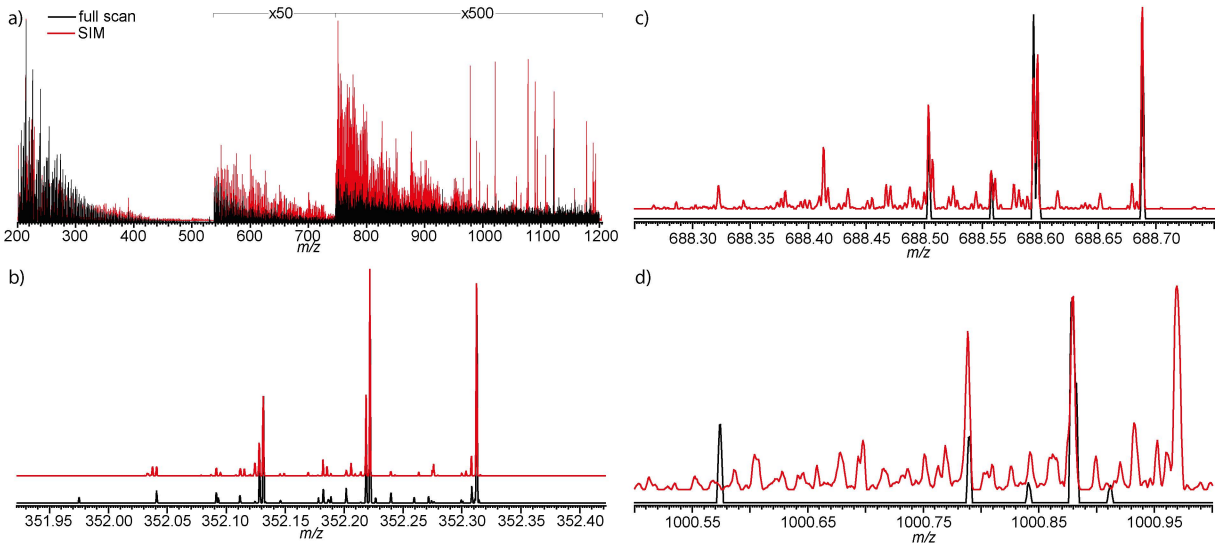

Figure 4-8: Comparison of spectra obtained in full scan mode (black lines) and by spectral stitching (SIM, red lines). Transient length for these spectra was set to 1.53 s (R = 480,000, FWHM at m/z 400). a) Entire mass range, with intensity scaled regions, b-d) Zooms into three different mass regions are shown, SIM mode spectra are set off from x-axis to help visualization.

4.6.3 Effect of high resolving power on the simultaneous detection of adjacent heteroatom classes

Figure 4-9 shows a Kendrick plot of the heteroatom classes of hydrocarbons (HC), S_1-, S_2- and S_3-compounds as assigned from the corresponding spectrum. As can be seen from the highlighted region in the figure, the problematic, adjacent heteroatom classes are easily detected beneath each other up until 1,200 Da when using the 3.04 s transient setting. Missing assignments here are mostly because of low abundances of the respective ions.

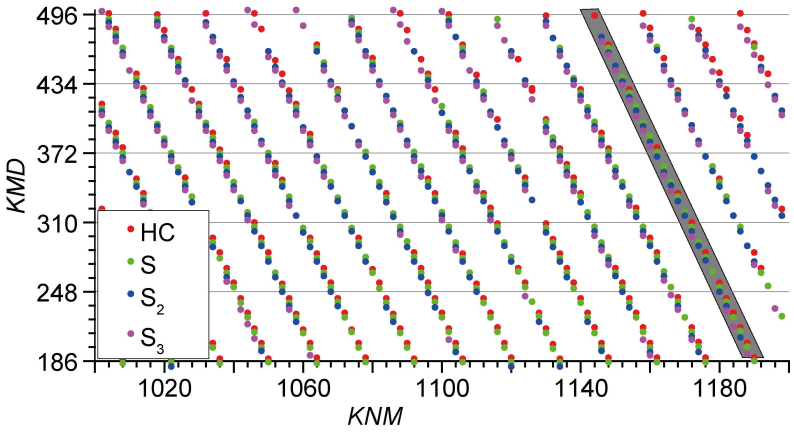

Figure 4-9: Zoom into a Kendrick plot of signals unambiguously assigned to radical cations of hydrocarbons (HC class, red), S_1-compounds (green), S_2-compounds (blue) and S_3-compounds (magenta) after measurement at highest resolving power (3.04 s transient) using spectral stitching.

When comparing the results obtained using the highest available resolving power (transient length of 3.04 s, green dots in Figure 4-10, left side) and an insufficient resolving power of $R = 240{,}000$ (FWHM at m/z 400, transient length of 0.768 s, red circles in Figure 4-10) a significant increase in assigned signals becomes apparent. The effect of increased resolving power is particularly pronounced above m/z 500. With the short transient (0.768 s) only a narrow portion of the neighboring heteroatom classes DBE distribution can be unambiguously detected. Increased resolving power allows the distinction of close-by peaks over the whole mass range. Thus, also less abundant DBE series can be detected along with compounds from neighboring classes. As a result, a broad range of DBE series is almost fully detected. The right side panels of Figure 4-10 show the amount of detected compositions for the single heteroatom classes by DBE. The solid line in each panel indicates the theoretical maximum of detected compositions within the recorded mass range.

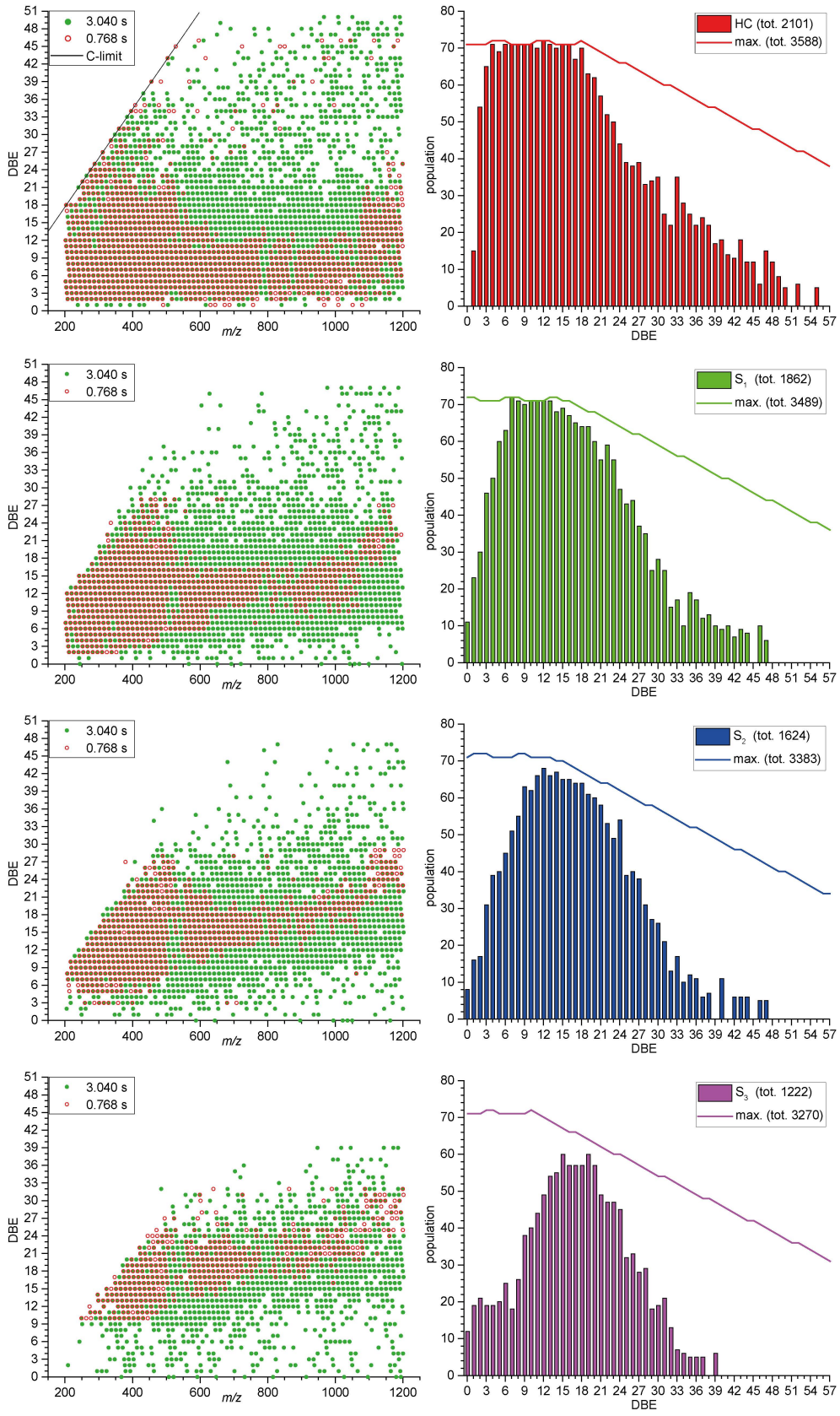

Figure 4-10: Carbon space coverage for selected heteroatom classes. Left: Plot of double bond equivalent (DBE) vs *m/z* for compositions unambiguously detected at 0.768 s transient (red) and at 3.04 s transient (green). Right: Plot of population (number of assigned compositions) vs DBE obtained from the 3.04 s transient. The lines depict the theoretical maxima within the scanned mass range.

4.6.4 Carbon space coverage for detected heteroatom classes

Table 4-1: Amount of theoretically possible and detected compositions (as radical cations) throughout selected heteroatom classes within the mass range covered. Values in brackets additionally include compositions only detected as protonated molecules. Data acquired from 3.04 s transient in SIM mode.

heteroatom class	max. num. of compositions	detected compositions	coverage [%]
HC	3588 / 4308[a]	2101 (2419)	58.6 (67.4)
S_1	3489 / 4119[a]	1862 (2140)	53.4 (61.3)
S_2	3383 / 3928[a]	1624 (1910)	48.0 (54.5)
S_3	3270 / 3737[a]	1222 (1580)	37.4 (48.3)
O_1	3539 / 4214[a]	1672 (2128)	47.2 (60.1)
O_2	3490 / 4120[a]	1581 (1984)	45.3 (56.8)
O_3	3438 / 4024[a]	1005 (1469)	29.3 (42.7)
O_4	3384 / 3929[a]	850 (1400)	25.1 (41.4)
N_1	3545 / 4225[a]	1708 (2134)	48.2 (60.2)
N_2	3501 / 4142[a]	1002 (1472)	28.6 (42.0)
N_3	3456 / 4059[a]	1035 (1485)	29.9 (43.0)
N_1S_1	3444 / 4036[a]	1228 (1541)	35.7 (44.7)
N_1S_2	3335 / 3845[a]	753 (1149)	22.6 (34.4)
N_1S_3	3219 / 3653[a]	495 (809)	15.4 (25.1)
N_2S_1	3397 / 3952[a]	602 (1002)	17.7 (29.5)
N_2S_2	3286 / 3762[a]	421 (763)	12.8 (23.2)
N_2S_3	3167 / 3570[a]	7 (22)	0.2 (0.7)
N_3S_1	3349 / 3869[a]	421 (763)	12.6 (22.8)
N_3S_2	3236 / 3679[a]	542 (842)	16.7 (26.0)
N_3S_3	3114 / 3487[a]	25 (63)	0.8 (2.0)
N_1O_1	3495 / 4131[a]	1406 (1846)	40.2 (52.8)
N_1O_2	3444 / 4036[a]	974 (1306)	28.3 (37.9)
N_1O_3	3391 / 3941[a]	793 (1314)	23.4 (38.7)
N_1O_4	3336 / 3846[a]	538 (918)	16.1 (27.5)
N_2O_1	3450 / 4048[a]	675 (1014)	19.6 (29.4)
N_2O_2	3397 / 3952[a]	709 (1047)	20.9 (30.8)
N_3O_1	3403 / 3964[a]	363 (655)	10.7 (19.2)
N_3O_2	3349 / 3869[a]	511 (881)	15.3 (26.3)
O_1S_1	3438 / 4024[a]	1445 (1781)	42.0 (51.8)
O_1S_2	3328 / 3833[a]	1238 (1531)	37.2 (46.0)
O_1S_3	3211 / 3641[a]	585 (868)	18.2 (27.0)
O_2S_1	3384 / 3929[a]	1235 (1621)	36.5 (47.9)
O_2S_2	3271 / 3737[a]	1136 (1449)	34.7 (44.3)
O_2S_3	3152 / 3547[a]	578 (836)	18.3 (26.5)
O_3S_1	3328 / 3833[a]	393 (595)	11.8 (17.9)
O_3S_2	3211 / 3641[a]	305 (590)	9.5 (18.4)
O_3S_3	3091 / 3452[a]	148 (252)	4.8 (8.2)
O_4S_1	3271 / 3737[a]	286 (487)	8.7 (14.9)
O_4S_2	3152 / 3547[a]	192 (398)	6.1 (12.6)
O_4S_3	3029 / 3357[a]	61 (148)	2.0 (4.9)
$N_1O_1S_1$	3391 / 3941[a]	988 (1463)	29.1 (43.1)
$N_2O_1S_1$	3343 / 3858[a]	537 (871)	16.1 (26.1)
$N_1O_2S_1$	3335 / 3845[a]	988 (1445)	29.6 (43.3)
$N_1O_1S_2$	3279 / 3750[a]	397 (762)	12.1 (23.2)
total	**147109 / 169117[a]**	**36655 (51153)**	**24.9 (34.8)**

[a]: Theoretical maximum of compositions without DBE limitation.

4.7 References

1. Dier, T. K. F.; Egele, K.; Fossog, V.; Hempelmann, R. and Volmer, D. A., *Enhanced Mass Defect Filtering To Simplify and Classify Complex Mixtures of Lignin Degradation Products* in: *Anal. Chem.* **2016**, *88*(2), 1328-1335.

2. Bingol, K.; Bruschweiler-Li, L.; Yu, C.; Somogyi, A.; Zhang, F. and Brüschweiler, R., *Metabolomics Beyond Spectroscopic Databases: A Combined MS/NMR Strategy for the Rapid Identification of New Metabolites in Complex Mixtures* in: *Anal. Chem.* **2015**, *87*(7), 3864-3870.

3. Fischer, K.; Fries, E.; Körner, W.; Schmalz, C. and Zwiener, C., *New developments in the trace analysis of organic water pollutants* in: *Appl. Microbiol. Biotechnol.* **2012**, *94*(1), 11-28.

4. Helmholz, H.; Lassen, S.; Ruhnau, C.; Pröfrock, D.; Erbslöh, H.-B. and Prange, A., *Investigation on the proteome response of transplanted blue mussel (Mytilus sp.) during a long term exposure experiment at differently impacted field stations in the German Bight (North Sea)* in: *Mar. Environ. Res.* **2015**, *110*, 69-80.

5. Scheurer, M.; Godejohann, M.; Wick, A.; Happel, O.; Ternes, T. A.; Brauch, H.-J.; Ruck, W. K. L. and Lange, F. T., *Structural elucidation of main ozonation products of the artificial sweeteners cyclamate and acesulfame* in: *Environ. Sci. Pollut. Res.* **2011**, *19*(4), 1107-1118.

6. Xiang, Y.; Fang, J. and Shang, C., *Kinetics and pathways of ibuprofen degradation by the UV/chlorine advanced oxidation process* in: *Water Res.* **2016**, *90*, 301-308.

7. Wu, X.; Fu, Q. and Gan, J., *Metabolism of pharmaceutical and personal care products by carrot cell cultures* in: *Environ. Pollut.* **2016**, *211*, 141-147.

8. Owen, B. C.; Haupert, L. J.; Jarrell, T. M.; Marcum, C. L.; Parsell, T. H.; Abu-Omar, M. M.; Bozell, J. J.; Black, S. K. and Kenttämaa, H. I., *High-Performance Liquid Chromatography/High-Resolution Multiple Stage Tandem Mass Spectrometry Using Negative-Ion-Mode Hydroxide-Doped Electrospray Ionization for the Characterization of Lignin Degradation Products* in: *Anal. Chem.* **2012**, *84*(14), 6000-6007.

9. Philippe, K. K.; Timmers, R.; van Grieken, R. and Marugan, J., *Photocatalytic Disinfection and Removal of Emerging Pollutants from Effluents of Biological Wastewater Treatments, Using a Newly Developed Large-Scale Solar Simulator* in: *Ind. Eng. Chem. Res.* **2016**, *55*(11), 2952-2958.

10. Gabarrón, S.; Gernjak, W.; Valero, F.; Barceló, A.; Petrovic, M. and Rodríguez-Roda, I., *Evaluation of emerging contaminants in a drinking water treatment plant using electrodialysis reversal technology* in: *J. Hazard. Mater.* **2016**, *309*, 192-201.

11. Zhu, X.; Xue, Y.; Li, X.; Zhang, Z.; Sun, W.; Ashida, R.; Miura, K. and Yao, H., *Mechanism study of degradative solvent extraction of biomass* in: *Fuel* **2016**, *165*, 10-18.

12. Gouilleux, B.; Charrier, B.; Danieli, E.; Dumez, J.-N.; Akoka, S.; Felpin, F.-X.; Rodriguez-Zubiri, M. and Giraudeau, P., *Real-time reaction monitoring by ultrafast 2D NMR on a benchtop spectrometer* in: *Analyst* **2015**, *140*(23), 7854-7858.

13. Knolhoff, A. M.; Callahan, J. H. and Croley, T. R., *Mass Accuracy and Isotopic Abundance Measurements for HR-MS Instrumentation: Capabilities for Non-Targeted Analyses* in: *J. Am. Soc. Mass. Spectrom.* **2014**, *25*(7), 1285-1294.

14. Marshall, A. G. and Rodgers, R. P., *Petroleomics: The Next Grand Challenge for Chemical Analysis* in: *Acc. Chem. Res.* **2004**, *37*(1), 53-59.

15. Santos, J. M.; dos Santos, L. O.; Silva, F. F.; Eberlin, M. N. and Wisniewski, A., Jr., *Comprehensive Characterization of Second-Generation Biofuel from Invasive Freshwater Plants by FT-ICR MS* in: *BioEnergy Res.* **2015**, *8*(4), 1938-1945.

16. Herzsprung, P.; Hertkorn, N.; von Tuempling, W.; Harir, M.; Friese, K. and Schmitt-Kopplin, P., *Molecular formula assignment for dissolved organic matter (DOM) using high-field FT-ICR-MS: chemical perspective and validation of sulphur-rich organic components (CHOS) in pit lake samples* in: *Anal. Bioanal. Chem.* **2016**, *408*(10), 2461-2469.

17. Gaspar, A.; Zellermann, E.; Lababidi, S.; Reece, J. and Schrader, W., *Impact of different ionization methods on the molecular assignments of asphaltenes by FT-ICR mass spectrometry* in: *Anal. Chem.* **2012**, *84*(12), 5257-5267.

18. Gaspar, A. and Schrader, W., *Expanding the data depth for the analysis of complex crude oil samples by Fourier transform ion cyclotron resonance mass spectrometry using the spectral stitching method* in: *Rapid Commun. Mass Spectrom.* **2012**, *26*(9), 1047-1052.

19. Schmitt-Kopplin, P.; Englmann, M.; Rossello-Mora, R.; Schiewek, R.; Brockmann, K. J.; Benter, T. and Schmitz, O. J., *Combining chip-ESI with APLI (cESILI) as a multimode source for analysis of complex mixtures with ultrahigh-resolution mass spectrometry* in: *Anal. Bioanal. Chem.* **2008**, *391*(8), 2803-2809.

20. Zhurov, K. O.; Kozhinov, A. N. and Tsybin, Y. O., *Hexagonal Class Representation for Fingerprinting and Facile Comparison of Petroleomic Samples* in: *Anal. Chem.* **2013**, *85*(11), 5311-5315.

21. Hertkorn, N.; Frommberger, M.; Witt, M.; Koch, B. P.; Schmitt-Kopplin, P. and Perdue, E. M., *Natural organic matter and the event horizon of mass spectrometry* in: *Anal. Chem.* **2008**, *80*(23), 8908-8919.

22. Panda, S. K.; Andersson, J. T. and Schrader, W., *Mass-spectrometric analysis of complex volatile and nonvolatile crude oil components: a challenge* in: *Anal. Bioanal. Chem.* **2007**, *389*(5), 1329-1339.

23. Panda, S. K.; Brockmann, K.-J.; Benter, T. and Schrader, W., *Atmospheric pressure laser ionization (APLI) coupled with Fourier transform ion cyclotron resonance mass spectrometry applied to petroleum samples analysis: comparison with electrospray ionization and atmospheric pressure photoionization methods* in: *Rapid Commun. Mass Spectrom.* **2011**, *25*(16), 2317-2326.

24. Marshall, A. G. and Rodgers, R. P., *Petroleomics: Chemistry of the underworld* in: *Proc. Natl. Acad. Sci. U. S. A.* **2008**, *105*(47), 18090-18095.

25. Zhurov, K. O.; Kozhinov, A. N. and Tsybin, Y. O., *Evaluation of High-Field Orbitrap Fourier Transform Mass Spectrometer for Petroleomics* in: *Energy Fuels* **2013**, *27*(6), 2974-2983.

26. Nikolaev, E. N., *Some notes about FT ICR mass spectrometry* in: *Int. J. Mass spectrom.* **2015**, *377*, 421-431.

27. Kaiser, N. K.; Quinn, J. P.; Blakney, G. T.; Hendrickson, C. L. and Marshall, A. G., *A Novel 9.4 Tesla FTICR Mass Spectrometer with Improved Sensitivity, Mass Resolution, and Mass Range* in: *J. Am. Soc. Mass. Spectrom.* **2011**, *22*(8), 1343-1351.

28. Gordon, E. F. and Muddiman, D. C., *Impact of ion cloud densities on the measurement of relative ion abundances in Fourier transform ion cyclotron resonance mass spectrometry: experimental observations of coulombically induced cyclotron radius perturbations and ion cloud dephasing rates* in: *J. Mass Spectrom.* **2001**, *36*(2), 195-203.

29. Denisov, E.; Damoc, E.; Lange, O. and Makarov, A., *Orbitrap mass spectrometry with resolving powers above 1,000,000* in: *Int. J. Mass spectrom.* **2012**, *325–327*, 80-85.

30. Kendrick, E., *A Mass Scale Based on CH2 = 14.0000 for High Resolution Mass Spectrometry of Organic Compounds* in: *Anal. Chem.* **1963**, *35*(13), 2146-2154.

31. Vetere, A. and Schrader, W., *1- and 2-photon ionization for online FAIMS-FTMS coupling allows new insights into the constitution of crude oils* in: *Anal. Chem.* **2015**, *87*(17), 8874-8879.

5. 1- and 2-photon ionization for online FAIMS-FTMS coupling allows new insights into the constitution of crude oils

Adapted with permission from:
Vetere, A. and Schrader, W., *1- and 2-photon ionization for online FAIMS-FTMS coupling allows new insights into the constitution of crude oils* in: *Anal. Chem.* **2015**, *87*(17), 8874-8879.

5.1 Abstract

Photoionization techniques (APPI and APLI) are important for the mass spectrometric analysis of crude oils, given the mainly unpolar character of the sample. Ultrahigh resolving Fourier transform mass spectrometry (FTMS) allows distinguishing between most isobaric compounds as well as to unambiguously determine the elemental compositions of the detected ions. Nevertheless, the complexity of crude oil makes its thorough analysis a difficult task. Besides discriminating effects that can be avoided and depth of information that can be gained by simplification of the sample prior to the MS analysis, the presence of numerous isomeric compounds limits the amount of information that can be gained by mass spectrometry alone. Ion mobility spectrometry (IMS) has been shown to be a valuable tool for isomer separation and has also been employed for the analysis of crude oils using IMS-TOF MS. The application of an online FAIMS-FTMS coupling after photoionization for the analysis of crude oils is shown here. With this setup, the complementarity of data obtained from both APPI and APLI ionization is demonstrated. Online separation and individual detection of different hydrocarbon isomers is achieved.

5.2 Introduction

Crude oils and associated products probably are – except for wood and stone – the natural products with the longest history in human technology.[1, 2] Ever since its beginning industrial exploitation in the 19th century analytical chemists have been striving for the thorough analysis of this most complex mixture of compounds. A detailed knowledge of the composition of crude oils is especially important for the refining industries as it would allow for the optimization of various refining processes like hydrodesulfurization or cracking procedures. Thus, an increased efficiency should sharply increase the economic value of the product. Compositional knowledge is equally important to consider the environmental effects of an exposure as well as for developing tailored methods for the remediation of oils that were released to the environment.[3]

To date most analytical methods that are routinely used during processing are only addressing the bulk features of the raw material like e.g. the API gravity, distillation profile or an interpretation of IR and/or NMR spectra of the whole material. This kind of information, however, cannot yield any knowledge on a molecular level, i.e. regarding the specific compounds actually present in the sample. Among others, chromatographic techniques, especially GC-MS and GC×GC-MS are used for analysis of the lower weight, volatile portion of a crude oil. These techniques are frequently employed in the assessment of a crude oils maturity or for source identification based on biomarker ratios.[4, 5] Headspace mass spectrometry was recently applied for oil spill identification.[6]

Fourier transform based ultrahigh resolution mass spectrometry (FTMS) as provided by Fourier transform ion cyclotron resonance mass spectrometry (FT-ICR MS), given its unmatched mass resolving power and high accuracy, allows the unambiguous determination of the molecular formulae of the distinct compounds present in complex crude oil mixtures.[7] However, due to the complexity of crude oils, discrimination effects can hardly be avoided. It has been shown that sample simplification prior to the mass spectrometric analysis is a key factor for the achievement of detailed information.[8] On the other hand a broad range from unpolar hydrocarbons to highly polar species has to be covered. To address this problem a set of different ionization techniques needs to be employed.[9, 10]

As for all mass spectrometric techniques also ultrahigh resolution MS cannot differentiate all individual compounds present in crude oils, especially the enormous variety of isomeric compounds cannot be addressed by using mass spectrometry alone. Normal-phase HPLC-MS

has been shown to be able to distinguish classes of isomeric compounds that differ largely in polarity, e.g. *N*-basic and *N*-alkylated nitrogen heterocycles.[11] A separation of chemically more similar isomers is on the other hand very difficult by traditional normal-phase HPLC. Online coupling of ion mobility spectrometry (IMS) to FTMS can be used to introduce a shape/size selective separation of compounds, i.e. possibly a separation of isomers, into the workflow without the need for any further sample preparation or the utilization of different instrumental setups.[12, 13]

While a variety of modern time-of-flight (TOF) MS instruments now incorporate an IMS module (mainly "drift tube" (DT) or "travelling wave" (TW) IMS) the mass resolving power of this instrumentation is usually not high enough to resolve important isobaric functionalities found in crude oil, e.g. C_3 vs SH_4 ($\Delta m = 3.4$ mDa). To distinguish between those at a mass range of around 500 Da a mass resolution of $R > 150{,}000$ (FWHM) is needed. This can be easily achieved by FT-ICR MS or modern FT Orbitrap technology, while even highly resolving TOF MS instruments that allow for a mass resolution of approx. 100,000 cannot separate such isobars above 300 Da.[14] Previous studies in crude oil research tried to circumvent the problem by combining data from analyses using IMS-TOF MS and FT-ICR MS both after electrospray ionization.[15-18] Due to the different characteristics of the MS analyzers the comparability of both datasets is, however, limited.

More straightforward results can be expected from a direct IMS-FTMS coupling. To match the time domains of IMS and FTMS (ms vs s) differential IMS methods, such as DIMS[19] or FAIMS[20] (high-field asymmetric waveform ion mobility spectrometry), are the method of choice. Here the mobility separation of ions occurs orthogonally to the flight path of the analytes, which enables a uniform stream of ions into the following mass spectrometer. The general usability of FAIMS has already been shown elsewhere using electrospray ionization.[12] While polar species are easily addressed by this setup, the majority of compounds present in crude oils is made up of unpolar hydrocarbons and naphthenes and low to medium polar polyaromatic heterocycles such as dibenzothiophenes or dibenzofurans. Such analytes are effectively ionized using photoionization techniques such as APPI (1-photon VUV ionization) or APLI (2-photon ionization using laser radiation).[9] APLI ionization is most efficient for unpolar hydrocarbons with extended, condensed aromatic systems and can as such be regarded as a very selective ionization technique.[21, 22] Compared to APPI ionization APLI is of advantage especially for the ionization of compounds with a high degree of unsaturation and/or aromaticity.[9]

Photoionization has been used for the analysis of chemical warfare agents with standalone ion mobility spectrometers, mainly as a non-harmful and "soft" replacement for the radioactive ^{63}Ni source.[23, 24] APPI-IMS-MS has been used by Laakia and co-workers for the characterization of pyridines, naphthols and amines using a triple-quadrupole mass spectrometer.[25, 26] APPI-IMS-TOF MS was used by Fernández-Lima and co-workers for the analysis of PAH in soil and LDI-IMS-TOF MS by Russell and co-workers for the analysis of crude oil.[18, 27] Yet, to date no studies are published that take advantage of an APPI/APLI-IMS-FTMS setup.

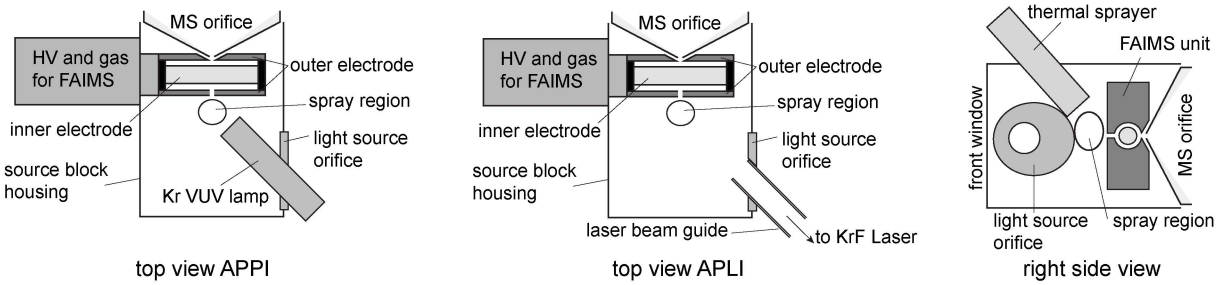

Figure 5-1. Schematic view of the experimental setup regarding the source region; left and center panel show a section through the source block from a top view with mounted FAIMS unit. High voltage and carrier gas leads are coming from the left hand side and connect the system to the waveform generator (not shown). The newly introduced light source orifice on the right side either fits a Kr VUV lamp for APPI or a beam guide for the KrF Laser (APLI). The right panel shows a section through the source block, looking from the right hand side. The positions of the light source orifice and the thermal sprayer are indicated.

Commercial availability of IMS modules that support photoionization on FTMS instruments is, however, limited. Especially the FAIMS unit used in our lab only allows for electrospray or atmospheric pressure chemical ionization in the default setup. Therefore, a new source block had to be designed to fit the light source into the system. Figure 5-1 shows the resulting setup with mounted light sources.

5.3 Experimental

5.3.1 Sample preparation

A heavy crude oil from a North American source was diluted in toluene to a final concentration of 500 $\mu g \cdot mL^{-1}$ and then analyzed without further treatment.

5.3.2 Instruments and methods

Mass spectra were recorded on a research-type Orbitrap Elite mass spectrometer (Thermo Fisher Scientific, Bremen, Germany) equipped with a FAIMS unit (Thermo Fisher Scientific,

San Jose, CA, USA). To fit the light sources into the system the default source block was replaced by a homemade design. Photoionization was performed by a Kr VUV lamp at 10.0 and 10.6 eV for APPI (Syagen Technologies, Tustin, CA, USA) or a KrF-Excimer Laser at 248 nm/5.0 eV for APLI (ATL Lasertechnik GmbH, Wermelskirchen, Germany) respectively. Positive mode mass spectra were recorded in a range of 200 – 1,000 Da at a mass resolving power *R* of 480,000 (FWHM at *m/z* 400) using the spectral stitching method[28] (windows of 70 Da with 5 Da overlap) while scanning the compensation voltage (CV) from -35 V to -5 V in 1 V steps. For each segment 6 to 7 single spectra were recorded.

5.3.3 Data analysis

Data analysis remains the crucial problem of online separations (HPLC as well as IMS) prior to an FTMS analysis of crude oils. Typically, non-target analysis is used to gain mass spectra that consist of several thousand distinct peaks each. Here not only the corresponding molecular formulae need to be assigned, important is also a data structure that allows for both adequate grouping and detailed information at the same time. While several approaches exist to comply with these demands for single mass spectra, to date no software is described that allows a fast, easy and thorough analysis of multi-dimensional FTMS data of such complexity, while providing a feasible structure of the results. Thus, spectra from discrete steps of a separation (here distinct CV values) need to be evaluated separately as distinct datasets. To recombine these datasets into one piece of information a MySQL database was built up that stores the resulting data and their relations to each other.

Separate mass segments of each CV were recombined to an averaged mass spectrum. The recombined spectra were individually analyzed using Composer (v1.06, Sierra Analytics, Modesto, CA, USA) and the results transferred to the homebuilt database for further interpretation.

5.4 Results and Discussion

As opposed to classical IMS methods ion transfer in FAIMS does not directly relate to the mobility and therefore the collisional cross section of an ion, but rather to the different cross sections/mobilities an ion exhibits under the influence of electrical fields of different strengths. Basis for the separation are therefore conformational changes and/or the tendency for clustering/declustering with the carrier gases at different field strengths rather than more direct structural differences.[24] One result of an IMS-MS coupling is a much increased peak capacity

as compounds are thus spread throughout an additional dimension, here the compensation voltage that is applied.

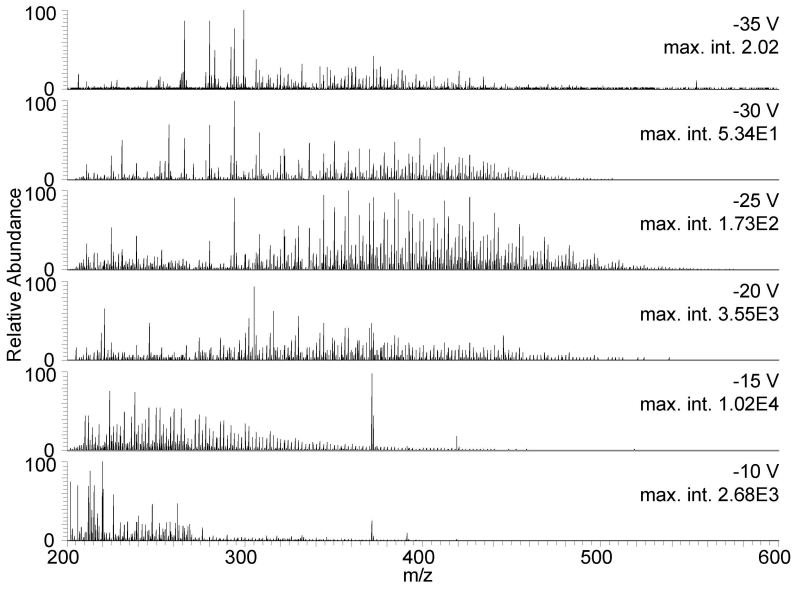

Figure 5-2. Mass spectra obtained for selected CV after APPI ionization.

With increasing compensation voltage, the observed mass value first increases slightly and then is followed by a sharp decrease. This is exemplarily shown for selected CV in Figure 5-2. Figure 5-3 shows a zoomed in portion of the same spectra. Here the sample simplification that is provided by the IMS separation becomes apparent. The changes in relative abundances monitor the different behavior of compounds belonging to the same heteroatom class, as well as of compounds of different classes. Especially regarding heteroatom classes that differ by the presence of one sulfur atom (i.e. HC vs S or S vs S_2) the corresponding compounds can be resolved and monitored individually thanks to the mass resolving power provided by the FTMS approach. For members of the same heteroatom class an additional trend can be observed. With increasing CV there is an increase in unsaturation (double bond equivalents, DBE) of the transmitted ions. This trend is most obvious for the pairs $C_{23}H_{34}S$ (DBE 7), $C_{24}H_{22}S$ (DBE 14) and $C_{21}H_{26}S_2$ (DBE 9), $C_{22}H_{14}S_2$ (DBE 16).

Both observed tendencies together suggest an increase in aromaticity and therefore compactness of the transmitted compounds with increasing CV (i.e. a CV value approaching 0 V). This is in accordance with the principle of FAIMS as it can be expected that more compact, polycyclic compounds with less and/or smaller aliphatic side chains can undergo less conformational changes under the influence of differing electrical fields. This in turn would

lead to high-field and low-field mobilities that are more similar and therefore only little compensation voltage should be needed to transmit the ion.

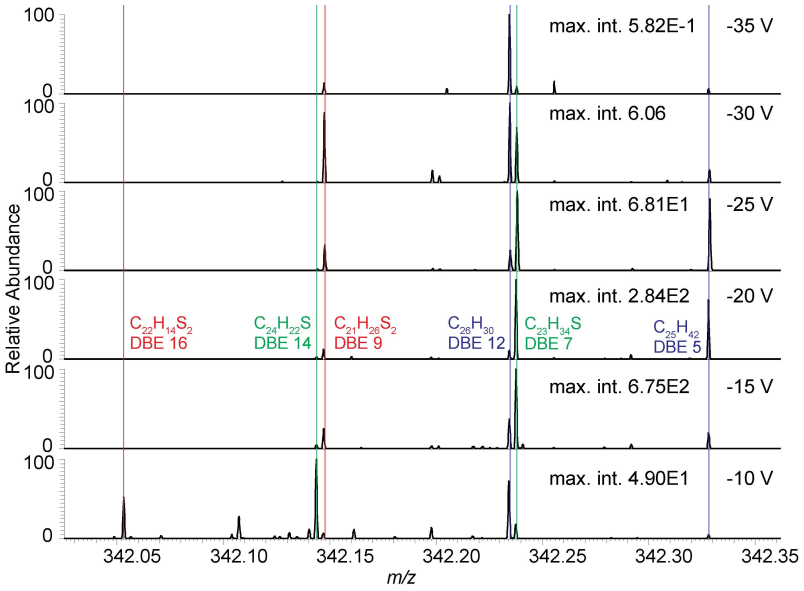

Figure 5-3. Zoomed-in mass spectra after APPI ionization for selected CV. Highlighted peaks represent members of the HC (blue), S (green) and S_2 (red) heteroatom classes.

Regarding the S heteroatom class intensity maxima evolve around DBE values of 3, 6, 9 and 12, which are commonly attributed to thiophenes, benzothiophenes, dibenzothiophenes and benzonaphthothiophenes, respectively (see Figure 5-4 for the corresponding core structures).

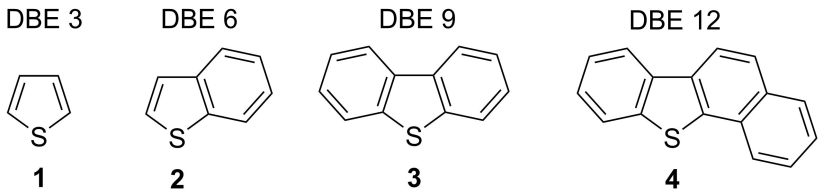

Figure 5-4. Core structures for polycyclic aromatic sulfur heterocycles (PASH). **1**: Thiophene, **2**: Benzo[*b*]thiophene, **3**: Dibenzo[*b*,*d*]thiophene, **4**: Benzo[*b*]naphtho[2,1-*d*]thiophene.

The behavior of the DBE distribution throughout the CV range is shown in the heatmaps in Figure 5-5. They show the summed intensities of all peaks that were assigned to an S_1-compound of the corresponding DBE series. Additionally, the traces along the CV range that correspond to the aforementioned DBE series are shown in the panels above. The panels on the right side of each heatmap show the DBE distributions for selected compensation voltages. The heatmap on the left side of Figure 5-5 shows APPI data while the right heatmap contains APLI data. For APPI the trend for increasing unsaturation with a compensation voltage that approaches 0 is again apparent. Distribution maxima occur at lower CV for higher DBE series

(see left upper panel in Figure 5-5). The distribution for DBE 9 (commonly attributed to dibenzothiophenes) in the APPI dataset is comparably broad, which hints towards a wide range of structural diversity for this group of compounds. As can be seen from the DBE distributions in the side panel (left side in Figure 5-5) the different core structures (see above) seem to be distributed onto a broad CV range.

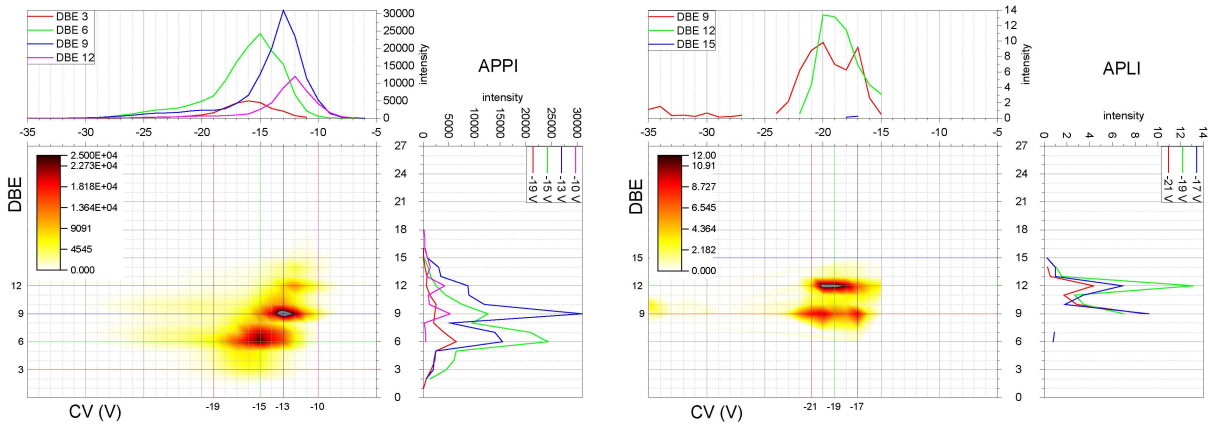

Figure 5-5. DBE distribution (contour plots, colors indicate the summed intensities) for sulfur class throughout the scanned CV range after APPI (left) and APLI (right) ionization. Top traces show the transmission behavior of selected DBE series throughout the CV range (CV on x-axis, y-axis shows summed intensity), right traces show the DBE distribution at selected compensation voltages (CV on y-axis, x-axis shows summed intensity). The corresponding cuts are indicated in the contour plot by colored lines.

The behavior of the S class after APLI ionization is shown in Figure 5-5 on the right side. Overall, intensities after APLI ionization were lower in comparison with APPI ionization. DBE values below 3 were not observed. This is in accordance with the preference of APLI ionization for condensed aromatic systems.[9, 21] The intensity maximum is observed for a DBE of 12 (benzonaphthothiophenes) with DBE 9 (dibenzothiophenes) being the next dominant series. As compared to APPI, ions belonging to both series are transmitted at compensation voltages that are 4-6 V lower when ionizing by APLI (see right upper panel in Figure 5-5).

The need for using a wider set of ionization techniques becomes apparent here, as obviously two (or more) different structural types are observed. The complementarity of the datasets obtained with either APPI or APLI ionization is further shown in Figure 5-6. Two examples are shown for DBE series 9 ($C_{21}H_{26}S$) and 12 ($C_{21}H_{20}S$). Although with the current setup no clear separation of isomers was achieved within one measurement, i.e. one ionization technique, when using both techniques the possible separation of two different structures or structure types becomes evident.

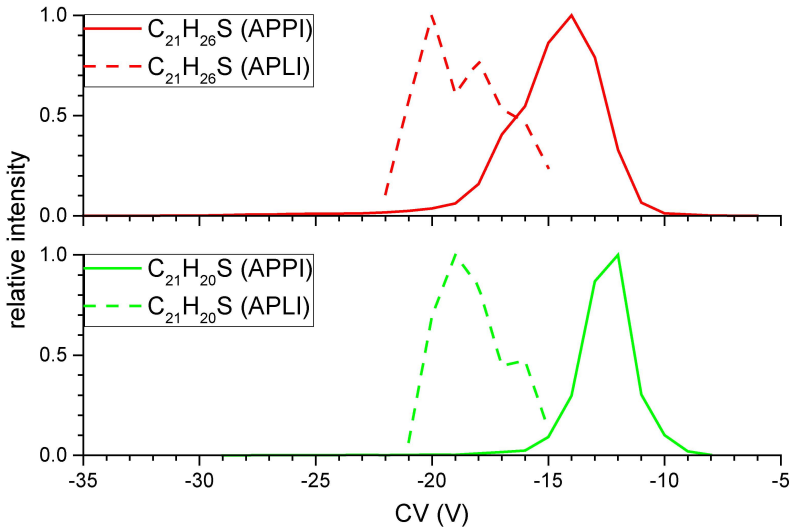

Figure 5-6. FAIMS transmission of ions corresponding to $C_{21}H_{26}S$ (DBE 9, top) and $C_{21}H_{20}S$ (DBE 12, bottom) after APPI (solid line) and APLI (dashed line) ionization (normalized intensities).

Compared with the S class, the group of pure hydrocarbons (HC class) seems to exhibit a broader structural variety. As can be seen in Figure 5-7 on the left side, the DBE distribution throughout the CV range is much less pronounced when using APPI ionization than as shown in Figure 5-5 for the S class. The DBE distributions of the HC class found for distinct CV values (see side panel on the left side of Figure 5-7) resemble a Gaussian type distribution, rather than exhibiting local maxima.

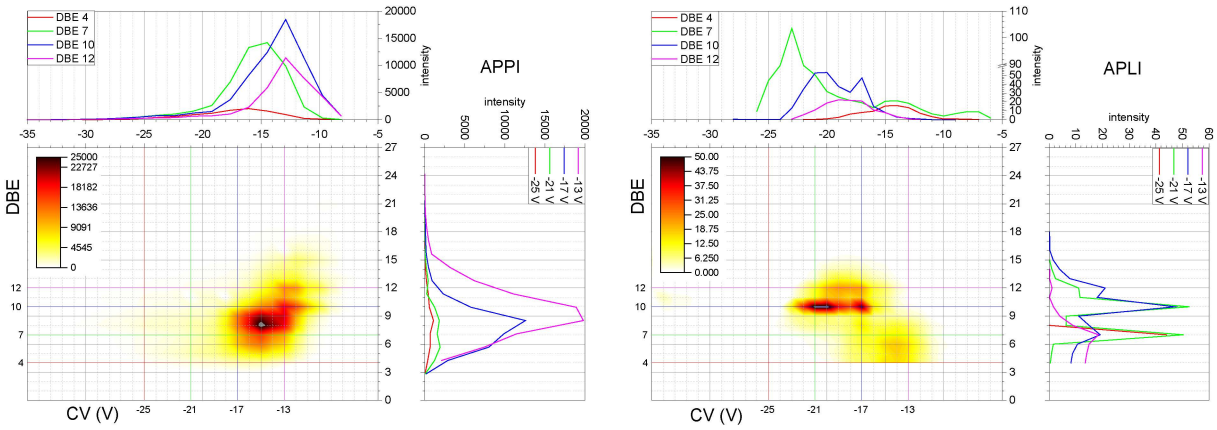

Figure 5-7. DBE distribution (contour plots, colors indicate the summed intensities) for hydrocarbon class throughout the scanned CV range after APPI (left) and APLI (right) ionization. Top traces show the transmission behavior of selected DBE series throughout the CV range (CV on x-axis, y-axis shows summed intensity), right traces show the DBE distribution at selected compensation voltages (CV on y-axis, x-axis shows summed intensity). The corresponding cuts are indicated in the contour plot by colored lines. Intensity from peaks corresponding to $C_{16}H_{20}$ (DBE 7) was removed from the heatmap of the APLI dataset for clarity but retained in the top trace. To help visualization of the other series the y-axis of the trace is broken as indicated.

Nevertheless, as can be estimated from the top panel distributions for selected DBE values, the tendency for a higher degree of unsaturation with increasing CV still persists. Most notably the maximum intensity originates from species belonging to the DBE 8 series. This behavior is rather unusual as typically series of fully aromatic, condensed systems are favored. Therefore, local maxima at DBE 7 (naphthalenes), 10 (phenanthrenes or anthracenes), 12 (pyrenes) and 15 (benzopyrenes) are expected (see Figure 5-8 for the corresponding core structures).

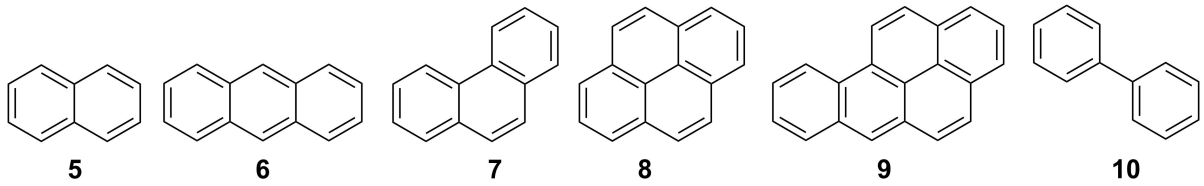

Figure 5-8. Core structures for polycyclic aromatic hydrocarbons (PAH). **5**: Naphthalene, **6**: Anthracene, **7**: Phenanthrene, **8**: Pyrene, **9**: Benz[*a*]pyrene, **10**: Biphenyl.

Probably, the majority of compounds of the DBE 8 series are alkylated biphenyls rather than naphthalenes with an additional double bond or ring closure. This is supported by the fact that the DBE 8 series is almost absent after APLI ionization. While biphenyls are readily ionized under APPI conditions, the ionization efficiency in APLI is comparably low for single phenyl substituents. This behavior was verified using 4,4'-di-*tert*-butyl-1,1'-biphenyl as a standard.

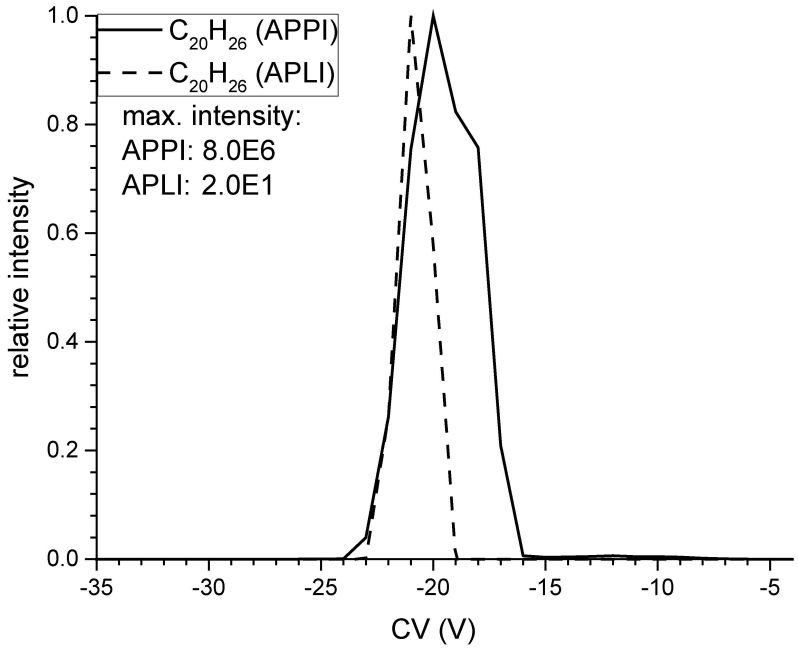

Figure 5-9. FAIMS transmission of 4,4'-di-*tert*-butyl-1,1'-biphenylium radical cation generated by APPI (solid line) and APLI (dashed line) respectively.

As can be seen from Figure 5-9 the ionization efficiency of the biphenyl standard is considerably lower when using APLI than with APPI (maximum intensity of $2.0 \cdot 10^1$ compared to $8.0 \cdot 10^6$). The compensation voltage needed to transmit the ion does, however, not change significantly.

The different CV ranges found for both ionization techniques can therefore not be attributed to potentially different ionization sites due to differing ionization mechanisms. While signal intensity was generally lower with APLI, the high difference in case of the standard can be partly attributed to a higher ionization efficiency of APLI for condensed aromatic structures due to an increased density of intermediate states.[22] Therefore ionization of a biphenylic structure is much less favorable in APLI, while it is still readily ionized by direct 1-photon ionization (APPI).

After APLI ionization the DBE distribution of the hydrocarbon class is dominated by the expected series of DBE 10 (anthracenes and phenanthrenes) and 12 (pyrenes). The DBE 7 series (naphthalenes) is dominated by ions from a single compound of the formula $C_{16}H_{20}$. The corresponding intensity was taken out of the heatmap (see Figure 5-7, right side) to help the visualization of the remaining distribution. The selected traces for DBE 7 and especially for compensation voltages of -25 V and -21 V (right upper panel and right side panel in Figure 5-7) still include the peak intensity of the corresponding peaks.

After APLI ionization no hydrocarbons with double bond equivalents below 4 were found, as expected. Some compounds with DBE 4-6 are, however, found at low intensity. The compensation voltages needed to transmit the corresponding ions fall into the same region as observed for APPI ionization. The transmitted ions are thus probably structurally related. For double bond equivalents 9-12 compensation voltages needed for transmission are 4-6 V lower, comparable with the data obtained for the sulfur class.

This is shown in Figure 5-10 for compounds with the molecular formula $C_{21}H_{24}$. The difference in compensation voltage needed to transmit the corresponding ions (of equal compositions) suggests that analytes of different structures must be ionized by either of the two methods employed (bottom panel). Most notably, the top panel shows the ion mobility behavior of a set of ions from compounds with the molecular formula $C_{22}H_{30}$ (top panel). The APLI dataset shows only one signal at a compensation voltage of -15 V that is also present after APPI ionization. For APPI however a second local maximum is found at a compensation voltage

of -25 V, respectively. Here a nearly full separation of two isomeric compounds that were both ionized with APPI must have occurred within the FAIMS unit.

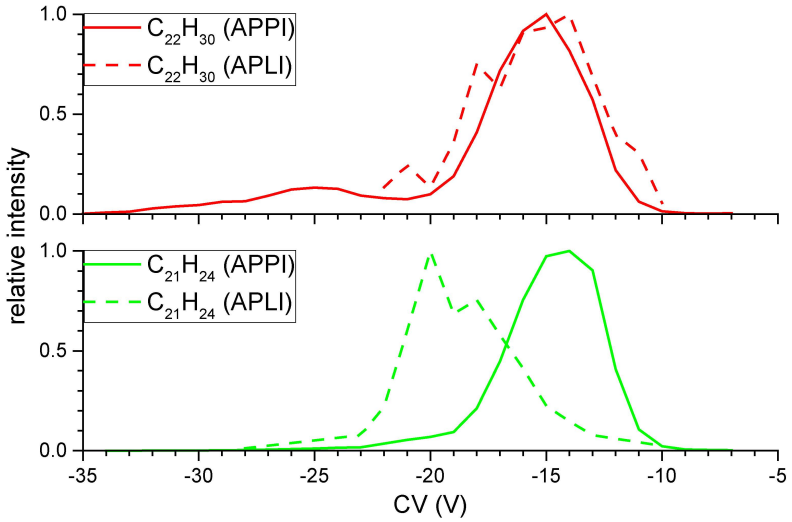

Figure 5-10. FAIMS transmission of ions corresponding to $C_{22}H_{30}$ (DBE 8, top) and $C_{21}H_{24}$ (DBE 10, bottom) after APPI (solid line) and APLI (dashed line) ionization (normalized intensities).

5.5 Conclusions

Ion mobility spectrometry has already been shown to be a valuable tool for the analysis of highly complex mixtures such as crude oils. It highly increases the peak capacity of a mass spectrometric analysis and helps avoiding discriminating effects by simplifying the portion of the sample that is introduced to the mass spectrometer at any time of the analysis. The application of photoionization techniques is important for the analysis of crude oils, given its mainly unpolar character. Here we demonstrated a first example for FAIMS-FTMS coupling to photoionization methods, using a homebuilt ion source block. By using both, APPI-FAIMS-FTMS as well as APLI-FAIMS-FTMS it was revealed, that both ionization methods yield data that are complementary in the sense of analyte structures that are observed. This is obvious from the difference in compensation voltage that is needed to transmit ions of the same composition after either APPI or APLI ionization. The combination of selective ionization and FAIMS separation can be further exploited in future studies for a more detailed analysis of crude oil mixtures. Additionally, we reported the first online separation of isomeric hydrocarbons in crude oil prior to FTMS analysis by means of an APPI-FAIMS-FTMS coupling. Thus, the impossibility to distinguish isomers by mass spectrometry was successfully overcome by hyphenation to a FAIMS separation. The major difficulty when using a filtering stage such as FAIMS is, that a compromise between (isomer) resolving power and ion transmission of the FAIMS unit has to be found, as both are hardly optimizable together. For

this study neither of both was explicitly optimized by hardware modifications. For future studies first ion transmission is to be addressed, before focusing on a more effective isomer separation.

5.6 References

1. Connan, J., *Use and trade of bitumen in antiquity and prehistory: molecular archaeology reveals secrets of past civilizations* in: *Philos. Trans. R. Soc. London, Ser. B* **1999**, *354*(1379), 33-50.

2. Forbes, R. J., *Neues zur ältesten Geschichte des Bitumens* in: *Bitumen* **1938**, *8*(6), 128–134.

3. Speight, J. G., *Handbook of petroleum analysis*. Chemical Analysis **2001**, Wiley-Interscience, New York, NY.

4. van Aarssen, B. G. K.; Bastow, T. P.; Alexander, R. and Kagi, R. I., *Distributions of methylated naphthalenes in crude oils: indicators of maturity, biodegradation and mixing* in: *Org. Geochem.* **1999**, *30*(10), 1213-1227.

5. Dong, T.; He, S.; Liu, G. O.; Hou, Y. G. and Harris, N. B., *Geochemistry and correlation of crude oils from reservoirs and source rocks in southern Biyang Sag, Nanxiang Basin, China* in: *Org. Geochem.* **2015**, *80*, 18-34.

6. Pavon, J. L. P.; Pinto, C. G.; Pena, A. G. and Cordero, B. M., *Headspace mass spectrometry methodology: application to oil spill identification in soils* in: *Anal. Bioanal. Chem.* **2008**, *391*(2), 599-607.

7. Hughey, C. A.; Hendrickson, C. L.; Rodgers, R. P. and Marshall, A. G., *Elemental Composition Analysis of Processed and Unprocessed Diesel Fuel by Electrospray Ionization Fourier Transform Ion Cyclotron Resonance Mass Spectrometry* in: *Energy Fuels* **2001**, *15*(5), 1186–1193.

8. Gaspar, A.; Zellermann, E.; Lababidi, S.; Reece, J. and Schrader, W., *Characterization of Saturates, Aromatics, Resins, and Asphaltenes Heavy Crude Oil Fractions by Atmospheric Pressure Laser Ionization Fourier Transform Ion Cyclotron Resonance Mass Spectrometry* in: *Energy Fuels* **2012**, *26*(6), 3481–3487.

9. Gaspar, A.; Zellermann, E.; Lababidi, S.; Reece, J. and Schrader, W., *Impact of different ionization methods on the molecular assignments of asphaltenes by FT-ICR mass spectrometry* in: *Anal. Chem.* **2012**, *84*(12), 5257-5267.

10. Panda, S. K.; Andersson, J. T. and Schrader, W., *Characterization of supercomplex crude oil mixtures: what is really in there?* in: *Angew. Chem. Int. Ed.* **2009**, *48*(10), 1788-1791.

11. Lababidi, S. and Schrader, W., *Online normal-phase high-performance liquid chromatography/Fourier transform ion cyclotron resonance mass spectrometry: effects of different ionization methods on the characterization of highly complex crude oil mixtures* in: *Rapid Commun. Mass Spectrom.* **2014**, *28*(12), 1345-1352.

12. Schrader, W.; Xuan, Y. and Gaspar, A., *Studying ultra-complex crude oil mixtures by using High Field Asymmetric Waveform Ion Mobility Spectrometry (FAIMS) coupled to an ESI-LTQ-Orbitrap Mass Spectrometer* in: *Eur. J. Mass Spectrom.* **2014**, *20*(1), 43.

13. Benigni, P.; Thompson, C. J.; Ridgeway, M. E.; Park, M. A. and Fernandez-Lima, F., *Targeted high-resolution ion mobility separation coupled to ultrahigh-resolution mass spectrometry of endocrine disruptors in complex mixtures* in: *Anal. Chem.* **2015**, *87*(8), 4321-4325.

14. Klitzke, C. F.; Corilo, Y. E.; Siek, K.; Binkley, J.; Patrick, J. and Eberlin, M. N., *Petroleomics by Ultrahigh-Resolution Time-of-Flight Mass Spectrometry* in: *Energy Fuels* **2012**, *26*(9), 5787–5794.

15. Fasciotti, M.; Lalli, P. M.; Klitzke, C. F.; Corilo, Y. E.; Pudenzi, M. A.; Pereira, R. C. L.; Bastos, W.; Daroda, R. J. and Eberlin, M. N., *Petroleomics by Traveling Wave Ion Mobility–Mass Spectrometry Using CO2as a Drift Gas* in: *Energy Fuels* **2013**, *27*(12), 7277-7286.

16. Ponthus, J. and Riches, E., *Evaluating the multiple benefits offered by ion mobility-mass spectrometry in oil and petroleum analysis* in: *Int. J. Ion Mobility Spectrom.* **2013**, *16*(2), 95-103.

17. Santos, J. M.; Galaverna, R. d. S.; Pudenzi, M. A.; Schmidt, E. M.; Sanders, N. L.; Kurulugama, R. T.; Mordehai, A.; Stafford, G. C.; Wisniewski, A. and Eberlin, M. N., *Petroleomics by ion mobility mass spectrometry: resolution and characterization of contaminants and additives in crude oils and petrofuels* in: *Anal. Methods* **2015**, *7*(11), 4450-4463.

18. Fernandez-Lima, F. A.; Becker, C.; McKenna, A. M.; Rodgers, R. P.; Marshall, A. G. and Russell, D. H., *Petroleum Crude Oil Characterization by IMS-MS and FTICR MS* in: *Anal. Chem.* **2009**, *81*(24), 9941-9947.

19. Isenberg, S. L.; Armistead, P. M. and Glish, G. L., *Optimization of peptide separations by differential ion mobility spectrometry* in: *J. Am. Soc. Mass. Spectrom.* **2014**, *25*(9), 1592–1599.

20. Guevremont, R., *High-field asymmetric waveform ion mobility spectrometry: A new tool for mass spectrometry* in: *J. Chromatogr. A* **2004**, *1058*(1-2), 3–19.

21. Constapel, M.; Schellenträger, M.; Schmitz, O. J.; Gäb, S.; Brockmann, K. J.; Giese, R. and Benter, T., *Atmospheric-pressure laser ionization: a novel ionization method for liquid chromatography/mass spectrometry* in: *Rapid Commun. Mass Spectrom.* **2005**, *19*(3), 326–336.

22. Lorenz, M.; Schiewek, R.; Brockmann, K. J.; Schmitz, O. J.; Gäb, S. and Benter, T., *The distribution of ion acceptance in atmospheric pressure ion sources: Spatially resolved APLI measurements* in: *J. Am. Soc. Mass. Spectrom.* **2008**, *19*(3), 400-410.

23. Chen, C.; Dong, C.; Du, Y.; Cheng, S.; Han, F.; Li, L.; Wang, W.; Hou, K. and Li, H., *Bipolar ionization source for ion mobility spectrometry based on vacuum ultraviolet radiation induced photoemission and photoionization* in: *Anal. Chem.* **2010**, *82*(10), 4151–4157.

24. Kotkovskii, G. E.; Sychev, A. V.; Tugaenko, A. V. and Chistyakov, A. A., *A laser spectrometer of field-asymmetric ion mobility* in: *Instrum. Exp. Tech.* **2011**, *54*(2), 256–261.

25. Laakia, J.; Adamov, A.; Jussila, M.; Pedersen, C. S.; Sysoev, A. A. and Kotiaho, T., *Separation of different ion structures in atmospheric pressure photoionization-ion mobility spectrometry-mass spectrometry (APPI-IMS-MS)* in: *J. Am. Soc. Mass. Spectrom.* **2010**, *21*(9), 1565–1572.

26. Laakia, J.; Kauppila, T. J.; Adamov, A.; Sysoev, A. A. and Kotiaho, T., *Separation of isomeric amines with ion mobility spectrometry* in: *Talanta* **2015**, *132*, 889–893.

27. Castellanos, A.; Benigni, P.; Hernandez, D. R.; DeBord, J. D.; Ridgeway, M. E.; Park, M. A. and Fernandez-Lima, F. A., *Fast Screening of Polycyclic Aromatic Hydrocarbons using Trapped Ion Mobility Spectrometry - Mass Spectrometry* in: *Anal. Methods* **2014**, *6*(23), 9328–9332.

28. Gaspar, A. and Schrader, W., *Expanding the data depth for the analysis of complex crude oil samples by Fourier transform ion cyclotron resonance mass spectrometry using the spectral stitching method* in: *Rapid Commun. Mass Spectrom.* **2012**, *26*(9), 1047-1052.

6. Structural motifs of crude oil constituents – Elucidation by APPI-FAIMS-MS/FTMS

Redrafted from:
Vetere, A. and Schrader, W., *Structural motifs of crude oil constituents – Elucidation by APPI-FAIMS-MS/FTMS*, will be submitted to *Analytical Chemistry*.

6.1 Abstract

Despite the enormous progress in analytical techniques and its importance for our energy-driven society, still little information is available on the real composition of crude oils. Ultrahigh resolution mass spectrometry allows gaining information down to the molecular level, thus enabling to determine elemental compositions of individual analytes. However, no structural information on the alkylation pattern or even on functional groups is achievable by mass spectrometry alone. Ion mobility spectrometry (IMS) is a suitable method to differentiate between isomeric compounds in the gas phase prior to a mass spectrometric analysis. The lab-built APPI/APLI-FAIMS source we introduced earlier was revised to optimize ion transmission and used to follow up on the ion mobility of crude oil constituents after photoionization. An MS/MS approach using collision-induced dissociation (CID) was used to elucidate structural motifs of the transmitted isomers.

6.2 Introduction

Although crude oil has been processed industrially for more than 150 years and notwithstanding its importance for our energy-driven society, it still is a vastly unknown mixture of very high complexity. Over the past decades a variety of analytical techniques have been developed for, or adapted to the analysis of crude oil, many of which focusing on certain bulk parameters like boiling point distribution, density, overall aromaticity or heteroatom content.[1-9] While these parameters are crucial for the refining process, information on the molecular level becomes increasingly important.

Substantial progress in this field has been made with the introduction of ultrahigh resolving mass spectrometry together with soft, non-fragmenting, ionization methods.[10-17] Fourier transform ion cyclotron resonance mass spectrometry (FT-ICR MS) and FT Orbitrap MS (together termed as FTMS) yield sub-ppm mass accuracy and a mass resolving power $R > 10^5$ (FWHM), thus allowing the unambiguous determination of the elemental composition that corresponds to a mass spectrometric signal. Still, one major problem of the mass spectrometric approach is the inability to distinguish the broad variety of isomeric species present within a single crude oil sample without prior separation.

A chromatographic pre-separation of isomeric compounds before a mass spectrometric analysis is typically done by one- or two-dimensional (GC×)GC-MS.[18-21] With these techniques structural isomers, at least with a low degree of alkylation and especially functional isomers can be separated from each other easily. However, a gas chromatographic analysis is only suitable for relatively light oils or fractions such as kerosene or diesel oil.

For heavier oils or fractions that are not amenable to GC, ion mobility spectrometry (IMS) is a suitable alternative that has the potential to separate isomeric compounds (ions) by their different shape and size in the gas phase. However, most studies so far use ion mobility together with time-of-flight mass spectrometry (TOF-MS) that suffers from insufficient mass resolving power. Additionally, studies often focus on electrospray ionization (ESI), thus neglecting the vast majority of non-polar compounds.[22-28]

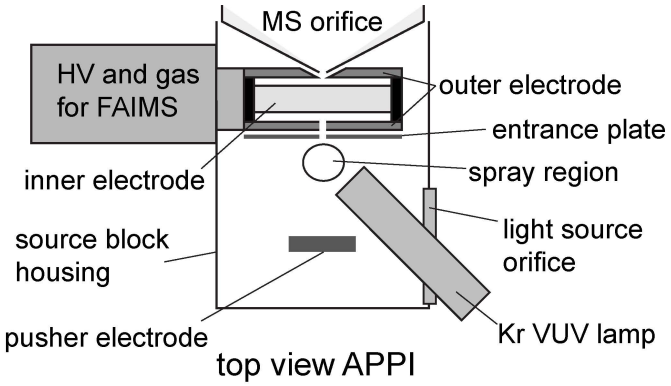

Figure 6-1: Schematic section of the reviewed source block design for APPI-FAIMS-FTMS. The pusher electrode is located behind the spray region such that formed ions are accelerated into the FAIMS unit. Not shown is the thermal sprayer located at the top of the view.

We recently introduced a new source block design that allows using photoionization together with FAIMS-FTMS.[29] With this initial design we were able to demonstrate the necessity for using multiple ionization techniques when analyzing a mixture as complex as crude oil. However, the setup was impaired by a relatively poor ion transmission due to an entrance plate potential on the FAIMS unit of 1 kV. For the present study, the source setup was reviewed to implement an additional pusher electrode as can be seen from Figure 6-1.

The new design was used to follow up on the IMS separation behavior of selected ions through fragmentation experiments.

6.3 Experimental

6.3.1 Sample preparation

A North American heavy crude oil was diluted in toluene to a final concentration of 500 µg·mL^{-1} and then analyzed without further treatment.

6.3.2 Instruments and methods

Mass spectra were recorded on a research-type Orbitrap Elite mass spectrometer (Thermo Fisher Scientific, Bremen, Germany) equipped with a FAIMS unit (Thermo Fisher Scientific, San Jose, CA, USA), while injecting the sample at a flow rate of 20 µL·min^{-1}. For use of photoionization (APPI) a lab-built source block was used and extended by a pusher electrode that was, after evaluation, set at 1.5 kV. The pusher electrode was operated externally by a high voltage power supply (PNC 30000-2, Heinzinger electronic GmbH, Rosenheim, Germany). Ionization was performed by a Kr VUV lamp at 10.0 and 10.6 eV for APPI (Syagen

Technologies, Tustin, CA, USA). Positive mode mass spectra were recorded in SIM mode using 30 Da mass windows for monitoring the IMS behavior of selected ions, while scanning the compensation voltage (CV) from -39 V to -9 V in steps of 0.2 V. The dispersion voltage was held at -5.0 kV with a carrier gas flow of 4.0 $L \cdot min^{-1}$ (N_2:He, 1:1). For each CV step, after recording of a SIM spectrum of ±15 Da around a preselected *m/z* (FTMS), an additional MS/MS scan was performed on selected ions after isolation and fragmentation by collision-induced dissociation (CID) in the linear ion trap (LTQ). The procedure is shown in detail in Figure 6-2.

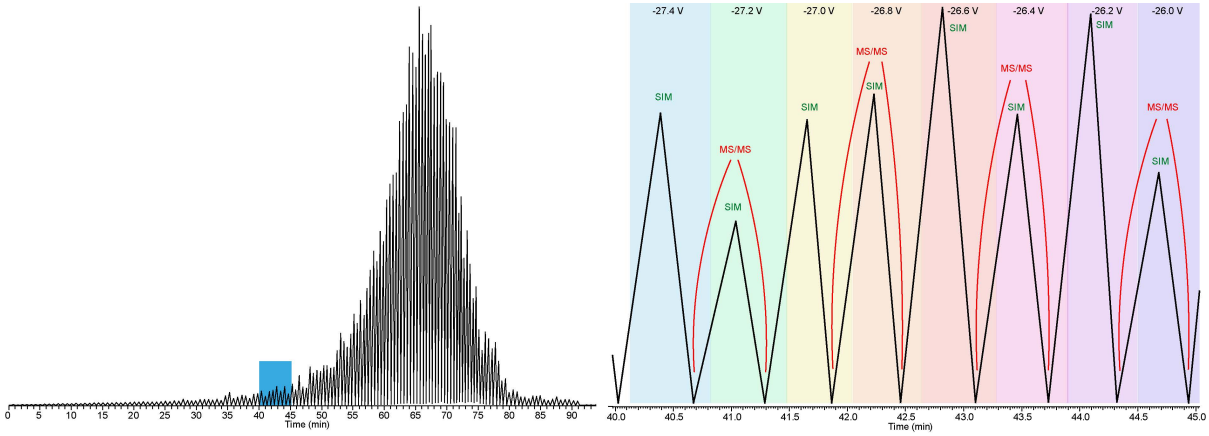

Figure 6-2: Experimental procedure with resulting total ion chromatogram (TIC, left). The compensation voltage set in the FAIMS unit is incremented over time after performing a SIM scan on a selected mass range, followed by an MS/MS scan on a selected ion (right).

Fragment spectra were recorded using FTMS in full scan mode. In all cases a total of 6 microscans was summed at a mass resolving power of 480,000 (FWHM at *m/z* 400).

Additionally, the electrode setup of the FAIMS unit was modified by replacing the inner electrode with a lab-built electrode that reduces the electrode gap from the standard of 2.50 mm to 2.25 mm. The previously described experiments were then repeated with the different electrode setup.

6.4 Results and Discussion

6.4.1 Optimization of ion transmission

The effect of the newly introduced pusher electrode was first evaluated using a set of PAH (polycyclic aromatic hydrocarbons) as model compounds. Figure 6-3 shows the development of analyte signal (absolute intensities) with increasing pusher electrode potential.

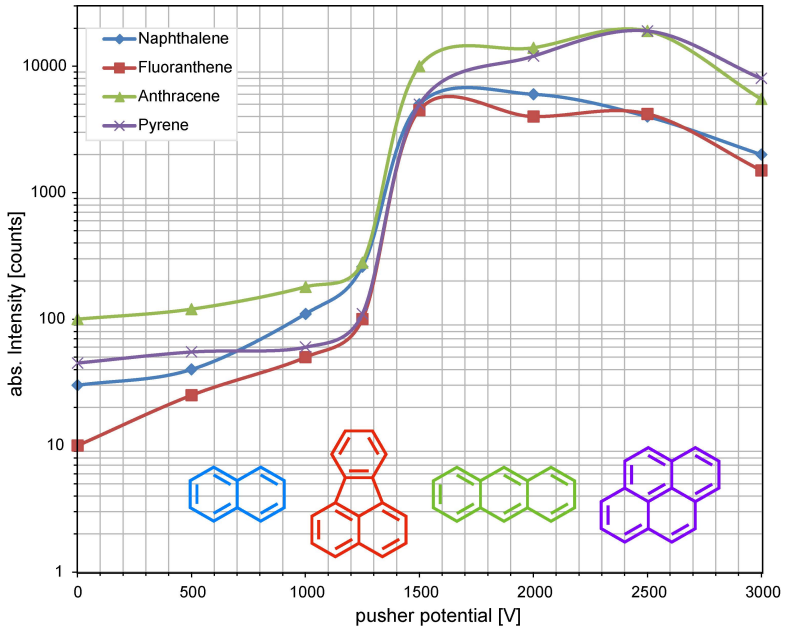

Figure 6-3: Signal intensities obtained from a PAH standard mixture after APPI-FAIMS-FTMS in relation to the potential applied to the pusher electrode.

The initially low signal intensity is increased by a factor of 2 to 5 when the pusher electrode is operated at the entrance plate potential (1 kV). Further raising of the potential to 1.5 kV results in a steep increase in signal intensity by a factor of 100 to 500. Incrementing the potential beyond this point does not enhance the signal, but partly leads to signal loss. This behavior is presumably caused by the ions being accelerated too strongly, leading to a collision with the central electrode.

For the remainder of this study a pusher electrode potential of 1.5 kV was thus chosen as the optimum operating condition. The IMS transmission of selected heteroatomic compounds was monitored and their fragmentation behavior recorded after CID. For the following discussion, only fragment ions are considered that contain the same number of heteroatoms as the parent ion. Especially fragments that contain only carbon and hydrogen are excluded from the discussion as they cannot be attributed to a single parent ion but might also originate from a different compound within the isolation window.

6.4.2 Fragmentation of $C_{42}H_{66}S^{\cdot+}$

Radical cations detected at *m/z* 602.48797 have an elemental composition of $C_{42}H_{66}S$, corresponding to a double bond equivalent (DBE) of 10. Such sulfur containing compounds are considered to be mostly thiophenic. Some possible structure types are shown in Figure 6-4. The possibilities include structures derived from benzo- (**1d**), dibenzo- (**1a**), benzonaphtho- (**1b**) or

phenanthrothiophenes (**1c**). Generally, sulfidic compounds or mercaptanes would also be possible, but are not typically considered to be equally important.

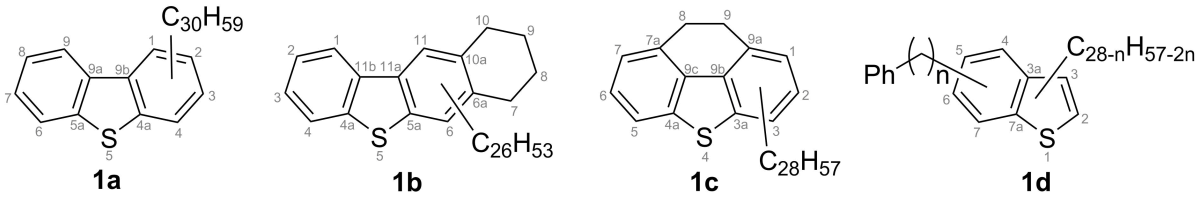

Figure 6-4: Possible isomeric structure types for $C_{42}H_{66}S$. Dibenzothiophenic (**1a**), tetrahydrobenzonaphthothiophenic (**1b**), dihydrophenanthrothiophenic (**1c**) or phenylated benzothiophenic (**1d**) structures are possible. Indicated alkyl chains might be split up into several smaller substituents. Atom positions on the aromatic core are indicated as shaded numbers.

The cumulative fragment ion spectra obtained while scanning the CV of the FAIMS unit are shown in Figure 6-5 on the left side. For a better overview the top axis shows the number of carbon atoms lost to generate the corresponding fragment. On first sight the observed 14 Da pattern does resemble electron impact (EI) spectra of alkyl chains with cleavage at arbitrary positions, as was also suggested by Porter and co-workers.[30] However, it has been shown that crude oil relevant aromatic compounds that bear a (hetero-)aromatic core fragment predominantly by benzylic cleavage of an entire alkyl chain or related mechanisms.[31]

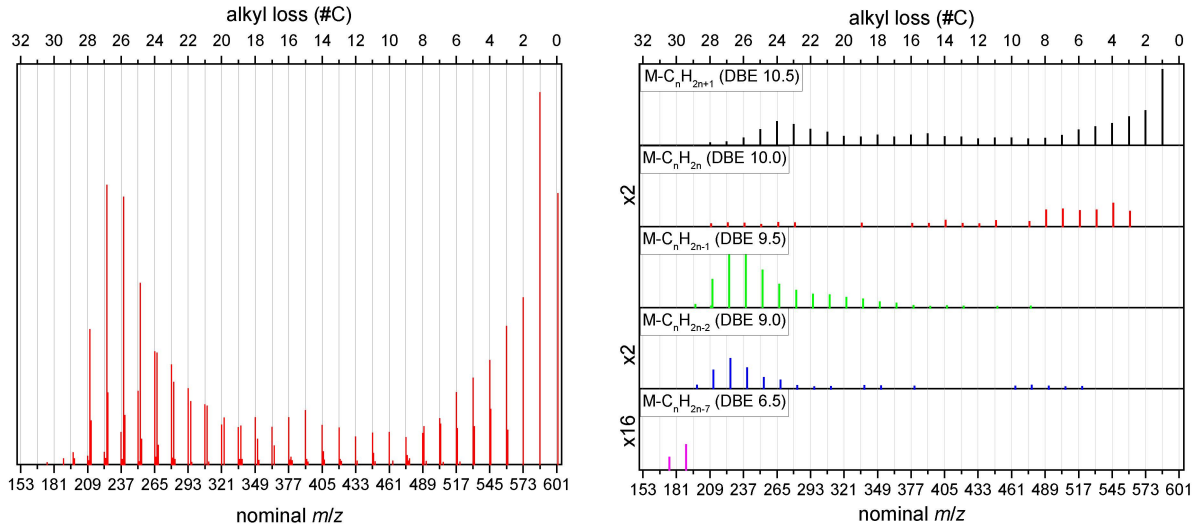

Figure 6-5: Fragment ion spectra of $C_{42}H_{66}S^{\cdot+}$ after summation over the entire CV range. The bottom axes show the nominal *m/z* of detected fragments ions, while the top axes show the number of carbon atoms lost during fragmentation. Left panel: Whole spectrum. Right panel: Spectrum separated into different series of fragment ions, corresponding to the indicated DBE values. Where applicable, zoom factors are indicated on the left side.

This is exemplarily shown in Figure 6-6 for a **1c** type core structure. Homolytic cleavage of an alkyl chain in benzylic position results in a diradical fragment ion with a DBE of 10.5 (top). If the sidechain is at least three carbon atoms long, an additional rearrangement of one hydrogen atom is also possible that ultimately leads to the loss of an alkene and formation of a DBE 10 fragment ion.[32]

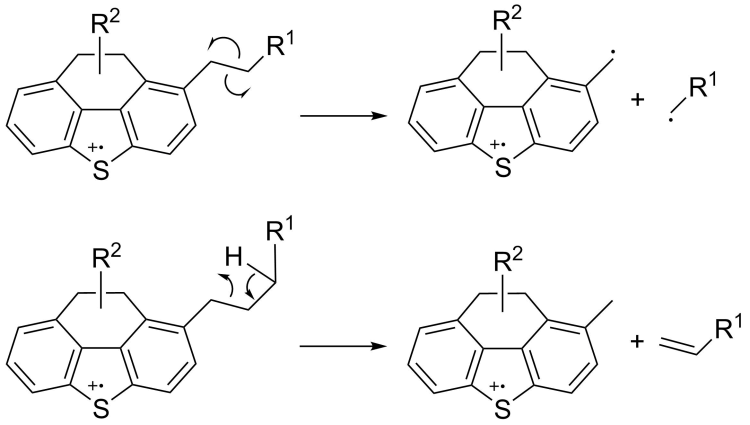

Figure 6-6: Basic mechanisms for the fragmentation of polycyclic aromatic compounds. Dominant is the homolytic cleavage in a benzylic position (top). With alkyl chains of three or more carbon atoms the fragmentation reaction competes with an additional 1,3-H-shift that results in the loss of an alkene (bottom).

Based on these results it needs to be concluded that each of the fragment ions observed must result from a parent ion that exhibits an alkyl chain of corresponding length, i.e. number of carbon atoms lost + 1. When multiple alkyl chains are present at an aromatic core, only one is fragmented during a single CID step, resulting in a statistical distribution of fragment ion signals. The intensity distribution given in Figure 6-5 indicates a strong preference of compounds exhibiting only few, relatively long alkyl chains. Apart from a methyl loss (resulting from cleavage of an ethyl group) the loss of an alkyl chain of 25 to 28 carbon atoms is dominating the spectrum.

This can be seen in more detail on the right side of Figure 6-5 by splitting the spectrum into different traces of fragment ion series, belonging to the same DBE value. The top trace (DBE 10.5) corresponds to the homolytic cleavage of a fully saturated alkyl chain. Considering the core structures given in Figure 6-4, a total number of 26 to 28 carbon atoms reside in aliphatic side chains that do not contain any double bond or ring closure. These can be statistically distributed over 6 (**1d**) to 8 (**1a-c**) benzylic positions, giving rise to an average of around 3 to 5 aliphatic carbon atoms per benzylic position.

If alkyl chains were statistically distributed around an aromatic core, the intensity distribution should therefore peak around a loss of 2 to 4 carbon atoms. The fragment series, however, shows local maxima at 1, 15 and 24 carbon atoms to be lost, indicating the presence of high amounts of ethyl, hexadecyl and pentaeicosyl sidechains. The smallest fragment observed within this series is at *m*/*z* 209, corresponding to a loss of $C_{28}H_{57}$. This is indicative of a **1c** type structure with a single alkyl chain located in position 8, which, in fact, is benzylic. Structure type **1d** allows only a maximum loss of $C_{27}H_{55}$ (with n = 0, compare Figure 6-4), while type **1b** allows a maximum loss of $C_{26}H_{53}$ from a benzylic position, if a single sidechain is located in position 7 or 10.

The fragment ion series with DBE 10.0 generally follows the same trend. This is expected, since for longer alkyl chains the rearrangement reaction shown in Figure 6-6 is competing with the direct homolytic fission. Additionally, the series contains fragment ions that result from retro-Diels-Alder reactions of **1b** type parent ions. Both types of reaction cannot be distinguished here, however, the overall intensity distribution indicates that the corresponding structure type is of relatively low abundance.

The following fragment ion series (DBE 9.5 and 9.0) originate from the same type of fragmentation reactions, but with a double bond equivalent – most probably a naphthenic ring – residing within the lost alkyl chain. These series of fragment ions therefore can be attributed to an **1a** type parent structure, where the naphthenic ring is not fused to the aromatic core. While the maximum intensity is observed for fragments after loss of a C_{27}-chain, loss of small fragments is absent for these series. The lowest mass fragments at *m*/*z* 197/198, indicative of a C_{29}-loss are in good accordance to the proposed type **1a** structure. No information, however, is available on the exact position of any sidechain, nor on its degree of branching. In case of type **1a** parent structures also the position of the naphthenic ring inside the substituent is not known.

Small alkyl fragments can occur for all four structure types proposed. Only two low intensity fragment signals are found that clearly indicate type **1d** parent compounds. Fragment ions at *m*/*z* 175 and 189 (DBE 6.5) result from the loss of a DBE 4 fragment, which is indicative of a standalone phenyl ring. In total 31/30 carbon atoms are lost to produce the fragments, which is close to the maximum number of 33 (n = 28 in Figure 6-4). Especially the absence of fragments within this series that indicate the loss of only few (> 6) carbon atoms reveals that the phenyl substituent, while not fused to the aromatic benzothiophene core, must still be in close vicinity to it. The aromatic centers are probably separated by a small alkyl bridge of only 2 to 4 carbon

atoms (compare Figure 6-7). Additionally, the phenyl ring must bear the majority of the remaining aliphatic sidechains. Otherwise more, larger fragments should be observed after loss of the phenyl moiety.

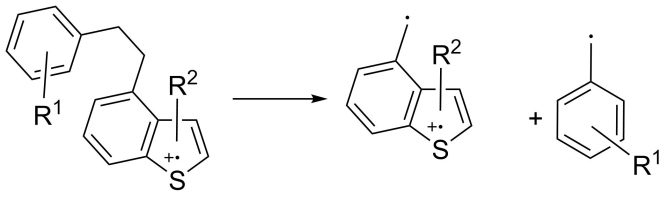

Figure 6-7: Fragmentation of a **1d** type compound with an ethylene bridge. Substituent positions are examples.

Apart from the structure types discussed so far, sulfidic compounds with the sulfur residing inside an open chain or a naphthenic ring are possible. Regarding the absence of sulfur containing low DBE fragments, such structures, however, do not seem to be very abundant.

As can be seen from Figure 6-8 the modified electrode setup does not offer a much better separation of isomeric compounds in this case. In both experiments fragment ion traces largely overlap within a CV range spanning 9-10 V. With the observed dominance of rather long alkyl chains, this can be expected. The ion mobility of the distinct isomers, i.e. the degree of conformational change between the high and low electric field portion of the wave, will be mostly affected by the folding abilities of these substituents. Minor changes in branching or position of long alkyl chains will only be of limited effect. However, due to the intrinsic simplification of the mixture passing the mobility unit at a given setting, discrimination effects are reduced, thus enabling the detection also of low abundant species.

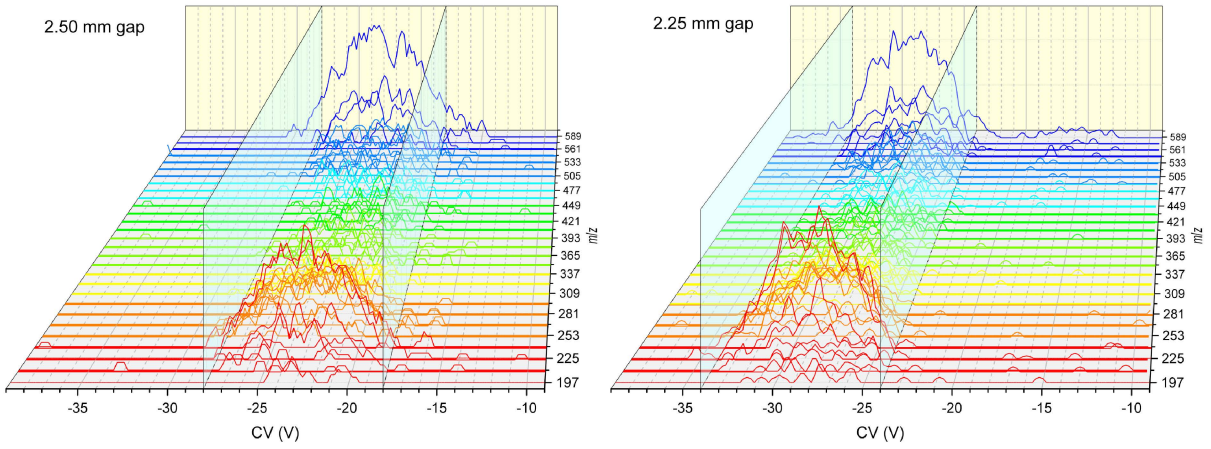

Figure 6-8: Occurrence of fragment ions throughout the ion mobility separation of the parent isomers of *m/z* 602.48797. Left: Standard electrode set (2.50 mm gap); right: Lab-built electrode set (2.25 mm gap). Shaded XZ-planes indicate occurrence of the majority of signals.

6.4.3 Fragmentation of $C_{19}H_{24}N^+$

Cations detected at *m/z* 266.19033 result from parent compounds of composition $C_{19}H_{23}N$ that have been ionized by protonation. Corresponding molecules bear a DBE of 9, with the observed ions being of DBE 8.5. While such species are mostly considered as being carbazole type compounds (see Figure 6-9, **2a**), also pyridinic (**2b** and **2d**) or aniline related structure types (**2c**) are possible.

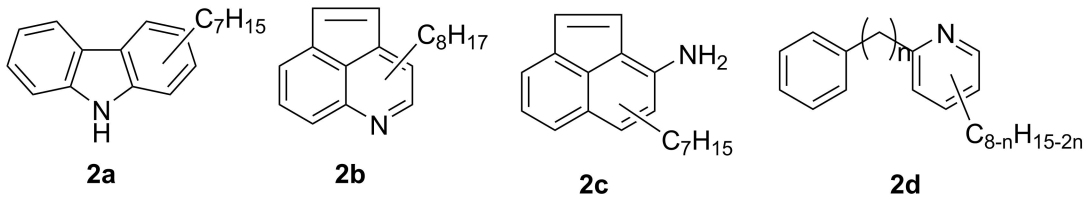

Figure 6-9: Possible isomeric structure types for $C_{19}H_{23}N$. Indicated alkyl chains might be split up into several smaller substituents, including possible *N*-alkylation for types **2a** and **2c**.

Compared to the previous example, the isomeric compounds investigated here are less extensively alkylated, with only 7 to 8 carbon atoms in aliphatic chains. The summarized fragment spectra shown in Figure 6-10 are therefore much less complicated. Loss of a methyl group is, again, by far the dominating fragmentation. This is indicative of small or branched alkyl chains being favored. The highest alkyl loss (Figure 6-10, right panel, DBE series 9.0 and 8.5) is of C_5H_{11} and C_6H_{12}, respectively. While this is not a clear criterion against type **2b** or **2d** isomers, with a maximum alkyl loss of C_7H_{15}, this corresponds well with type **2a** or **2c** structures.

Remarkable is the relatively high abundance of DBE 9.5 fragments. These correspond to a loss of fully saturated alkanes, starting from methane, up to pentane, with the maximum intensity observed for the loss of C_2H_6. Such behavior has so far only been reported for *N*-alkylated amines, where nitrogen is not part of an aromatic system, which also includes anilinic **2c** type compounds.[33, 34]

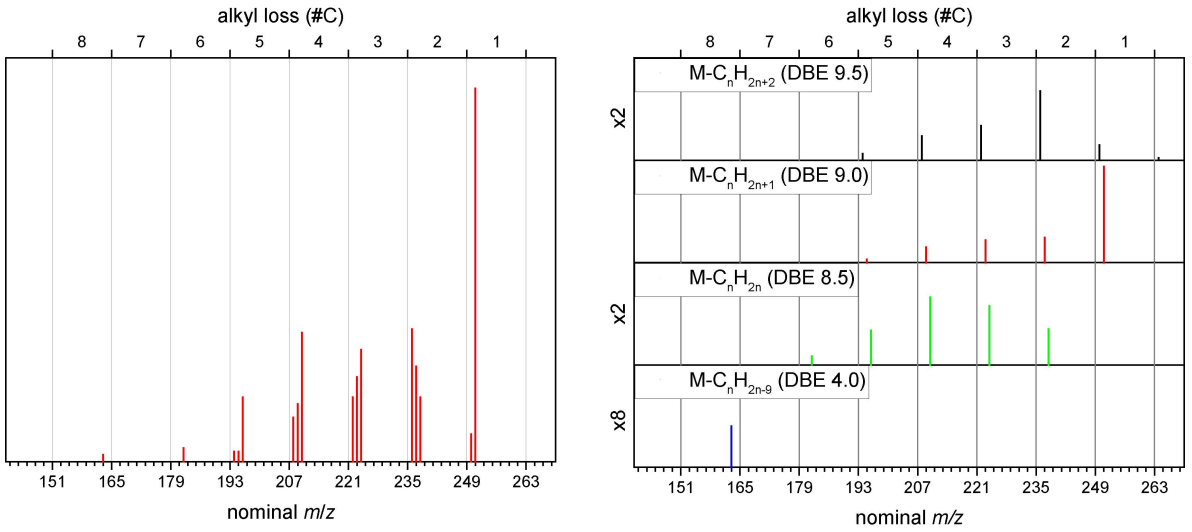

Figure 6-10: Fragment ion spectra of $[C_{19}H_{23}N+H]^+$ after summation over the entire CV range. The bottom axes show the nominal *m/z* of detected fragments ions, while the top axes show the number of carbon atoms lost during fragmentation. Left panel: Summarized spectrum throughout CV range. Right panel: Spectrum separated into different series of fragment ions, corresponding to the indicated DBE values. Where applicable, zoom factors are indicated on the left side.

Two reaction pathways are discussed for this kind of fragmentation. The reaction can progress via a concerted rearrangement, leading to the removal of an alkane. Alternatively, an alkyl radical can be lost from the nitrogen atom, followed by further loss of a second radical from the metastable product. Both pathways, as depicted in Figure 6-11, lead to the formation of a C-N double bond and the net loss of an alkane. In case of a radical mechanism, the formation of an alkane from both radical fragments is, however, unlikely. The present data do not allow any differentiation between both pathways.

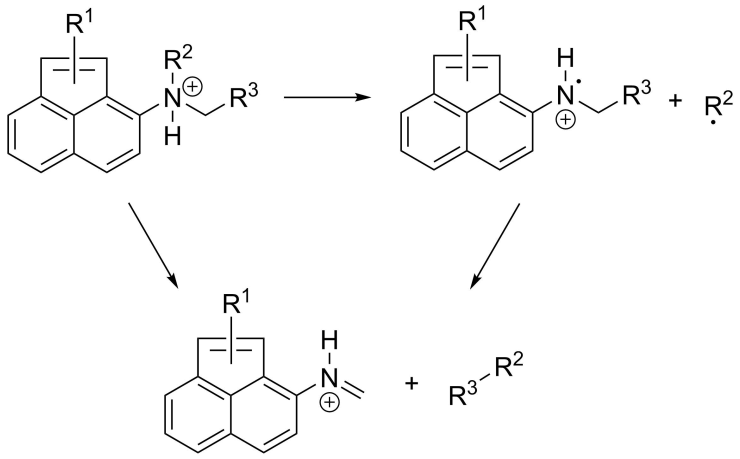

Figure 6-11: Reaction pathways leading to loss of an alkane from *N*-alkylated type **2c** amines. Either a two-step radical process or a concerted rearrangement are possible.

Interesting here is the relative high intensity of the corresponding signals with the loss of ethane being the second most abundant fragmentation observed. This finding is contrasting earlier studies which report aliphatic amines or even anilinic species to be either fully absent or of relatively low abundance.[35-37]

Similar to the previous examples of sulfur containing compounds only one low intensity signal is observed that indicates the loss of an aromatic substructure. The fragment ion observed at *m/z* 163 (bottom trace in Figure 6-10, right side) results from the loss of a C_8H_7 radical, leaving a protonated DBE 4 fragment behind.

Considering the limited possibilities for a reasonable substructure, we propose that this fragmentation originates from some kind of **2d** type pyridinic species with a styrene type substituent as shown in Figure 6-12. To the best of our knowledge no indication has so far been reported for such compounds in crude oil.

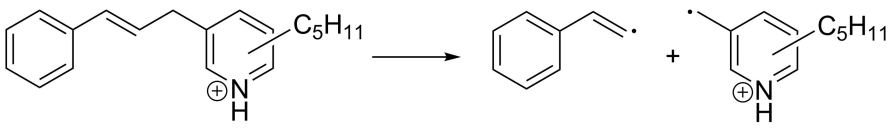

Figure 6-12: Proposed **2d** type parent structure and mechanism for fragmentation resulting in a loss of C_8H_7.

When repeating the experiment with the lab-built electrode setup, the presence of additional isomeric compounds of this type is revealed. The fragment ion traces throughout the scanned CV range are shown in Figure 6-13.

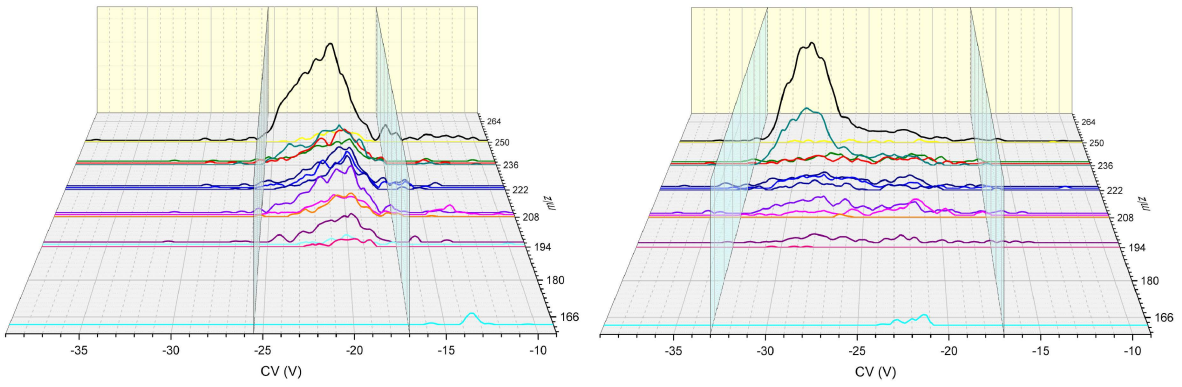

Figure 6-13: Occurrence of fragment ions throughout the ion mobility separation of the parent isomers of *m/z* 266.19033. Left: Standard electrode set (2.50 mm gap); right: Lab-built electrode set (2.25 mm gap). Shaded XZ-planes indicate occurrence of the majority of signals.

As above, here also an overall shift towards more negative compensation voltages is observed. Additionally, for this less complex system, all fragment traces are generally flattened out, while spanning over an increased CV range (~9 V vs ~16 V). Although no single isomers were clearly separated from the rest, this is indicative of a more efficient separation. Regarding the fragment ion at *m/z* 163 three local maxima are observed using the 2.25 mm gap electrodes, at -23.0 V, -22.0 V and -21.4 V.

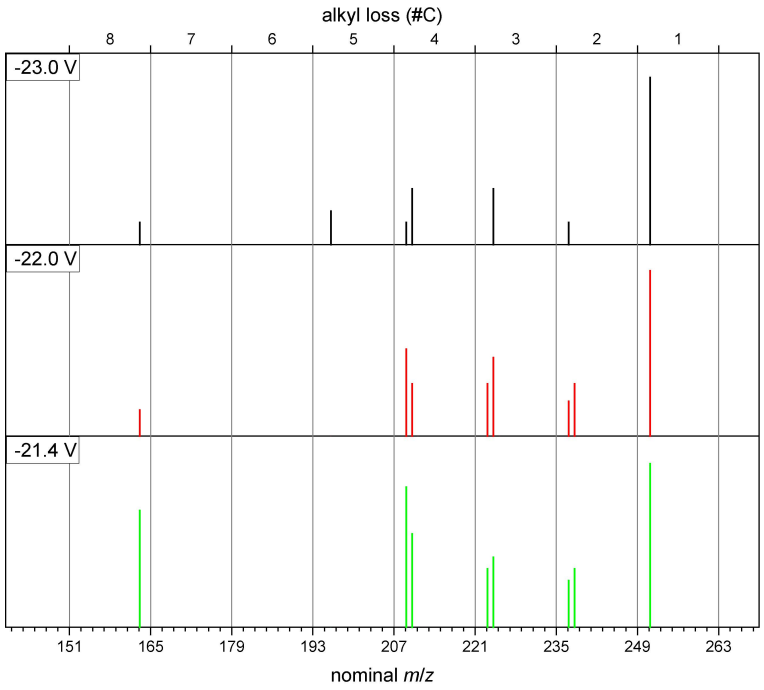

Figure 6-14: Fragment ion spectra, resulting from CID on the parent ion at *m/z* 266.19033. Spectra were recorded at the indicated compensation voltages using the lab-built electrode setup.

The fragment spectra obtained at these compensation voltages are shown in Figure 6-14. It cannot be assumed, that all observed signals originate from a **2d** type structure as a complete separation of isomeric compounds is not likely. Nevertheless, differences in details can be observed, especially between the spectra recorded at -23.0 V and -21.4 V. In the first case loss of a methyl group is the dominating fragmentation pathway, indicating the presence of multiple short alkyl chains, while styryl loss yields only about 10% of the total intensity. For the isomeric compound transmitted at -21.4 V, however, losses of a styryl or a butyl radical (indicating a pentyl substituent) are almost equally abundant. Figure 6-15 shows two possible isomeric structures that might lead to the fragmentation pattern observed at -23 V (**2d-1**) and -21.4 V (**2d-2**). As for all structures shown here, these are possible examples, while no information is available, especially on the positioning of single substituents.

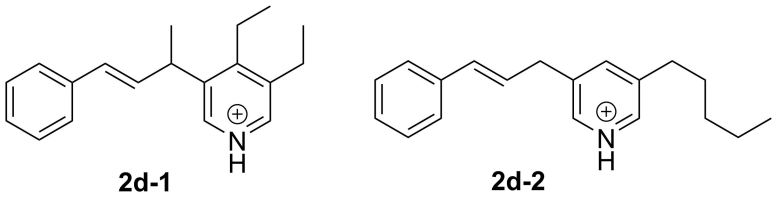

Figure 6-15: Possible structures, leading to the fragmentation pattern shown in Figure 6-14.

6.5 Conclusion

Ultrahigh resolving mass spectrometry has enabled a huge progress in crude oil analysis by its potential to determine elemental compositions of the various analytes present. Still, assumptions on the structure and therefore compound types of detected species mostly rely on the heteroatom content and double bond equivalent only. This will arguably lead to an over-simplification, as it limits the findings to the most common compound classes. Detailed information on the occurrence of isomeric species can only be gained by additional separation techniques. Ion mobility spectrometry is a feasible alternative, especially for heavy crude oils that are not amenable to gas chromatography.

The modification of the source block presented here allows a detailed study also of non-polar compounds in crude oil by photoionization-FAIMS-FTMS. Transmission problems of the initial setup have successfully been addressed. The intrinsic sample simplification within the FAIMS unit also allows monitoring low abundant isomers, which, together with high resolving MS/MS experiments reveals some unexpected features.

The preference of few but long alkyl chains over a more arbitrary distribution in case of the $C_{42}H_{66}S$ isomers is indicative of such species being formed by some selective pathways. Further investigations on the positioning and branching of the alkyl substituents might lead to a deeper understanding on the formation of thiophenic compounds.

Also the high abundance of fragment ions resulting from the loss of an alkyl chain including a non-fused naphthenic ring is remarkable, as DBE 11 and 10 sulfur compounds are typically attributed to di- and tetrahydrobenzonaphthothiophenes. While no indications of high amounts of such compounds are found, phenanthrothiophenic compounds seem to play a certain role within the analyzed sample.

Surprisingly, only little evidence was found for benzothiophenic compounds with a remote phenyl substituent. However, results show that compounds of this type bear the unique

structural feature of the phenyl substituent being in close vicinity to the aromatic core, additionally, holding the majority of the aliphatic portion.

Regarding the nitrogen compounds discussed, an unexpectedly high abundance of fragments from aliphatic amines was observed. Additionally, a peculiar group of compounds was identified that most probably consists of alkylated pyridines, bearing a 3-phenyl-2-propene-1-yl substituent. With the modified set of FAIMS electrodes we were also able to further separate this group of compounds into several isomeric species.

Some of these findings were unexpected and might present compositional features that are special to the crude oil under investigation. The method presented here might therefore also be a useful approach for fingerprinting purposes like source elucidation of oil spills or authentication of blended fuels.

6.6 References

1. Espada, J. J.; Fernández, S.; Velasco, L. and Coto, B., *Evaluation of different methodologies to determine the n-paraffin distribution of petroleum fractions* in: *Fuel* **2013**, *109*, 470-475.

2. O'Donnell, R. J., *Measurement of Fractionation in Analytical Distillation of Crude Oil* in: *Ind. Eng. Chem. Process Des. Dev.* **1973**, *12*(2), 208-211.

3. Argirov, G.; Ivanov, S. and Cholakov, G., *Estimation of crude oil TBP from crude viscosity* in: *Fuel* **2012**, *97*, 358-365.

4. Alomair, O.; Jumaa, M.; Alkoriem, A. and Hamed, M., *Heavy oil viscosity and density prediction at normal and elevated temperatures* in: *J. Pet. Explor. Prod. Technol.* **2016**, *6*(2), 253-263.

5. Rogel, E.; Ovalles, C.; Bake, K. D.; Zuo, J. Y.; Dumont, H.; Pomerantz, A. E. and Mullins, O. C., *Asphaltene Densities and Solubility Parameter Distributions: Impact on Asphaltene Gradients* in: *Energy Fuels* **2016**, *30*(11), 9132-9140.

6. Jia, Z.; Xiao, L.; Wang, Z.; Liao, G.; Zhang, Y. and Liang, C., *Molecular dynamics and composition of crude oil by low-field nuclear magnetic resonance* in: *Magn. Reson. Chem.* **2016**, *54*(8), 650-655.

7. Kovalenko, E. Y.; Golushkova, E. B. and Sagachenko, T. A., *The study of the composition of oils and structure of their components during the preliminary refining of oil feedstock with metal powders* in: *Pet. Chem.* **2016**, *56*(2), 101-108.

8. Corilo, Y. E.; Rowland, S. M. and Rodgers, R. P., *Calculation of the Total Sulfur Content in Crude Oils by Positive-Ion Atmospheric Pressure Photoionization Fourier Transform Ion Cyclotron Resonance Mass Spectrometry* in: *Energy Fuels* **2016**, *30*(5), 3962-3966.

9. Walkner, C.; Gratzer, R.; Meisel, T. and Bokhari, S. N. H., *Multi-element analysis of crude oils using ICP-QQQ-MS* in: *Org. Geochem.* **2017**, *103*, 22-30.

10. Purcell, J. M.; Hendrickson, C. L.; Rodgers, R. P. and Marshall, A. G., *Atmospheric Pressure Photoionization Fourier Transform Ion Cyclotron Resonance Mass Spectrometry for Complex Mixture Analysis* in: *Anal. Chem.* **2006**, *78*(16), 5906-5912.

11. Gaspar, A. and Schrader, W., *Expanding the data depth for the analysis of complex crude oil samples by Fourier transform ion cyclotron resonance mass spectrometry using the spectral stitching method* in: *Rapid Commun. Mass Spectrom.* **2012**, *26*(9), 1047-1052.

12. Gaspar, A.; Zellermann, E.; Lababidi, S.; Reece, J. and Schrader, W., *Characterization of Saturates, Aromatics, Resins, and Asphaltenes Heavy Crude Oil Fractions by Atmospheric Pressure Laser Ionization Fourier Transform Ion Cyclotron Resonance Mass Spectrometry* in: *Energy Fuels* **2012**, *26*(6), 3481–3487.

13. McKenna, A. M.; Williams, J. T.; Putman, J. C.; Aeppli, C.; Reddy, C. M.; Valentine, D. L.; Lemkau, K. L.; Kellermann, M. Y.; Savory, J. J.; Kaiser, N. K.; Marshall, A. G. and Rodgers, R. P., *Unprecedented Ultrahigh Resolution FT-ICR Mass Spectrometry and Parts-Per-Billion Mass Accuracy Enable Direct Characterization of Nickel and Vanadyl Porphyrins in Petroleum from Natural Seeps* in: *Energy Fuels* **2014**, *28*(4), 2454-2464.

14. Cho, Y.; Ahmed, A.; Islam, A. and Kim, S., *Developments in FT-ICR MS instrumentation, ionization techniques, and data interpretation methods for petroleomics* in: *Mass Spectrom. Rev.* **2015**, *34*(2), 248-263.

15. Santos, J. M.; Santos, F. M. L.; Eberlin, M. N. and Wisniewski, A., *Advanced Aspects of Crude Oils Correlating Data of Classical Biomarkers and Mass Spectrometry Petroleomics* in: *Energy Fuels* **2017**, *31*(2), 1208-1217.

16. Zhurov, K. O.; Kozhinov, A. N. and Tsybin, Y. O., *Evaluation of High-Field Orbitrap Fourier Transform Mass Spectrometer for Petroleomics* in: *Energy Fuels* **2013**, *27*(6), 2974-2983.

17. Vetere, A. and Schrader, W., *Mass Spectrometric Coverage of Complex Mixtures: Exploring the Carbon Space of Crude Oil* in: *ChemistrySelect* **2017**, *2*(3), 849-853.

18. Robson, W. J.; Sutton, P. A.; McCormack, P.; Chilcott, N. P. and Rowland, S. J., *Class Type Separation of the Polar and Apolar Components of Petroleum* in: *Anal. Chem.* **2017**, *89*(5), 2919-2927.

19. Zhang, W.; Zhu, S.; Pang, L.; Gao, X.; Zhu, G.-T. and Li, D., *Determination of diamondoids in crude oils using gas purge microsyringe extraction with comprehensive two dimensional gas chromatography-time-of-flight mass spectrometry* in: *J. Chromatogr. A* **2016**, *1478*, 75-83.

20. Byer, J. D.; Siek, K. and Jobst, K., *Distinguishing the C3 vs SH4 Mass Split by Comprehensive Two-Dimensional Gas Chromatography–High Resolution Time-of-Flight Mass Spectrometry* in: *Anal. Chem.* **2016**, *88*(12), 6101-6104.

21. Genuit, W. and Chaabani, H., *Comprehensive two-dimensional gas chromatography-field ionization time-of-flight mass spectrometry (GCxGC-FI-TOFMS) for detailed hydrocarbon middle distillate analysis* in: *Int. J. Mass spectrom.* **2016**, *413*, 27-32.

22. Ahmed, A.; Cho, Y.; Giles, K.; Riches, E.; Lee, J. W.; Kim, H. I.; Choi, C. H. and Kim, S., *Elucidating Molecular Structures of Nonalkylated and Short-Chain Alkyl (n < 5, (CH2)n) Aromatic Compounds in Crude Oils by a Combination of Ion Mobility and Ultrahigh-Resolution Mass Spectrometries and Theoretical Collisional Cross-Section Calculations* in: *Anal. Chem.* **2014**, *86*(7), 3300-3307.

23. Ahmed, A.; Cho, Y. J.; No, M.-H.; Koh, J.; Tomczyk, N.; Giles, K.; Yoo, J. S. and Kim, S., *Application of the Mason−Schamp Equation and Ion Mobility Mass Spectrometry To Identify Structurally Related Compounds in Crude Oil* in: *Anal. Chem.* **2011**, *83*(1), 77-83.

24. Ibrahim, Y. M.; Garimella, S. V. B.; Prost, S. A.; Wojcik, R.; Norheim, R. V.; Baker, E. S.; Rusyn, I. and Smith, R. D., *Development of an Ion Mobility Spectrometry-Orbitrap Mass Spectrometer Platform* in: *Anal. Chem.* **2016**, *88*(24), 12152-12160.

25. Lalli, P. M.; Jarvis, J. M.; Marshall, A. G. and Rodgers, R. P., *Functional Isomers in Petroleum Emulsion Interfacial Material Revealed by Ion Mobility Mass Spectrometry and Collision-Induced Dissociation* in: *Energy Fuels* **2017**, *31*(1), 311-318.

26. Maleki, H.; Ghassabi Kondalaji, S.; Khakinejad, M. and Valentine, S. J., *Structural Assignments of Sulfur-Containing Compounds in Crude Oil Using Ion Mobility Spectrometry-Mass Spectrometry* in: *Energy Fuels* **2016**, *30*(11), 9150-9161.

27. Santos, J. M.; Galaverna, R. d. S.; Pudenzi, M. A.; Schmidt, E. M.; Sanders, N. L.; Kurulugama, R. T.; Mordehai, A.; Stafford, G. C.; Wisniewski, A. and Eberlin, M. N., *Petroleomics by ion mobility mass spectrometry: resolution and characterization of contaminants and additives in crude oils and petrofuels* in: *Anal. Methods* **2015**, *7*(11), 4450-4463.

28. Schrader, W.; Xuan, Y. and Gaspar, A., *Studying ultra-complex crude oil mixtures by using High Field Asymmetric Waveform Ion Mobility Spectrometry (FAIMS) coupled to an ESI-LTQ-Orbitrap Mass Spectrometer* in: *Eur. J. Mass Spectrom.* **2014**, *20*(1), 43.

29. Vetere, A. and Schrader, W., *1- and 2-photon ionization for online FAIMS-FTMS coupling allows new insights into the constitution of crude oils* in: *Anal. Chem.* **2015**, *87*(17), 8874-8879.

30. Porter, D. J.; Mayer, P. M. and Fingas, M., *Analysis of Petroleum Resins Using Electrospray Ionization Tandem Mass Spectrometry* in: *Energy Fuels* **2004**, *18*(4), 987-994.

31. Alachraf, W.; Panda, S. K.; Andersson, J. T. and Schrader, W., *Studying the fragmentation behavior of crude oil relevant compounds by CID mass spectrometry* in: **in submission**.

32. Budzikiewicz, H.; Djerassi, C. and Williams, D. H., *Interpretation of mass spectra of organic compounds* **1964**, Holden-Day, San Francisco.

33. Bosma, N. L. and Harrison, A. G., *An energy-resolved study of the fragmentation reactions of alkyl ammonium ions* in: *Can. J. Chem.* **1994**, *72*(11), 2205-2211.

34. Peters, J.; Clemen, M. and Grotemeyer, J., *Fragmentation of deuterated rhodamine B derivates by laser and collisional activation in an FT-ICR mass spectrometer* in: *Anal. Bioanal. Chem.* **2013**, *405*(22), 7061-7069.

35. Flego, C. and Zannoni, C., *N-containing species in crude oil fractions: An identification and quantification method by comprehensive two-dimensional gas chromatography coupled with quadrupole mass spectrometry* in: *Fuel* **2011**, *90*(9), 2863-2869.

36. Lissitsyna, K.; Huertas, S.; Quintero, L. C. and Polo, L. M., *Novel simple method for quantitation of nitrogen compounds in middle distillates using solid phase extraction and comprehensive two-dimensional gas chromatography* in: *Fuel* **2013**, *104*, 752-757.

37. Singh, D.; Chopra, A.; Patel, M. B. and Sarpal, A. S., *A Comparative Evaluation of Nitrogen Compounds in Petroleum Distillates* in: *Chromatographia* **2011**, *74*(1), 121-126.

7. Quantitative and qualitative analysis of three classes of sulfur compounds in crude oil

Redrafted from:
Vetere, A.; Pröfrock, D. and Schrader, W., *Quantitative and qualitative analysis of three classes of sulfur compounds in crude oil*, submitted to *Angewandte Chemie*.

7.1 Abstract

Due to environmental hazards arising from sulfur containing combustion products, strong legal regulations exist to reduce the sulfur content of transportation fuels down to a few ppm. With the ongoing depletion of low-sulfur crude oil reservoirs, increased technological efforts are needed for crude oil refining to meet these requirements. The desulfurization step is a critical part of the refining process but partly suffers from recalcitrance of certain species against sulfur removal and the inability to quantitatively understand the behavior of individual classes during the process. Here a new and simple approach for the parallel quantification of three different classes of sulfur species present in crude oils using LC-separation and an online detection and quantification by ICP-MS/MS is shown. This new and simple approach will help to estimate the amount of recalcitrant species and thus to allow a better optimization of desulfurization conditions during fuel production.

7.2 Introduction

Albeit strong efforts are undertaken to move from fossil to renewable material based transportation fuels, crude oil is estimated to remain a major energy resource throughout the next decades. Reservoirs of light and sweet (low-sulfur) crudes are meanwhile mostly depleted and heavier and sourer (high-sulfur) oils with sulfur contents of up to 14 wt.-% are shifting into focus.[1] Sulfur containing compounds form SO_{2-3} on combustion and have thus been mainly responsible for the formation of acid rain.[2, 3] Nowadays, strong legal requirements force oil refineries to remove sulfur from any transportation fuel. Limits in the European Union as well as in the United States are as low as 10 ppm.[4, 5] The removal of sulfur by hydrodesulfurization (HDS) arguably is one of, if not the most widely used catalytic reaction in industry. It uses hydrogen at elevated pressures and temperatures on heterogeneous catalysts to yield gaseous H_2S and sulfur-free products.[6] The process, however, is rather unselective and also results in the undesired hydrogenation of aromatic moieties.[7] An example of the reaction and possible byproducts is shown in Scheme 7-1.

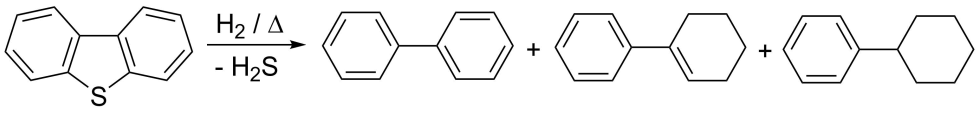

Scheme 7-1: Products of the hydrodesulfurization process with dibenzothiophene as an example.

Unfortunately, a number of sulfur containing compounds withstand the process. Among these recalcitrant species are mostly condensed thiophenic compounds, while non-condensed thiophenes and aliphatic thiols or thioethers (sulfides) are relatively easily converted.[6, 7] To gain high-quality fuels in a cost-efficient and resource saving manner the HDS process needs to be optimized and fine-tuned for any given feedstock that is, in turn, characterized by the large variety of different compounds present therein. This optimization, however, can only be achieved when quantitative information on the total amount of different sulfur species and their distribution into relevant compound classes is available.

To the best of our knowledge no single method has yet been reported for the group-selective quantification of sulfur or any other group of compounds within a full crude oil. Total sulfur content is commonly determined as a bulk parameter through elemental analysis as part of the characterization. However, no molecular information regarding its chemical surrounding is gained with this method.

Numerous studies dealt with the characterization and quantification of sulfur containing compounds in fossil materials. These studies used mostly a gas chromatographic (GC) approach, some relying on molecular mass spectrometry.[8, 9] However, a full quantification of sulfur in a given crude oil sample is not possible by this approach. Response factors of single compounds differ largely from each other and cannot – as often done – be assumed to be unity. Unfortunately, also no reference standards are available for most compounds found in a crude oil since the number of unique compounds is expected to exceed one million.[10] This problem can be avoided by sulfur selective detection with uniform response, because in such a case the response is independent from the chemical surrounding of a sulfur atom and only one reference standard is needed. For this purpose the sulfur chemiluminescence detector (SCD), the atomic emission detector (AED) or inductively coupled plasma mass spectrometry (ICP-MS) have been used after one- and two-dimensional GC separations.[11-16] However, only volatile, thermally stable compounds are amenable by GC, while a considerable portion of a crude oil is non-volatile with molecular weights being well above 500 Da.[17, 18]

Here, a simple, one-step alternative based on an HPLC separation approach developed by Andersson and co-workers is presented.[17, 19, 20] They reported ligand exchange chromatography (LEC) on a Pd(II) coated stationary chromatographic phase for the separation of the aromatic fraction of crude oils into sulfur-free, thiophenic and sulfidic compounds without chemical conversion. Thiophenic compounds are further separated, as non-condensed (1-ring) thiophenes are reported to elute into the sulfur-free fraction, hence the three groups of sulfur containing compounds that differ most in recalcitrance towards HDS – thioethers, 1-ring thiophenes and condensed thiophenes – can be analyzed separately with one method.

For sulfur selective detection and quantification in the liquid phase, inductively coupled plasma mass spectrometry (ICP-MS) is the method of choice as it provides a uniform response due to all analytes being atomized within the plasma. Nonetheless, sulfur quantification by ICP-MS has long been problematic due to low ionization efficiency and molecular interferences on all sulfur isotopes. Most problematic is the interference between the main isotope $^{32}S^{+}$ and $^{16}O_2^{+}$.[21] A novel ICP-MS instrument that includes a collision/reaction cell in a triple-quadrupole (QqQ) setup allows avoiding such interferences.[22] Further details on the principle can be found in section 7.6.2.

The method presented here combines for the first time the liquid chromatographic (LEC) separation of sulfur containing compound classes from a full crude oil with powerful online

detection by different types of mass spectrometry. This allows qualitative assignments of the molecular species by ultrahigh resolution mass spectrometry using direct coupling to an Orbitrap analyzer[23] and additionally, online sulfur selective detection and quantification by ICP-MS/MS. Prior to quantification by ICP-MS/MS the separation conditions were altered from the original protocol and verified by online HPLC-FTMS using photoionization in a separate experiment. The general experimental setup is depicted in Figure 7-1. Details on alterations of the original LC-protocol can be found in section 7.6.1.

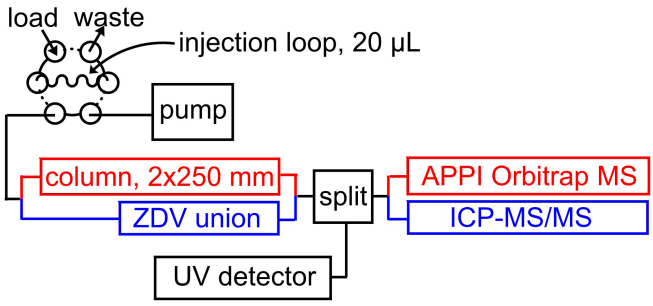

Figure 7-1: Experimental setup for the course of this study, red and blue routes are alternatives with only one active at a time. Qualitative analyses were performed by hyphenation of the HPLC separation to APPI Orbitrap MS. Alternatively, quantitative analyses were run using ICP-MS/MS. Calibration for ICP-MS/MS and loop injections of the full samples were done after replacing the LC column with a Zero-Dead-Volume (ZDV) union. In all cases the mobile phase flow was split 1:20 and the larger flow routed to a UV detector for alignment of the mass spectrometric datasets.

7.3 Experimental

The stationary phase for LEC was prepared by suspending pre-dried (240 °C, 24 h) silica gel (10 g, LiChrosorb® Si-100, 10 µm, Merck KGaA, Darmstadt, Germany) in dry toluene (100 mL). After addition of 3-mercaptopropanotrimethylsiloxane (18 mL) the mixture was refluxed under argon for 24 h. Afterwards the mercaptopropano-modified silica gel (MPSG) was filtered off, washed with toluene and methanol (100 mL each) and stored overnight at 50 °C. The dried material was then suspended in water (150 mL), $PdCl_2$ was added (1.60 g) and the mixture was stirred for 1 h, until the color of the suspension changed from light brown to deep red. The Pd-loaded MPSG was then filtered off, washed with water and methanol (100 mL each) and stored overnight at 50 °C for further use.

HPLC columns were prepared by wet-packing of the prepared Pd-MPSG (slurry in propan-2-ol) into empty stainless steel columns (Vertex Plus, 2×250 mm, Knauer Wissenschaftliche Geräte GmbH, Berlin, Germany) at an operating pressure of 400 bar.

HPLC separations were performed using an Ultimate 3000 HPLC system (DIONEX Softron GmbH, Germering, Germany), with parameters as follows:

- Stationary phase: Pd-MPSG, 2×250 mm, column temperature 25 °C
- Mobile phase: A: pre-mixed cyclohexane/toluene (9:1, *V*/*V*), B: tetrahydrofuran
- Gradient: 0-12 min: 0 % B – 12-25 min: 4 % B – 25-35 min: 15 % B – 35-40 min: 100 % B – 47-60 min: 0 % B
- Injection volume: 20 µL
- Flowrate: 300 $\mu L \cdot min^{-1}$, post-column split: 1:20 (high flow to UV, low flow to MS)
- UV-detection: 287 nm and 357 nm

Online MS detection for qualitative evaluation of the separation behavior was performed using ultrahigh resolution FTMS (Orbitrap Elite, Thermo Fisher Scientific, Bremen, Germany) with atmospheric pressure photoionization (APPI). As light source a Kr VUV lamp with photon emission at 10.0/10.6 eV (Syagen Technology, Santa Ana, CA, USA) was used. Mass spectra were recorded in full scan mode (m/z 200-1,200) at a scan rate of 0.67 Hz ($R > 480{,}000$ at m/z 400, FWHM). Peak assignment and data evaluation was performed using Composer64 software (v1.5, Sierra Analytics, Modesto, CA, USA).

Sulfur quantification was performed by ICP-MS/MS (8800 Triple Quadrupole ICP-MS, Agilent Technologies, Santa Clara, CA, USA). Since only organic solvents were used for the chromatographic separation, Pt cones, a low i.d. torch, a cooled spray chamber as well as O_2 addition have been utilized to eliminate any carbon build up during the measurements. To overcome the interference problem when analyzing sulfur via ICP based techniques the MS/MS reaction mode was used to monitor the transition from S^+ to SO^+ (m/z 32 → 48) using the following instrumental settings:

- RF Power: 1600 W
- Nebulizer: Elemental Scientific PFA micro flow
- Carrier Gas Flow: 0.7 $L \cdot min^{-1}$
- Make up gas flow: 0.1 $L \cdot min^{-1}$
- Optional Gas setting: 29.5 % (10 % O_2 (6.0 purity) in 90 % Ar (5.0 purity))
- Torch i.d.: 1.0 mm
- Spray chamber: -2 °C

- Cell gas 4 setting: 30 % O_2 (6.0 purity)
- Wait time: 2 ms
- Dwell time: 0.1 s
- Monitored Isotopes/Transitions: $^{32}S^+ \rightarrow {}^{32}S^{16}O^+$, $^{105}Pd^+ \rightarrow {}^{105}Pd^+$

Calibration and sulfur quantification for the unseparated sample were done by duplicate loop injections (20 µL) into a continuous mobile phase flow (300 µL·min^{-1}, 0 % B) with the HPLC column removed from the system. As calibrant dibenzo[*b*,*d*]thiophene (Sigma-Aldrich, Taufkirchen, Germany, 98 %), diluted in mobile phase A was used. Samples were diluted in mobile phase A to a final concentration of 25 µg·mL^{-1} for loop injection and 1000 µg·mL^{-1} for HPLC separation. Peak integration and data evaluation were performed using Origin software (v9.2G, OriginLab Corporation, Northhampton, MA, USA).

The crude oil was a gift from industry without any further information of its origin and properties.

7.4 Results and Discussion

Wang and co-workers recently introduced an alternative approach to separate thiophenic from sulfidic compounds.[24] Their protocol, however, included several derivatization procedures with a total of seven single steps over the course of about two weeks, each of which bearing the risk of errors. This is a rather tedious and time consuming procedure and therefore, here a method is introduced that allows the analysis of different sulfur containing classes directly after online separation by HPLC. The separation performance of our protocol was verified by online coupling of the LC system to an ultrahigh resolving FT Orbitrap Elite mass spectrometer (Thermo Fisher Scientific, Bremen, Germany). The chromatographic behavior of the sulfur containing classes was monitored by piecewise summation of the mass spectra obtained and assignment of elemental compositions to the resulting peaks. This allows a thorough characterization of the eluting compounds. At the mass resolving power given, hydrocarbons are easily distinguished from sulfur containing compounds, also in minute amounts. With the change of mobile phase three main fractions were eluted, as expected (Figure 7-2, left panel). The first fraction (F1), eluted between 2-15.5 min, mainly consists of sulfur-free hydrocarbons, with sulfur containing compounds being only of minor abundance as is shown in the class distribution in the right panel of Figure 7-2.

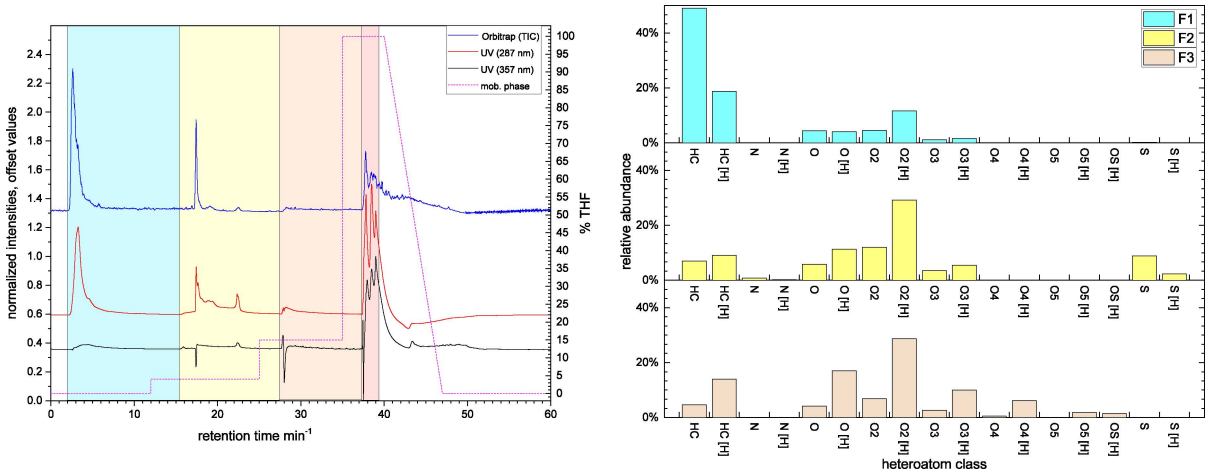

Figure 7-2: Qualitative evaluation of the LC separation. The left panel shows the UV-chromatograms (black and red) and the total ion chromatogram (TIC) obtained for Orbitrap-MS (blue). Shaded boxes indicate fraction boundaries, containing the distinct compound groups. The amount of THF in the mobile phase is indicated by the purple dashed line (right axis). The right panel shows intensity based class distributions throughout the given fractions. Note that with the given setup, sulfidic species in fractions 3 and 4 are mostly detected as oxidized, protonated molecules ($[M+OH]^+$ and $[M+O_2H]^+$).

These species include non-condensed thiophenic species with double bond equivalents (DBE) of 3 or higher (see also top panel in Figure 7-3). The DBE 4 series corresponds to tetrahydrobenzothiophenes, the next high abundance DBE series 7 corresponds to thiophenes with an additional non-condensed phenyl-group or four naphthenic rings in a side chain.

The second fraction (F2, 15.5-27.5 min), eluted by the addition of 4 % THF, contains condensed thiophenic species (DBE 6 and higher), with local maxima for benzothiophenes (DBE 6), dibenzothiophenes (DBE 9) and benzonaphthothiophenes (DBE 12).

For the remainder of the chromatographic run sulfidic species are eluted, as can be seen from the changed DBE distribution (Figure 7-3). The last fraction (27.5-39.5 min) can be divided into two sub-fractions. Compounds with DBE 8 or 9 are eluting first (F3, 27.5-37 min). These correspond to thioethers with two phenyl substituents on the sulfur that are more easily released due to a lower nucleophilicity. In fact, the most abundant signal here represents diphenyl sulfide ($C_{12}H_{10}S$).

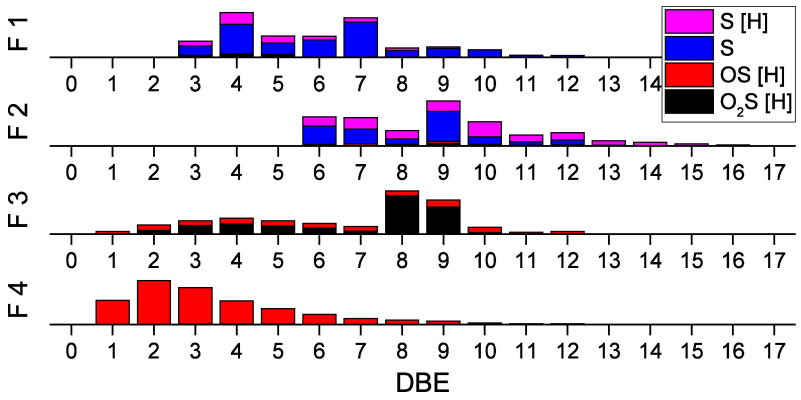

Figure 7-3: Intensity based DBE distributions of the sulfur containing classes throughout the different fractions.

Sulfides with no direct attachment of aromatic groups are predominantly eluted by very high concentrations of competitive ligand (THF) during minutes 37-39.5 (F4). Here, DBE series 1 to 3 dominate, indicating the aliphatic nature of the corresponding compounds. Common among the later fractions is that sulfur containing compounds are mostly detected as oxidized, protonated species. Sulfoxides are not typically abundant in crude oils and also data from measurements using electrospray ionization do not suggest that such species are present in high amounts in this sample. It has previously been shown that easily oxidizable compounds (such as sulfides) are susceptible to in-source oxidation when using atmospheric pressure photo-ionization (APPI) as was the case here.[25]

Focus here was the group-type resolved quantification of sulfur in a whole crude oil in a one-step analysis, using liquid chromatographic separation. For external calibration the chromatographic column was replaced by a ZDV union, such that injection loop fillings of dibenzo[*b*,*d*]thiophene (DBT) were directly introduced into a continuous flow of mobile phase (100 % A). The same setup was used for direct loop injection of the full crude oil sample (25 µg·mL^{-1}) without chromatographic separation. The calibration curve spanned a range between 2 and 34 ng sulfur per injection, with the linear correlation coefficient being R = 0.998. Loop injections were performed in duplicate. The overall sulfur content of the whole crude oil was found to be 0.475±0.007 wt.-%. The result was confirmed by standard addition of DBT to the sample, resulting in a content of 0.48±0.03 wt.-%.

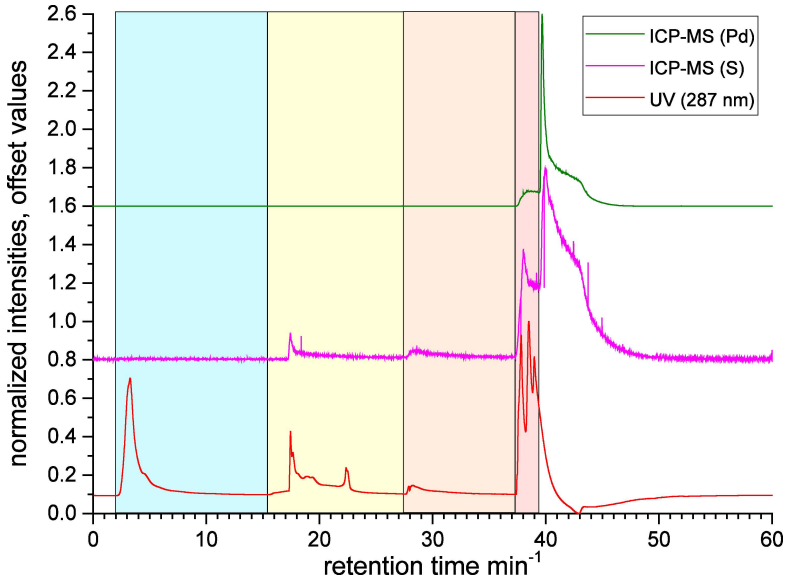

Figure 7-4: LC-ICP-MS/MS chromatograms obtained after separation of the crude oil sample. The red trace represents the UV-chromatogram at 287 nm, used for alignment of the datasets. Additionally, the S (magenta) and Pd (green) selective chromatograms obtained by ICP-MS/MS are shown. Shaded boxes indicate fraction boundaries, containing the distinct compound groups.

For group type separated quantification the LC column was introduced into the system as shown in Figure 7-1 and the crude oil sample (1,000 µg·mL^{-1}) was injected onto the column. As depicted in Figure 7-4 the sulfur selective chromatogram of the ICP-MS/MS follows the UV trace (and therefore also the Orbitrap MS data) as expected. The area of the first peak, representing 1-ring thiophenes, is relatively small and therefore not seen in the figure due to scaling. This is expected, as non-condensed thiophenes are typically not very abundant compared with (di-)benzothiophenes. A major difference between the sulfur selective trace in ICP-MS/MS and the chromatograms obtained by HPLC-UV and HPLC-FTMS is an additional sharp increase in intensity at 39.5 min with the mobile phase being 100 % THF. This signal coincides with the appearance of significant amounts of palladium (see green trace in Figure 7-4) in the effluent. It seems that small amounts of Pd are released from the stationary phase when using such high amounts of competitive ligand. However, the sulfur eluted along with the Pd cannot be attributed to the injected sample. No relevant amounts of corresponding species are found during qualitative FTMS analysis. Also is the overall amount of sulfur detected after 39.5 min by far exceeding expectations. This portion alone would account for a sulfur recovery of 342 %. One suggestion is that a considerable portion of the sulfur detected after 39.5 min originates from sulfur directly bound to the Pd-ion, such as the used mercaptopropano linker. For these reasons, integration of the sulfur trace was only performed

until the valley before significant Pd-elution begins (39.5 min), giving a total sulfur recovery of 95.8 %.

Overall integration results, given in Table 7-1, show that the total amount of sulfur eluted from this sample is mainly present in sulfidic species (79.8 %), followed by condensed thiophenes (19.1 %). Only a minor amount of sulfur is present as non-condensed thiophenes (1.1 %). Compared with loop injection results 95.8 % recovery of sulfur compounds was achieved. A few, though typically minor compound classes cannot be addressed by this method. Thiols and disulfides have been reported to be irreversibly retained by the column and will therefore contribute to the non-recovered portion of the crude. However, both classes as well as the non-eluting sulfides can be considered as easily desulfurizable.

Table 7-1: Quantitative results of sulfur content after direct loop injection (total sulfur) and after LC fractionation into different compound classes (F1-4). LC recoveries are compared with loop injection results. Values are wt.-% sulfur within the sample.

total sulfur (wt.-%)	F1[a] wt.-% S	F2[b] wt.-% S	F3[c] wt.-% S	F4[c] wt.-% S	recovery (F1-3)	recovery (F1-4)
0.475 ±0.007	0.005 ±0,001	0.087 ±0,001	0.063 ±0,001	0.300 ±0,001	32.7% ±0.6%	95.8% ±0.8 %

[a] non-condensed (1-ring) thiophenes. [b] condensed thiophenes. [c] sulfides.

7.5 Conclusion

The direct quantification of individual species in crude oil suffers from the complexity given by more than one million distinct chemical compounds present in such samples. In general, quantification requires a pure signal and an individually determined response factor for each compound of interest. Here, for the first time the quantitative analysis of compound groups present in a complex crude oil is presented by combining uniform response detection via ICP-MS/MS with molecular detection using APPI-Orbitrap MS, both utilizing separation capabilities from liquid chromatography.

The online HPLC-FTMS data gained by FT Orbitrap mass spectrometry clearly show a successful separation of sulfur containing species into three main groups of compounds, namely non-condensed thiophenes, condensed thiophenes and thioethers. Overall, the results shown here present a new fast and group-selective quantification of sulfur present in a whole crude oil. The method does not require any sample pretreatment, other than dilution, and is additionally capable of analyzing also non-volatile and/or thermally labile compounds. The information

gained by this technique should enable processing refineries to optimize their desulfurization workflows and thus support the manufacturing of high-quality fuels at economical costs with lower environmental contamination.

Despite the high signal intensity observed when washing the column with 100 % THF the integration results using the chromatographic data still agree well with the results from the loop injection measurements. Thus, when loop injections are used for a determination of the total sulfur content of the sample, the chromatographic approach followed here can be used to easily and quantitatively distinguish between different groups of sulfur containing species. Still, further investigations should be undertaken to avoid the release of palladium from the stationary phase, which should also lead to a prolonged lifetime of the chromatographic columns.

7.6 Appendix

7.6.1 Adaption of the original LEC protocol

For the course of this study an adaption of the chromatographic method introduced by Andersson and co-workers was necessary as their mobile phase system was not suitable for our purpose. The basic mobile phase was changed from a cyclohexane (CH) / dichloromethane (DCM) mixture, replacing DCM with toluene. Thus, solubility for the entire sample is assured, while reducing the risk of rapidly corroding the cones and lenses of the ICP-MS/MS system by large amounts of chlorinated solvents. Additionally, the presence of ammonia as strong competitive ligand for the elution of sulfides was avoided. This increased the reproducibility of the separation, as the addition of ammonia often leads to a loss in retention of the sulfur containing species. Finally, propan-2-ol (^{i}PrOH) was replaced with tetrahydrofuran (THF) during this work as experiments showed a high background for the *m*/*z* 32 → 48 transition when adding ^{i}PrOH to the mobile phase.

7.6.2 Operating principle of 8800 Triple Quadrupole ICP-MS for the analysis of sulfur

A major problem for the ICP-MS analysis of sulfur is the presence of isobaric interferences for all stable isotopes. The most dominant interference being between $^{16}O_2^+$ and $^{32}S^+$ (*m*/*z* 32). The instrument used during this study has a triple-quadrupole setup, including a collision/reaction cell. The setup allows selected reaction monitoring (SRM) to follow the transition from $^{32}S^+$ to $^{32}S^{16}O^+$ (*m*/*z* 32 → 48).[22] A sulfur ion selected in the first quadrupole stage (along with $^{16}O_2^+$) is reacted with oxygen gas in the collision cell and the resulting SO^+ ion (*m*/*z* 48) is selected in the third quadrupole, while all other interfering masses are rejected (compare Figure 7-5). Thus,

interference from both $^{16}O_2^+$ (*m/z* 32) with $^{32}S^+$ and also from $^{36}Ar^{12}C^+$ (*m/z* 48) with SO^+ are eliminated.

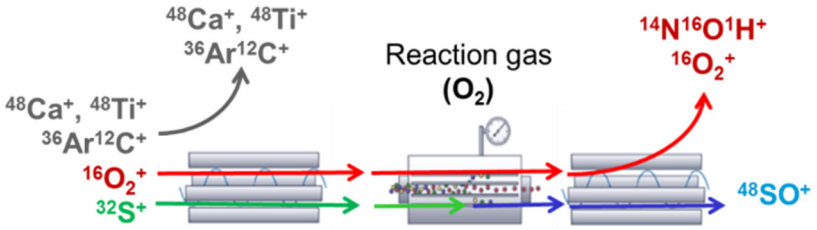

Figure 7-5: Operation principle of ICP-MS/MS in the O_2 mass shift mode for sulfur detection. Q1 is set to allow the transition of all ions with *m/z* 32, while all other ions, which show the same nominal mass as the targeted reaction product (SO^+) are rejected. Inside the cell $^{32}S^+$ reacts with O_2 to form its oxide, while the interfering $^{16}O_2^+$ dimer does not indicate any reactivity. Q2 is finally set to allow only the transition of *m/z* 48, while all other masses are rejected, which allows the sensitive, interference free determination of sulfur using its main isotope ^{32}S.

7.7 References

1. Andersson, J. T., *Schwefel in Erdöl: Ein problematisches Element?* in: *Chem. unserer Zeit* **2005**, *39*(2), 116-120.

2. Likens, G. E. and Bormann, F. H., *Acid Rain: A Serious Regional Environmental Problem* in: *Science* **1974**, *184*(4142), 1176-1179.

3. Galloway, J. N.; Dianwu, Z.; Jiling, X. and Likens, G. E., *Acid rain: china, United States, and a remote area* in: *Science* **1987**, *236*(4808), 1559-1562.

4. *E. Parliament Directive 98/70/EC of 13 October 1998 relating to the quality of petrol and diesel fuels and amending Council Directive 93/12/EEC.*

5. *CFR, Title 40, Chapter I , Subchapter C, Part 80, Subpart O, Section 80.1603 of Gasoline sulfur standards for refiners and importers.*

6. Javadli, R. and de Klerk, A., *Desulfurization of heavy oil* in: *Appl. Petrochem. Res.* **2012**, *1*(1), 3-19.

7. Sun, Y. and Prins, R., *Hydrodesulfurization of 4,6-dimethyldibenzothiophene over noble metals supported on mesoporous zeolites* in: *Angew. Chem. Int. Ed.* **2008**, *47*(44), 8478-8481.

8. Li, M.; Wang, T. G.; Simoneit, B. R. T.; Shi, S.; Zhang, L. and Yang, F., *Qualitative and quantitative analysis of dibenzothiophene, its methylated homologues, and benzonaphthothiophenes in crude oils, coal, and sediment extracts* in: *J. Chromatogr. A* **2012**, *1233*, 126-136.

9. Müller, H.; Adam, F. M.; Panda, S. K.; Al-Jawad, H. H. and Al-Hajji, A. A., *Evaluation of Quantitative Sulfur Speciation in Gas Oils by Fourier Transform Ion Cyclotron Resonance Mass Spectrometry: Validation by Comprehensive Two-Dimensional Gas Chromatography* in: *J. Am. Soc. Mass. Spectrom.* **2012**, *23*(5), 806-815.

10. Blomberg, J.; Schoenmakers, P. J.; Beens, J. and Tijssen, R., *Compehensive two-dimensional gas chromatography (GC×GC) and its applicability to the characterization of complex (petrochemical) mixtures* in: *J. High. Resolut. Chromatogr.* **1997**, *20*(10), 539-544.

11. Behbehani, H. and Andari, M. K., *Determination of Organic Sulfur Compound Types in Vacuum Gas Oils Using Gc-Fid-Scd Method* in: *Pet. Sci. Technol.* **2000**, *18*(1-2), 51-61.

12. Hua, R.; Li, Y.; Liu, W.; Zheng, J.; Wei, H.; Wang, J.; Lu, X.; Kong, H. and Xu, G., *Determination of sulfur-containing compounds in diesel oils by comprehensive two-dimensional gas chromatography with a sulfur chemiluminescence detector* in: *J. Chromatogr. A* **2003**, *1019*(1–2), 101-109.

13. Hua, R.; Wang, J.; Kong, H.; Liu, J.; Lu, X. and Xu, G., *Analysis of sulfur-containing compounds in crude oils by comprehensive two-dimensional gas chromatography with sulfur chemiluminescence detection* in: *J. Sep. Sci.* **2004**, *27*(9), 691-698.

14. López García, C.; Becchi, M.; Grenier-Loustalot, M. F.; Païsse, O. and Szymanski, R., *Analysis of Aromatic Sulfur Compounds in Gas Oils Using GC with Sulfur Chemiluminescence Detection and High-Resolution MS* in: *Anal. Chem.* **2002**, *74*(15), 3849-3857.

15. Mössner, S. G. and Wise, S. A., *Determination of Polycyclic Aromatic Sulfur Heterocycles in Fossil Fuel-Related Samples* in: *Anal. Chem.* **1999**, *71*(1), 58-69.

16. Bouyssiere, B.; Leonhard, P.; Pröfrock, D.; Baco, F.; Lopez Garcia, C.; Wilbur, S. and Prange, A., *Investigation of the sulfur speciation in petroleum products by capillary gas chromatography with ICP-collision cell-MS detection* in: *J. Anal. At. Spectrom.* **2004**, *19*(5), 700-702.

17. Müller, H.; Andersson, J. T. and Schrader, W., *Characterization of high-molecular-weight sulfur-containing aromatics in vacuum residues using Fourier transform ion cyclotron resonance mass spectrometry* in: *Anal. Chem.* **2005**, *77*(8), 2536-2543.

18. Panda, S. K.; Andersson, J. T. and Schrader, W., *Characterization of supercomplex crude oil mixtures: what is really in there?* in: *Angew. Chem. Int. Ed.* **2009**, *48*(10), 1788-1791.

19. Japes, A.; Penassa, M. and Andersson, J. T., *Analysis of Recalcitrant Hexahydrodibenzothiophenes in Petroleum Products Using a Simple Fractionation Process* in: *Energy Fuels* **2009**, *23*(4), 2143-2148.

20. Nolte, T.; Posch, T. N.; Huhn, C. and Andersson, J. T., *Desulfurized Fuels from Athabasca Bitumen and Their Polycyclic Aromatic Sulfur Heterocycles. Analysis Based on Capillary Electrophoresis Coupled with TOF MS* in: *Energy Fuels* **2013**, *27*(1), 97-107.

21. Giner Martínez-Sierra, J.; Galilea San Blas, O.; Marchante Gayón, J. M. and García Alonso, J. I., *Sulfur analysis by inductively coupled plasma-mass spectrometry: A review* in: *Spectrochim. Acta, Part B* **2015**, *108*, 35-52.

22. Hanousek, O.; Brunner, M.; Profrock, D.; Irrgeher, J. and Prohaska, T., *The performance of single and multi-collector ICP-MS instruments for fast and reliable 34S/32S isotope ratio measurements* in: *Anal. Methods* **2016**, *8*(42), 7661-7672.

23. Vetere, A. and Schrader, W., *Mass Spectrometric Coverage of Complex Mixtures: Exploring the Carbon Space of Crude Oil* in: *ChemistrySelect* **2017**, *2*(3), 849-853.

24. Wang, M.; Zhao, S.; Chung, K. H.; Xu, C. and Shi, Q., *Approach for Selective Separation of Thiophenic and Sulfidic Sulfur Compounds from Petroleum by Methylation/Demethylation* in: *Anal. Chem.* **2015**, *87*(2), 1083-1088.

25. Panda, S. K.; Brockmann, K. J.; Benter, T. and Schrader, W., *Atmospheric pressure laser ionization (APLI) coupled with Fourier transform ion cyclotron resonance mass spectrometry applied to petroleum samples analysis: comparison with electrospray ionization and atmospheric pressure photoionization methods* in: *Rapid Commun. Mass Spectrom.* **2011**, *25*(16), 2317-2326.

8. Combining HPLC-FTMS and HPLC-ICP-MS/MS: Qualitative and quantitative analysis of sulfur compounds in heavy crude oil and its fractions

Redrafted from:
Vetere, A.; Pröfrock, D. and Schrader, W., *Combining HPLC-FTMS and HPLC-ICP-MS/MS: Qualitative and quantitative analysis of sulfur compounds in heavy crude oil and its fractions*, submitted to *Analytical Chemistry*.

8.1 Abstract

Sulfur and its efficient removal are among the most discussed issues in crude oil refining and processing. Strong legislative regulations are in effect that force producers to virtually remove sulfur from their products. This is commonly done by hydrodesulfurization (HDS) using hydrogen and heterogenous catalysts. The optimization of the process, however, requires a good understanding of the amount and nature of the sulfur containing compounds in the raw material. Here, we present for the first time the combination of a sulfur selective chromatographic separation of crude oil fractions on a Pd-coated stationary phase with direct sulfur quantification by ICP mass spectrometry.

8.2 Introduction

A major concern in crude oil refining and processing and therefore for evaluation of feedstock rentability is the sulfur content. Sulfur in crude oil and related subfractions is mostly present as thiophenes (aromatic sulfur) or as sulfides/thioethers or disulfides (aliphatic sulfur).[1] Sulfur containing species form SO_2 on combustion and are thus held responsible for adverse environmental effects such as acid rain. Therefore strong regulations are in place in the United States as well as in the European Union and in other countries that limit the amount of sulfur present in any end-product (transportation or heating fuel). For land-based vehicles these limitations are as low as 10-15 $mg \cdot kg^{-1}$ sulfur.[2] Considering an average initial sulfur content of 2-5 wt.-% (with as much as 14 wt.-% reported for specific single feedstocks [3]) this means that a substantial effort has to be undertaken to virtually remove all sulfur from the original supply before a high quality product can be produced.

During refinery, sulfur is typically removed from single distillation cuts by treatment with hydrogen at elevated pressures and temperatures (hydrodesulfurization, HDS). However, certain components like alkylated dibenzothiophenes show some resistance towards the process that is performed on a heterogenous (solid) catalyst. Removal of these recalcitrant compounds requires somewhat harsher conditions, i.e. higher hydrogen pressure and/or temperature. This, on the other hand, leads to unwanted side-effects such as over-hydrogenation of aromatic structures.[4]

To economically produce a high-quality fuel that meets the current as well as future legislative requirements, a feedstock dependent fine-tuning of the HDS process is desirable. This, however, can only be achieved if information is available on the amount and distribution of sulfur containing species present. Especially information on the amount of recalcitrant compounds, i.e. condensed thiophenes like benzo- and especially dibenzothiophenes is of great importance. Other compounds such as non-condensed thiophenes or sulfidic species are less problematic and can be desulfurized with relative ease.[4]

A group-selective quantification of sulfur within a crude oil or a crude oil subfraction requires either a quantitative method using a detector that allows the distinction of the different groups of analytes or the employment of a separation step that allows analyzing the different groups one after the other.

Numerous studies have been carried out using gas chromatography as a separation step, due to its unmatched separating power for volatile compounds.[1, 5-12] Detectors used range from sulfur selective detection using either a chemiluminescence detector (SCD)) or an atomic emission detector (AED) to mass spectrometric detection (MS), mostly involving low resolving mass spectrometers. For a comprehensive and group-selective analysis all of these approaches suffer from different drawbacks. Sulfur quantification by GC-MS using electron ionization or atmospheric pressure ionization techniques is only possible for known compounds that are available as pure reference materials. Response factors of various compounds differ largely and cannot be assumed to be uniform. Unfortunately, only a very limited number of naturally occurring compounds is commercially available or can easily be synthesized at the required purity. Zimmermann and co-workers reported circumvention of the problem for volatile petroleum constituents by determination of average response factors for groups of compounds with no to three aromatic rings and interpolation of the data based on the effective carbon number.[13, 14] However, uncertainties of the determined response factors increased strongly with molecular weight, rendering the approach not useful for heavy crude oils. The problem of unknown response is alternatively avoided fully when using sulfur selective detectors with a uniform response as is the case for SCD and AED.[15] However, the analysis will still be limited to only volatile compounds, while constituents of crude oils easily excess a molecular weight of 500 Da. Additionally, a true gas chromatographic separation of compound groups according to the chemical surrounding of the embedded sulfur has yet to be reported.

An alternative separation approach has been reported by Andersson and co-workers who employed a liquid chromatographic separation using ligand exchange chromatography (LEC) on a Pd-coated stationary phase.[9, 16-20] Their main separation, using the aromatic fraction of a crude oil, resulted in three fractions. The first fraction (Pd1) holding mainly sulfur-free hydrocarbons, the second (Pd2) consisting of condensed thiophenic species (benzothiophenes and above) and a third fraction (Pd3) containing sulfidic species. However, reports show non-condensed thiophenes to be eluted into the first (Pd1) fraction.[16, 18] This separation approach is therefore adequate to separate the most recalcitrant condensed thiophenes from the less problematic non-condensed thiophenes and from easily desulfurized thioethers. Additionally, compound volatility is not an issue here as liquid chromatography is used.

The analytical approach presented here, uses an online separation based on the work presented by Andersson and co-workers combined with sulfur selective detection using inductively coupled plasma mass spectrometry (ICP-MS/MS). The separation behavior was verified by

separate measurements in an online HPLC-MS approach using ultra-high resolving Fourier transform Orbitrap Mass Spectrometry (FTMS).

Sulfur quantification by ICP-MS has long been a challenging task due to low sensitivity and/or omnipresent polyatomic interferences for all sulfur isotopes.[21-24] Recently, a new ICP mass spectrometer was introduced that takes advantage of a triple quadrupole setup (8800 Triple Quadrupole ICP-MS, Agilent Technologies, Santa Clara, CA, USA). The second analyzer stage is a collision/reaction cell with an octopole ion guide (ORS), rather than a conventional quadrupole. For sulfur quantification the system can be run in selected reaction monitoring (SRM) mode. In the first quadrupole stage ions of *m/z* 32 (S^+ and O_2^+) are selected and transmitted to the reaction cell, where they are reacted with oxygen gas. Thus, sulfur is oxidized to form SO^+ ions, which are detectred at *m/z* 48 by the second quadrupole. Thus, the transition *m/z* 32 → 48 is monitored, effectively avoiding any polyatomic interferences.[25-27]

8.3 Experimental

8.3.1 Sample preparation

Crude oil fractions were obtained from a very heavy crude oil of North American origin following a modified SARA fractionation (**S**aturates, **A**romatics, **R**esins, **A**sphaltenes) scheme developed in our lab that is based on a modified IP 143 procedure for the separation of asphaltenes as published elsewhere,[28] followed by a modified open tubular chromatography, collecting an additional, second resin fraction. Briefly, asphaltenes were precipitated from a heavy crude oil (8.626 g) after refluxing in *n*-heptane (30 mL·g^{-1}) for an hour and subsequent storing overnight. The precipitate was filtered off, washed with hot *n*-heptane (50 mL) and residual maltenes were removed by soxhlet extraction with *n*-heptane for 2 h. Final asphaltenes were recovered as black flakes (0.970 g) by replacing the extraction solvent with toluene and continuous extraction for 20 h, followed by evaporation of the solvent in vacuo (50 mbar). *n*-Heptane extracts were combined with the filtrate for further separation of the maltene fraction. Activated neutral alumina (10 g, Brockman I grade) was suspended in the solution prior to evaporation to dryness and the maltene loaded alumina was placed on top of a chromatographic column (activated neutral alumina, 3×40 cm). Four fractions were eluted consecutively using cyclohexane (300 mL), cyclohexane/dichloromethane (1:1, 600 mL), methanol (500 mL) and ethyl acetate (500 mL). Fraction boundaries were monitored by UV absorption (254 nm) of the effluent. All solvents were evaporated in vacuo (50 mbar) to give the final fractions of saturates (0.762 g, colorless liquid), aromatics (4.540 g, yellow liquid),

resins I (0.774 g, brown, highly viscous oil) and resins II (0.511 g, brown solid). A total recovery of 87.6 % was achieved. For further analyses the samples were dissolved in cyclohexane/toluene (9:1).

8.3.2 Preparation of HPLC columns

The stationary phase for ligand exchange chromatography was prepared based on the protocol by Andersson and co-workers.[16] Briefly, silica gel (10 g, LiChrosorb® Si 100, 10 µm, Merck KgAA, Darmstadt, Germany), was dried for 24 h at 240 °C and then suspended in dry toluene (50 mL). 3-Mercaptopropyltrimethoxysilane (18 mL) was added and the mixture was refluxed under argon for 24 h. The colorless mercaptopropano modified silica gel (MPSG) was then filtered off, washed consecutively with toluene and methanol (100 mL each) and stored at 50 °C overnight. Palladium loading was performed by suspending MPSG (6 g) in water (50 mL) and adding $PdCl_2$ (1 g). The mixture was vigorously stirred for 1 h, during which the color changed from brownish to red. The Pd-loaded silica gel (Pd-MPSG) was then filtered off, washed with water (100 mL) and acetone (50 mL) and stored at 50 °C overnight to give the final stationary phase as an orange-red powder. HPLC columns (2×250 mm) were prepared by wet-packing the prepared stationary phase (slurry in propan-2-ol) using a pneumatic pump (Smartline 1950, Knauer Wissenschaftliche Geräte GmbH, Berlin, Germany) at a packing pressure of 400 bar.

8.3.3 Liquid Chromatography

The chromatographic conditions were changed from the protocol developed by Andersson and co-workers to meet our purposes. To avoid excessive contamination and corrosion of the ICP-MS/MS cones and lens stack the original mobile phase was altered from a mixture of cyclohexane (CH) and dichloromethane to cyclohexane with toluene (TOL). The presence of 10% toluene within the mobile phase additionally proves beneficial for the mass spectrometric analysis using photoionization (APPI), as it serves as an efficient dopant.[29] Also the competitive ligand was modified as propan-2-ol showed a high background on the *m/z* 32 → 48 transition. Thus, the mobile phase system was changed to tetrahydrofuran (THF) as competitive ligand. Also the use of ammonia was avoided, as it results in poor reproducibility and also bad column reusability due to deterioration of the stationary phase. Instead, a highly increased amount of THF was used for the elution of sulfidic compounds. HPLC separations were performed using an Ultimate 3000 HPLC system (DIONEX Softron GmbH, Germering, Germany) with parameters as follows: stationary phase: Pd-MPSG, 2×250 mm, mobile phase: A: pre-mixed CH/TOL (9:1, *V/V*), B: THF, gradient: 0-12 min: 0 % B – 12-25 min: 4 % B –

25-35 min: 15 % B – 35-40 min: 100 % B – 47-60 min: 0 % B; injection volume: 20 µL; flowrate: 300 µL·min^{-1}, post-column split: 1:6 (250 µL·min^{-1} to UV, 50 µL·min^{-1} to MS for Orbitrap MS), 1:20 (285 µL·min^{-1} to UV, 15 µL·min^{-1} to MS for ICP-MS/MS); UV-detection: 287 nm and 357 nm.

Thus, three main fractions were obtained between 2-17 min (Pd1), 17-27 min (Pd2) and 27-38 min (Pd3), as stated above. The final 13 minutes of the gradient are used to recondition the column for the following run. Fractions were directly analyzed by online hyphenation to both mass spectrometric devices used.

8.3.4 FT Orbitrap Mass Spectrometry

Qualitative analyses of the crude oil and its fractions after HPLC separation were performed using online FTMS on a research-type Orbitrap Elite (Thermo Fisher Scientific, Bremen, Germany).[30] Ionization was performed by APPI using a Kr VUV lamp with photon emission at 10.0 and 10.6 eV (Syagen Technology, Santa Ana, CA, USA). Source settings used were a vaporizer temperature of 350 °C, sheath gas flow of 40, auxiliary gas flow of 10 and sweep gas flow of 5 (arbitrary units each). Mass spectra were recorded in full scan mode between *m/z* 200 and *m/z* 1,200 at a mass resolution of 480,000 (FWHM at *m/z* 400). Sample flow rate was adjusted to 50 µL·min^{-1} using a post-column split. Data analysis was performed using Composer64 software (v1.50, Sierra Analytics, Modesto, CA, USA) after accumulation of several individual spectra. For a more detailed investigation of the chromatographic behavior of the whole crude oil bins of 1 min width were analyzed individually and results transferred to a lab-written database for further interpretation. Alternatively, bins covering the entire fractions were averaged and the results used for verification of the overall separation process.

8.3.5 ICP Mass Spectrometry

Quantitative analysis of sulfur content was performed on a 8800 Triple Quadrupole ICP-MS (Agilent Technologies, Santa Clara, CA, USA) using the following instrument parameters: RF Power: 1600 W, Nebulizer: Elemental Scientific PFA micro flow, Carrier Gas Flow: 0.7 L·min^{-1}**,** Make up gas flow: 0.1 L·min^{-1}**,** Optional Gas setting: 29.5 % (10 % O_2 (6.0 purity) in 90 % Ar (5.0 purity)), Torch i.d.: 1.0 mm, Spray chamber: -2 °C, Cell gas 4 setting: 30 % O_2 (6.0 purity), Wait time: 2 ms, Dwell time: 0.1 s, Monitored Isotopes/Transitions: $^{32}S^+ \rightarrow {}^{32}S^{16}O^+$, $^{105}Pd^+ \rightarrow {}^{105}Pd^+$.

Sample/mobile phase flow rate was provided by the HPLC system at a flow rate of 300 µL·min^{-1}. Before entering the plasma, any flow from the HPLC system was split down to 15 µL·min^{-1}. Calibration and total sulfur quantification without separation were performed by duplicate loop injections into a continuous flow of mobile phase A. For this purpose, the chromatographic column was removed from the system and bypassed using a ZDV union. As calibrant dibenzo[*b*,*d*]thiophene, diluted in mobile phase A was used. Peak integration and data evaluation were done using Origin software (v9.2G, OriginLab Corporation, Northhampton, MA, USA).

8.4 Results and Discussion

8.4.1 Qualitative analysis of sulfur compounds

The original chromatographic protocol, published by Andersson and co-workers, was based on a different mobile phase system and was only performed on the aromatic fraction of crude oils or fuels. Figure 8-1 shows results from a first implementation of the method for online HPLC-FTMS using a scan rate of 2 Hz, yielding a mass resolution of 120,000 (FWHM at *m/z* 400).

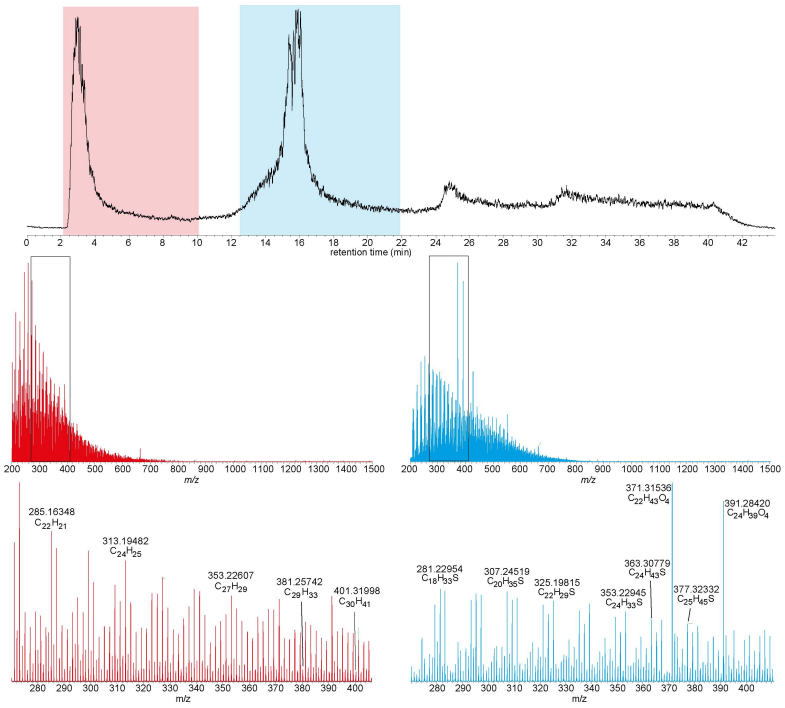

Figure 8-1: Total ion chromatogram (TIC) recorded from HPLC-FTMS analysis of a heavy crude oil, using the original protocol published by Andersson and co-workers (top). Mass spectra gained throughout the first (red) and second (blue) chromatographic peak are shown in the center panel. Examples for assigned elemental compositions are given for the distinct zoomed portions of the spectra (bottom).

The lower panels show spectra that were gained throughout the first two chromatographic peaks and zoomed portions thereof. A clear separation of sulfur-free hydrocarbons and sulfur containing thiophenic compounds can be observed. These results also show how the method reduces the need for utmost mass resolving power, as the most problematic isobars are chromatographically separated from each other.

Prior to using it for online separation/quantification by HPLC-ICP-MS/MS the method had, however, to be modified as stated above. The modified method was additionally verified using high resolving FTMS of molecular species with APPI as a rather unselective but soft ionization method, using a mass resolution of 480,000 (FWHM at *m/z* 400).

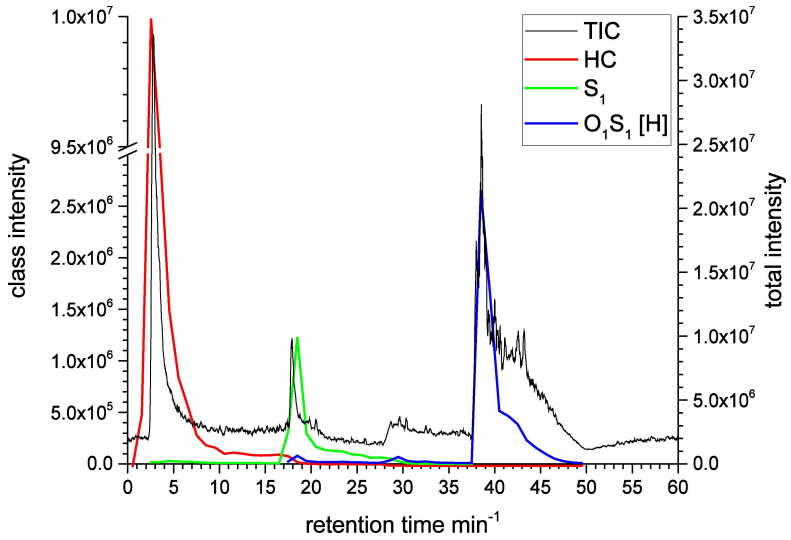

Figure 8-2: TIC recorded from HPLC-FTMS analysis of whole crude oil (black). Additionally, reconstructed class chromatograms (RCC) for hydrocarbons (radical cations, red), S_1-compounds (radical cations, green) and oxygenated S_1-compounds (O_1S_1, protonated molecules, blue) are shown. Note the axis break for the left y-axis (class intensity).

As can be seen in Figure 8-2, a series of broad, major peaks is observed in the total ion chromatogram (TIC, black). These coincide with the elution of sulfur-free hydrocarbons (red, Pd1) and different groups of sulfur containing compounds (green (Pd2) and blue (Pd3)) that are effectively separated from each other. The figure shows “reconstructed class chromatograms” (RCC), giving the summed intensities of all signals attributed to members of the respective class. Nitrogen containing compounds elute predominately around 18-30 min into the Pd2 fraction, while a variety of oxygenated compounds is observed throughout the entire chromatogram.

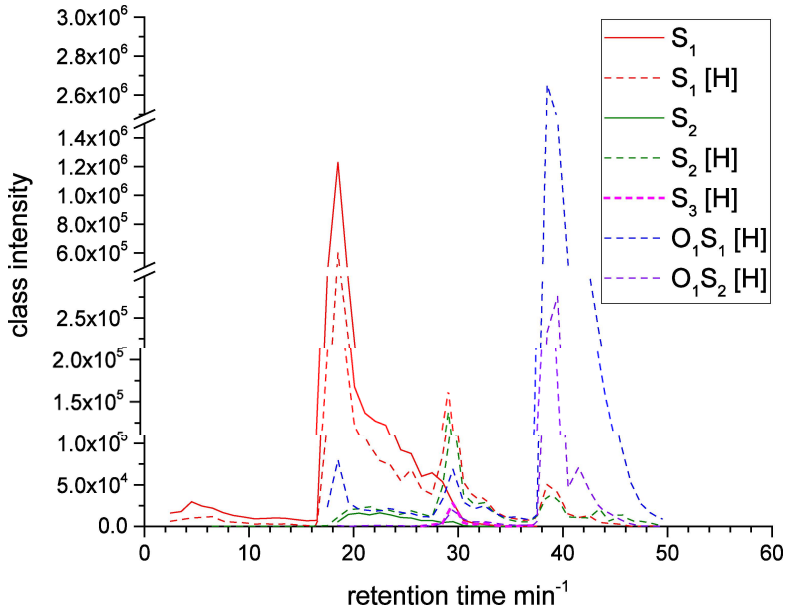

Figure 8-3: RCC for sulfur containing compounds in the whole crude oil sample. S_1 (red), S_2 (green) and S_3 (magenta) compounds are shown as well as oxygenated compounds O_1S_1 (blue) and O_1S_2 (purple). Solid lines represent radical cations, dashed lines account for protonated molecules. Note the axis break for the y-axis.

A closer look onto the sulfur containing compounds is given in Figure 8-3. The RCC of the S_1 class (radical cations, red solid line) shows two local maxima, one around 5 (Pd1), the other around 20 minutes (Pd2) retention time. According to expectation, these can be attributed to non-condensed thiophenes that are only weakly retained by the used stationary phase and to condensed thiophenes (benzothiophenes and above) respectively.

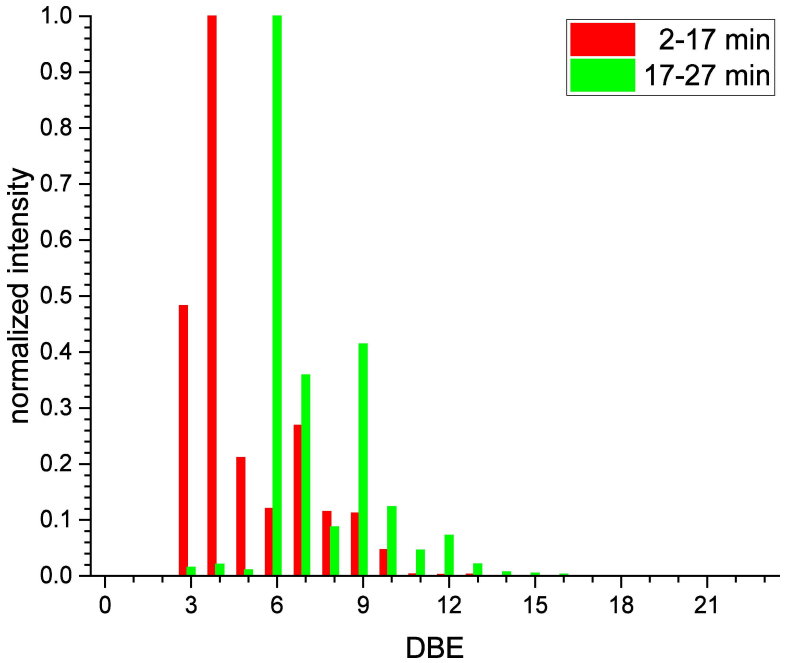

Figure 8-4: Double bond equivalent (DBE) distribution of S_1 class (radical cations), summed over time ranges 2-17 min (Pd1, red) and 17-27 min (Pd2, green). For a clearer representation, intensities were normalized.

As can be seen from Figure 8-4, double bond equivalents (DBE) of the sulfur containing compounds eluting into Pd1 fraction (red bars) start from 3, as is expected for thiophenes. Local maxima are observed at DBE 4 and 7, which correspond to tetrahydrobenzothiophenes and to phenyl-substituted thiophenes, respectively. Compounds eluted into Pd2 fraction (green bars) start at DBE 6, which corresponds to benzothiophenes, with additional local maxima at 9 and 12 (dibenzothiophenes and benzonaphthothiophenes), as is expected. The distinct 3-DBE-pattern is typical for thiophene related structures.[31] Only neglectable carry-over of DBE 3-5 compounds from the first fraction is observed.[16, 18]

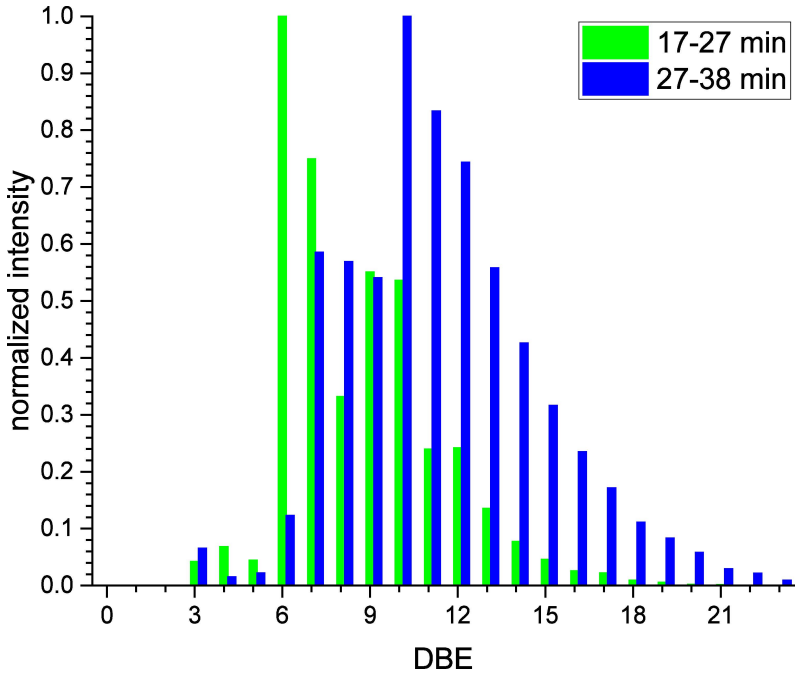

Figure 8-5: DBE distribution of S_1 class (protonated molecules), summed over time ranges 17-27 min (Pd2, green) and 27-38 min (Pd3, blue). For a clearer representation, intensities were normalized.

Also the RCC of S_1-compounds detected as protonated molecules (red dashed line in Figure 8-3) shows two local maxima, corresponding with Pd2 and Pd3 fractions. The DBE distribution of compounds eluting into Pd2 fraction largely follows that of compounds detected as radical cations (see green bars in Figure 8-5). Although ionization as radical cations seems favored in case of thiophenic compounds,[32] dopant-assisted photoionization does yield a certain amount of protonated molecules from the same analytes.[33] These compounds can therefore be considered thiophenic as well. The DBE distribution of compounds eluted into Pd3 fraction shows a distinctly different behavior. While radical cations of S_1-compounds are almost absent from the mass spectra, protonated molecules are still observed. Local maxima of the DBE distribution are, however, shifted to 3, 7 and 10. These values can be attributed to

hexahydrobenzothiophenes and naphthalene and phenanthrene substituted thioethers respectively.

A large portion of sulfur containing compounds that are eluted into Pd3 fraction is detected as oxygenated compounds, mostly as protonated molecules with a heteroatom content of O_1S_1. The DBE distribution of these compounds is compared to that of the respective, oxygen-free S_1-compounds in Figure 8-6. The majority of the eluted compounds is remarkably less aromatic, the DBE maximum being 2. The corresponding species must contain sulfur in a non-aromatic environment, i.e. they must be thioethers or sulfides. However, the species are detected as ions containing both sulfur and oxygen. As sulfoxides are not commonly abundant in crude oil and as this finding is reproducible throughout a variety of different samples, the observed ions must have been oxidized. To date, it cannot be concluded whether this oxidation is happening on column with palladium acting as a catalyst or whether this is happening in the ion source during the ionization process. It has been shown, however, that easily oxidizable species – such as aliphatic thioethers – are susceptible to in-source oxidation during photoionization, most likely by an OH-radical initiated ion-molecule reaction.[34]

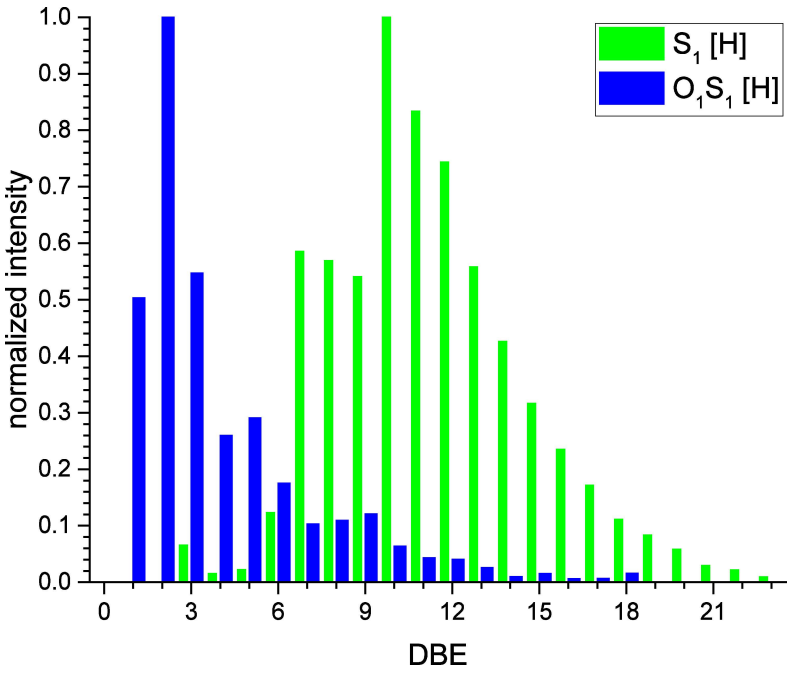

Figure 8-6: DBE distribution of S_1 (green) and O_1S_1 (blue) classes (protonated molecules), summed over the time range 27-38 min (Pd3). For a clearer representation intensities were normalized.

The majority of O_1S_1-compounds is eluted after 38 min, largely dominated by DBE 1-3. This can also be seen from the left panel in Figure 8-7. Here, the area of individual dots is based on the summed signal intensity for the corresponding DBE series. O_1S_1-compounds observed

during Pd2 fraction largely follow the DBE distribution observed for thiophenic species. These can therefore be regarded as belonging to the same group of compounds that have been oxidized during the analysis.

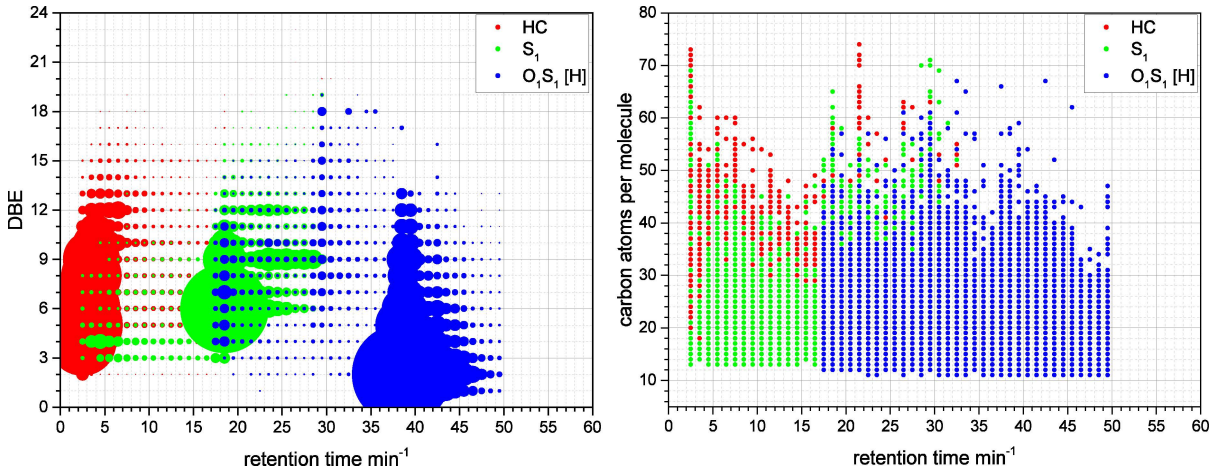

Figure 8-7: Elution behavior of hydrocarbons (red), S_1 compounds (green) and O_1S_1 compounds (blue) throughout the chromatogram. The left panel shows data grouped by DBE of eluting substances. Dot size is based on summed total intensity of the corresponding series. The right panel shows data based on the amount of carbon per molecule of eluting compounds.

Within Pd3 fraction sulfidic compounds with a higher degree of aromaticity (higher DBE) are eluted earlier, while low DBE, aliphatic compounds are only eluted with very high amounts of competitive ligand (THF). This can be explained given the strong interaction of aliphatic sulfur with palladium on the stationary phase. Compounds with an aryl-substituted sulfur atom, however, are expected to be recovered more easily due to the lower electron density at the sulfur center and therefore a weaker interaction with the stationary phase.

Additionally, we observed that not all sulfidic species can be fully recovered from the column, but are largely irreversibly bound to the stationary phase. This finding is also verified by TEM-EDX data that reveals sulfur to be built up on the particles of the stationary phase after repetitive usage.

Interestingly, the behavior for hydrocarbons and aromatic sulfur components seems to be opposite. As can be seen from the left panel in Figure 8-7 for both heteroatom classes compounds with lower DBE are eluted slightly earlier. For hydrocarbons, compounds with DBE below 10 are eluted first (2-5 min), while compounds with DBE above 10 are mostly eluted after 4-10 min. In case of sulfur compounds, thiophenes elute before benzothiophenes, which, in turn, are eluted earlier than dibenzothiophenes. As can be seen from the right panel of

Figure 8-7, also compounds with a higher degree of alkylation (higher amount of carbon per molecule) are eluted first in the case of hydrocarbons and thiophenes. Both trends suggest that a slight interaction exists between the stationary phase and the π-system of the analytes. In case of aliphatic sulfur compounds, these trends are counteracted by the strong interaction of the sulfur, such that the more aromatic compounds are eluted earlier. With both factors competing, no clear trend can be observed regarding the degree of alkylation of sulfidic compounds.

8.4.2 Quantitative analysis of sulfur within crude oil and its fractions

For the group-selective quantification of sulfur the same chromatographic method was used. However, instead of molecular mass spectrometry by FTMS a sulfur selective detection with uniform response had to be used. This was done by direct coupling of the chromatographic separation to ICP-MS/MS. Calibration was performed by loop injection into a continuous flow of mobile phase A. Measurements were performed with loop injections of the samples without chromatographic separation as well, by replacing the chromatographic column with a ZDV union. Loop injections of crude oil samples were done for quantification of the total sulfur content and for evaluation of sulfur recovery from the chromatographic system. Sample concentrations for later chromatographic separations were estimated based on the data obtained from loop injections.

The sulfur content of the entire crude oil was determined to be 3.34±0.02 wt.-% with values varying between a minimum of 0.036±0.002 wt.-% for the saturate fraction and a maximum of 4.76±0.13 wt.-% for the resin II fraction. Detailed values for each fraction are given in Table 8-1.

The sulfur content of the asphaltene fraction seems unexpectedly low, as it is commonly the fraction most rich in sulfur compounds. This effect is probably related to the fact that asphaltene components become increasingly less soluble and volatile, making the nebulization process less effective. Also, whether very large asphaltenic compounds are fully atomized by the ICP is open to debate. However, the combined and weighted sulfur content of all individual fractions, being 3.59 wt.-%, matches well with the data obtained from the whole crude oil, when taking into account that only 87.6 wt.-% of the original sample have been recovered after SARA fractionation. The difference includes compounds that did not elute from the chromatographic column as well as volatile species that were evaporated at 50 mbar. The non-recovered fraction of the sample (12.4 wt.-%) is thus assumed to have a total sulfur content of around 1.57 wt.-%.

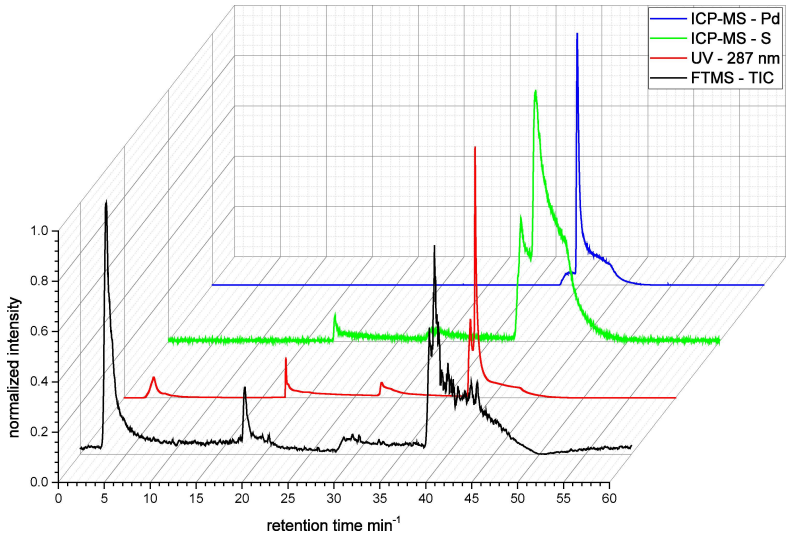

Figure 8-8: Stacked chromatograms, combining HPLC-FTMS data (TIC) and HPLC-ICP-MS/MS data (S and Pd ion traces) of a crude oil sample. Alignment of the different chromatograms was done using the UV trace recorded in each case.

For the group-selective quantification of sulfur the chromatograms obtained using HPLC-FTMS and HPLC-IPC-MS/MS were aligned according to the UV absorption at 287 nm recorded during both experiments. This is exemplarily shown in Figure 8-8 for the whole crude oil sample. On the sulfur selective trace, monitoring the *m/z* 32 → 48 transition, peaks are observed at the same positions, as expected. The sulfur peak during fraction Pd1 is not seen in the figure due to scaling.

Additionally, a fourth peak, eluting after 38 min, is seen. However, this peak coincides with the appearance of large amounts of palladium in the effluent when using 100 % THF as mobile phase, as can be seen from Figure 8-8. Under these conditions small amounts of the metal are obviously released from the stationary phase. As both the palladium and the sulfur trace directly coincide, the sulfur detected after 38 min retention time cannot be related to the injected sample. If considered, this portion alone would make up for a 100-200 % recovery of sulfur from the sample. We suggest that a considerable amount of the sulfur detected here is directly bound to the Pd-ions eluted, e.g. in form of the mercaptopropano linker used. Therefore, integration of the sulfur trace was performed only until minute 38. The crude oil investigated here is relatively rich in sulfidic compounds with 61.8 % of the detected sulfur falling into the sulfidic fraction Pd3 (see Table 8-1).

The majority of thiophenic compounds is found within the aromatic fraction (30.2 % of all sulfur detected), as is expected. For later fractions a shift towards excess sulfidic compounds is observed. For the increasingly less soluble fractions of resin I and II and asphaltenes only a

poor recovery of less than 25 % was achieved. This will be partly due to solubility issues of the less soluble fraction in the used mobile phase system. This also shows the possibilities and limits of this method. Especially for the asphaltene fraction a generally poor solubility within the mobile phase and therefore a poor chromatographic recovery can be presumed. Also, as already stated above, the nebulization and ionization process might not have been optimal for the detection of the corresponding species.

Table 8-1: Mass balance of SARA fractionation and results of sulfur quantification. Total S content is based on loop injection experiments. Values are given as mass fraction within the given fraction as well as regarding the whole crude oil. Mass fractions w_{Pdx} are calculated from HPLC-ICP-MS/MS analysis, with LC recovery being calculated based on the findings of loop injections.

sample	m g SARA	m wt.-% SARA	w_{total}(S) wt.-% fraction	w_{total}(S) wt.-% crude	w_{Pd1}(S) wt.-% LC-ICP	w_{Pd2}(S) wt.-% LC-ICP	w_{Pd3}(S) wt.-% LC-ICP	w_{Pd1-3}(S) wt.-% LC-ICP	recovery % LC-ICP
wh. crude	**8.626**	**100**	**3.34(2)**		**0.019**	**1.47**	**2.39**	**3.87**	**116.0**
saturates	0.762	8.834	0.036(2)	0.003	0.006	0.025	0.004	0.036	99.3
aromatics	4.540	52.632	3.91(2)	2.06	0.020	1.81	0.951	2.78	71.1
resins I	0.774	8.973	4.74(3)	0.425	0.041	0.501	0.478	1.02	21.5
resins II	0.511	5.924	4.76(13)	0.282	0.013	0.291	0.371	0.675	14.2
asphaltenes	0.970	11.245	3.32(13)	0.373	0.018	0.292	0.264	0.575	17.3
Σ(fractions)	**7.557**	**87.607**	**3.59**	**3.14**	**0.020**	**1.20**	**0.680**	**1.90**	**52.9**

Overall, the results from the individual fractions match well with those obtained from the whole crude. In both cases the amount of non-condensed thiophenes adds up to 0.020 wt.-%, while slightly less condensed thiophenes are found when summing over the fractions (1.47 vs 1.20 wt.-%).

8.5 Conclusion

The results presented here show the first application of an online HPLC-FTMS analysis for the detailed analysis of sulfur species in heavy crude oil and its fractions. The protocol developed by Andersson and co-workers was successfully implemented to allow for a fast and thorough analysis of sulfur species in crude oil without the need of previous fraction collection.

An additional benefit of this approach is the almost complete separation of some of the most problematic isobars for the mass spectrometric analysis of crude oil. Typically, utmost resolving power is required to differentiate between compounds differing by C_3 vs SH_4 (Δm = 3.4 mDa). As the majority of the relevant compounds is now eluting at different times, mass spectrometers

that are more frequently available or more suitable for hyphenation to chromatography, such as fast scanning Exactive Orbitraps or high performance Q-TOF instruments, can be used for a comprehensive analysis instead of more expensive FTMS systems.

Qualitative data gained by HPLC-FTMS coupling show that assumptions on the chromatographic behavior made for the stationary phase have been correct. Additionally, the chromatographic procedure was successfully modified to meet the requirements of HPLC-ICP-MS/MS couplings, while keeping up the known separating power.

Using these findings, we have successfully implemented the separation step into a simple, single-step procedure for the easy quantification of sulfur in crude oil and its individual fractions by ICP-MS/MS. To the best of our knowledge, this is the first time detailed information on the distribution of non-condensed and condensed thiophenes as well as sulfidic species and their abundance in crude oil fractions is reported.

For this study a very heavy crude oil was chosen to evaluate the limits of the methodology. Especially the large portion of the asphaltene fraction, which is the least soluble and non-volatile portion of the crude oil, shows unexpectedly low sulfur recoveries during chromatographic separation. This indicates the potential and the limits of the method for such heavy feedstocks with the current solvent system, due to solubility issues. Further improvement of the method, especially regarding mobile phase composition and the nebulization/ionization process is therefore necessary. Also, additional fine tuning of the method should help avoiding the release of palladium from the stationary phase.

8.6 References

1. Hua, R.; Li, Y.; Liu, W.; Zheng, J.; Wei, H.; Wang, J.; Lu, X.; Kong, H. and Xu, G., *Determination of sulfur-containing compounds in diesel oils by comprehensive two-dimensional gas chromatography with a sulfur chemiluminescence detector* in: *J. Chromatogr. A* **2003**, *1019*(1–2), 101-109.

2. *E. Parliament Directive 98/70/EC of 13 October 1998 relating to the quality of petrol and diesel fuels and amending Council Directive 93/12/EEC*.

3. Andersson, J. T., *Schwefel in Erdöl: Ein problematisches Element?* in: *Chem. unserer Zeit* **2005**, *39*(2), 116-120.

4. Javadli, R. and de Klerk, A., *Desulfurization of heavy oil* in: *Appl. Petrochem. Res.* **2012**, *1*(1), 3-19.

5. Andersson, J. T.; Hegazi, A. H. and Roberz, B., *Polycyclic aromatic sulfur heterocycles as information carriers in environmental studies* in: *Anal. Bioanal. Chem.* **2006**, *386*(4), 891-905.

6. Beens, J. and Tijssen, R., *An on-line coupled HPLC-HRGC system for the quantitative characterization of oil fractions in the middle distillate range* in: *J. Microcolumn Sep.* **1995**, *7*(4), 345-354.

7. Beens, J. and Tijssen, R., *The characterization and quantitation of sulfur-containing compounds in (heavy) middle distillates by LC-GC-FID-SCD* in: *J. High. Resolut. Chromatogr.* **1997**, *20*(3), 131-137.

8. Behbehani, H. and Andari, M. K., *Determination of Organic Sulfur Compound Types in Vacuum Gas Oils Using Gc-Fid-Scd Method* in: *Pet. Sci. Technol.* **2000**, *18*(1-2), 51-61.

9. Hegazi, A. H. and Andersson, J. T., *Limitations to GC-MS Determination of Sulfur-Containing Polycyclic Aromatic Compounds in Geochemical, Petroleum, and Environmental Investigations* in: *Energy Fuels* **2007**, *21*(6), 3375-3384.

10. Li, M.; Wang, T. G.; Simoneit, B. R. T.; Shi, S.; Zhang, L. and Yang, F., *Qualitative and quantitative analysis of dibenzothiophene, its methylated homologues, and benzonaphthothiophenes in crude oils, coal, and sediment extracts* in: *J. Chromatogr. A* **2012**, *1233*, 126-136.

11. López García, C.; Becchi, M.; Grenier-Loustalot, M. F.; Païsse, O. and Szymanski, R., *Analysis of Aromatic Sulfur Compounds in Gas Oils Using GC with Sulfur Chemiluminescence Detection and High-Resolution MS* in: *Anal. Chem.* **2002**, *74*(15), 3849-3857.

12. Lu, H.; Shi, Q.; Lu, J.; Sheng, G.; Peng, P. a. and Hsu, C. S., *Petroleum Sulfur Biomarkers Analyzed by Comprehensive Two-Dimensional Gas Chromatography Sulfur-Specific Detection and Mass Spectrometry* in: *Energy Fuels* **2013**, *27*(12), 7245-7251.

13. Jennerwein, M. K.; Eschner, M.; Gröger, T.; Wilharm, T. and Zimmermann, R., *Complete Group-Type Quantification of Petroleum Middle Distillates Based on Comprehensive Two-Dimensional Gas Chromatography Time-of-Flight Mass Spectrometry (GC×GC-TOFMS) and Visual Basic Scripting* in: *Energy Fuels* **2014**, *28*(9), 5670-5681.

14. Jennerwein, M. K.; Sutherland, A. C.; Eschner, M.; Gröger, T.; Wilharm, T. and Zimmermann, R., *Quantitative analysis of modern fuels derived from middle distillates – The impact of diverse compositions on standard methods evaluated by an offline hyphenation of HPLC-refractive index detection with GC×GC-TOFMS* in: *Fuel* **2017**, *187*, 16-25.

15. Hsu, C. S. and Shi, Q., *Prospects for petroleum mass spectrometry and chromatography* in: *Sci. China: Chem.* **2013**, *56*(7), 833-839.

16. Japes, A.; Penassa, M. and Andersson, J. T., *Analysis of Recalcitrant Hexahydrodibenzothiophenes in Petroleum Products Using a Simple Fractionation Process* in: *Energy Fuels* **2009**, *23*(4), 2143-2148.

17. Moustafa, N. E. and Andersson, J. T., *Analysis of polycyclic aromatic sulfur heterocycles in Egyptian petroleum condensate and volatile oils by gas chromatography with atomic emission detection* in: *Fuel Process. Technol.* **2011**, *92*(3), 547-555.

18. Müller, H.; Andersson, J. T. and Schrader, W., *Characterization of high-molecular-weight sulfur-containing aromatics in vacuum residues using Fourier transform ion cyclotron resonance mass spectrometry* in: *Anal. Chem.* **2005**, *77*(8), 2536-2543.

19. Panda, S. K.; Schrader, W.; al-Hajji, A. and Andersson, J. T., *Distribution of Polycyclic Aromatic Sulfur Heterocycles in Three Saudi Arabian Crude Oils as Determined by Fourier Transform Ion Cyclotron Resonance Mass Spectrometry* in: *Energy Fuels* **2007**, *21*(2), 1071-1077.

20. Sripada, K. and Andersson, J. T., *Liquid chromatographic properties of aromatic sulfur heterocycles on a Pd(II)-containing stationary phase for petroleum analysis* in: *Anal. Bioanal. Chem.* **2005**, *382*(3), 735-741.

21. Balcaen, L.; Woods, G.; Resano, M. and Vanhaecke, F., *Accurate determination of S in organic matrices using isotope dilution ICP-MS/MS* in: *J. Anal. At. Spectrom.* **2013**, *28*(1), 33-39.

22. Giner Martínez-Sierra, J.; Galilea San Blas, O.; Marchante Gayón, J. M. and García Alonso, J. I., *Sulfur analysis by inductively coupled plasma-mass spectrometry: A review* in: *Spectrochim. Acta, Part B* **2015**, *108*, 35-52.

23. Heilmann, J. and Heumann, K. G., *Sulfur trace determination in petroleum products by isotope dilution ICP-MS using direct injection by thermal vaporization (TV-ICP-IDMS)* in: *Anal. Bioanal. Chem.* **2009**, *393*(1), 393-397.

24. Pröfrock, D. and Prange, A., *Inductively Coupled Plasma–Mass Spectrometry (ICP-MS) for Quantitative Analysis in Environmental and Life Sciences: A Review of Challenges, Solutions, and Trends* in: *Appl. Spectrosc.* **2012**, *66*(8), 843-868.

25. Bouyssiere, B.; Leonhard, P.; Pröfrock, D.; Baco, F.; Lopez Garcia, C.; Wilbur, S. and Prange, A., *Investigation of the sulfur speciation in petroleum products by capillary gas chromatography with ICP-collision cell-MS detection* in: *J. Anal. At. Spectrom.* **2004**, *19*(5), 700-702.

26. Pröfrock, D.; Leonhard, P. and Prange, A., *Determination of sulfur and selected trace elements in metallothionein-like proteins using capillary electrophoresis hyphenated to inductively coupled plasma mass spectrometry with an octopole reaction cell* in: *Anal. Bioanal. Chem.* **2003**, *377*(1), 132-139.

27. Profrock, D.; Leonhard, P.; Wilbur, S. and Prange, A., *Sensitive, simultaneous determination of P, S, Cl, Br and I containing pesticides in environmental samples by GC hyphenated with collision-cell ICP-MS* in: *J. Anal. At. Spectrom.* **2004**, *19*(5), 623-631.

28. Molnarne Guricza, L. and Schrader, W., *Electrospray ionization for determination of non-polar polyaromatic hydrocarbons and polyaromatic heterocycles in heavy crude oil asphaltenes* in: *J. Mass Spectrom.* **2015**, *50*(3), 549-557.

29. Kauppila, T. J.; Kersten, H. and Benter, T., *Ionization of EPA Contaminants in Direct and Dopant-Assisted Atmospheric Pressure Photoionization and Atmospheric Pressure Laser Ionization* in: *J. Am. Soc. Mass. Spectrom.* **2015**, *26*(6), 1036-1045.

30. Vetere, A. and Schrader, W., *Mass Spectrometric Coverage of Complex Mixtures: Exploring the Carbon Space of Crude Oil* in: *ChemistrySelect* **2017**, *2*(3), 849-853.

31. Barrow, M. P.; Peru, K. M.; McMartin, D. W. and Headley, J. V., *Effects of Extraction pH on the Fourier Transform Ion Cyclotron Resonance Mass Spectrometry Profiles of Athabasca Oil Sands Process Water* in: *Energy Fuels* **2016**, *30*(5), 3615-3621.

32. Griffiths, M. T.; Da Campo, R.; O'Connor, P. B. and Barrow, M. P., *Throwing Light on Petroleum: Simulated Exposure of Crude Oil to Sunlight and Characterization Using Atmospheric Pressure Photoionization Fourier Transform Ion Cyclotron Resonance Mass Spectrometry* in: *Anal. Chem.* **2014**, *86*(1), 527-534.

33. Vaikkinen, A.; Kauppila, T. J. and Kostiainen, R., *Charge Exchange Reaction in Dopant-Assisted Atmospheric Pressure Chemical Ionization and Atmospheric Pressure Photoionization* in: *J. Am. Soc. Mass. Spectrom.* **2016**, *27*(8), 1291-1300.

34. Panda, S. K.; Brockmann, K.-J.; Benter, T. and Schrader, W., *Atmospheric pressure laser ionization (APLI) coupled with Fourier transform ion cyclotron resonance mass spectrometry applied to petroleum samples analysis: comparison with electrospray ionization and atmospheric pressure photoionization methods* in: *Rapid Commun. Mass Spectrom.* **2011**, *25*(16), 2317-2326.

9. Conclusion

For millennia mankind has been using what we know today to be crude oil. With the upcoming of the industrial age it has developed from a convenient material into an indispensable natural resource as energy carrier and as feedstock for the chemical industry. Despite this long usage and despite the rapid development of analytical techniques, however, crude oil still is a vastly unknown mixture regarding its composition. A detailed and comprehensive analysis of crude oil is prevented by the sample itself. Due to its unmatched complexity, with estimations of more than one million distinct compounds being present, no single analytical method exists that enables a full view on the composition of a crude oil.

Among the most powerful analytical techniques is ultra-high resolving Fourier transform mass spectrometry (FTMS). The method allows the parallel detection of several thousand distinct compounds by means of the accurately determined mass-to-charge ratio of the corresponding ions and thus their elemental composition. During this work a newly developed research-type Orbitrap Elite mass spectrometer was evaluated. The instrument allows recording 3 s transient spectra, yielding a mass resolving power of $R > 900{,}000$ (FWHM at m/z 400). With the given mass resolving power and sensitivity more than 110,000 individual ion compositions were unambiguously identified, including isotopolog signals, which correspond to more than 70,000 distinct molecular compositions. Such a high number is, so far, unmatched and shows the general potential of the instrument.

Mass spectrometry alone, however, is still not sufficient for a detailed understanding of crude oil. It has been shown that discrimination effects of the very sample play an important role and that each simplification prior to mass spectrometric detection is beneficial for the depth of data that can be achieved. Additionally, mass spectrometry does not allow distinguishing between isomeric compounds. Main topic of the present work was, therefore, the development of hyphenated techniques that combine sample simplification and potentially isomer separation with a mass spectrometric analysis.

Ion mobility spectrometry (IMS) has recently gained interest as an isomer separating technique. For this work, the differential variant of IMS, high-field asymmetric waveform ion mobility spectrometry (FAIMS), was adapted for the FTMS analysis of crude oil. Until now FAIMS-FTMS was only reportedly used with electrospray ionization (ESI). Therefore, a new ion source block was developed that allows using photoionization, both atmospheric pressure

photoionization (APPI) and atmospheric pressure laser ionization (APLI) for FAIMS-FTMS. Photoionization is an important alternative to the more common ESI, given that the majority of crude oil constituents are unpolar hydrocarbons.

It has been shown that using multiple ionization techniques is crucial for a comprehensive analysis of crude oil. However, when using different methods on the same crude oil sample, typically a portion of elemental compositions is detected with either of them. Mass spectrometry alone is not sufficient to judge whether these common elemental compositions represent the same analytes that are ionized by multiple ionization techniques or whether they represent different analytes that are selectively ionized by only one method. With the newly developed photoionization FAIMS-FTMS setup it was now shown that some compounds with the same elemental composition appear at different compensation voltages when ionized by different methods. It is thus clear that with APPI and APLI partly different, complementary analytes are ionized.

The original design of the source block showed a relatively low sensitivity and was thus optimized by the introduction of a pusher electrode to accelerate the ions into the FAIMS unit. The optimized APPI ion source was then used to investigate the structural composition of individual compounds within a very complex crude oil sample. For this purpose, fragment spectra of selected ions were recorded by collision-induced dissociation (CID) while scanning through the compensation voltage range. Several structural details were thus shown within a whole crude oil, such as a formerly unseen preference of long alkyl chains on thiophenic compounds or the unexpectedly high presence of alkylated amines. A modification of the FAIMS electrode setup additionally led to an increase of resolving power that allowed separating a group of unique, probably pyridinic isomers.

Another important method that allows sample simplification and isomer separation is liquid chromatography. During this work, normal phase chromatography was used in the form of ligand exchange chromatography (LEC) on a laboratory-made Pd-based stationary phase. Here, the method was for the first time implemented for crude oil separation in an online HPLC-FTMS approach, using APPI as ionization method. It was thus possible to follow up on the chromatographic behavior of distinct compound classes in detail. The results indicate a weak interaction of the π-systems of the analytes with the stationary phase that leads to a slightly stronger retention of compounds with larger π-systems and fewer/shorter alkyl substituents.

A major problem for the mass spectrometric analysis of crude oil is the need for ultra-high resolving power, to date only offered by high-performance FTMS instruments. This results from the presence of isobaric species with close-by masses. Most problematic in this aspect are sulfur containing species, as the molecular masses of compounds that differ by C_3 vs SH_4 are only 3.4 mDa apart.

The chromatographic method used in this work separates sulfur-free hydrocarbons from sulfur containing compounds. With the most problematic isobars being chromatographically separated, also fast scanning instruments that are more adequate for coupling to chromatographic methods, like Exactive Orbitraps or TOF mass spectrometers, can be used, instead of more expensive FTMS systems.

The comprehensive, qualitative analysis of crude oil by LEC-FTMS showed that the chromatographic method effectively separates three main groups of sulfur containing compounds, non-condensed from condensed thiophenes and in turn from sulfidic compounds. The distinction of these groups of compounds is essential for the optimization of refining processes. The successful chromatographic separation of these groups offers a solution to one of the most pressing problems in crude oil processing: The direct quantification of individual compounds within a very complex crude oil mixture. This had not been possible before due to unresolved response issues. Here, quantification was successfully achieved by using the same chromatographic separation in an LEC-ICP-MS/MS setup that profits from the uniform, compound independent, response of sulfur offered by ICP-MS/MS.

By combining the quantitative analysis of crude oil by LEC-FTMS and its quantitative analysis by LEC-ICP-MS/MS the group-selective quantification of sulfur was, for the first time, possible within a whole crude oil and its SARA fractions in a simple, single-step procedure.

10. Appendix

10.1 List of Abbreviations

(Pd-)MPSG	(Pd loaded) mercaptopropano modified silica gel
∑	sum
°C	degree Celsius
µg	microgram
µL	microliter
A	amplitude
AED	atomic emission detector
APCI	atmospheric pressure chemical ionization
API	atmospheric pressure ionization
	American Petroleum Institute
APLI	atmospheric pressure laser ionization
APPI	atmospheric pressure photoionization
avg.	average
BC	before Christ
CCS	collisional cross section
CH	cyclohexane
CV	compensation voltage
Da	Dalton
DBE	double bond equivalent

DBE/C	DBE per carbon ratio
DCM	dicloromethane
DIMS	See FAIMS
DMS	differential ion mobility spectrometry
DTIMS	drift tube IMS
DV	dispersion voltage
E	electrical field strength
e.g.	*exempli gratia* (lat.), for example
EDX	energy dispersive x-ray spectroscopy
eFT	enhanced Fourier transform
EI	electron ionization
ESI	electrospray ionization
eV	electron Volt
FAIMS	high-field asymmetric waveform ion mobility spectrometry
FT	Fourier transform
FT-ICR	Fourier transform ion cyclotron resonance
FTIR	Fourier transform infrared spectroscopy
FTMS	Fourier transform mass spectrometry
FWHM	full width at half maximum height
g	gram
GC	gas chromatography

GC×GC	2-dimensional GC
h	hour
HC	hydrocarbons
HDS	hydrodesulfurization
HOMO	highest occupied molecular orbital
HPLC	high performance liquid chromatography
HRMS	high resolution mass spectrometry
HSL	hue, saturation, luminance, a representation of an additive color model
HTML	Hypertext Markup Language
HV	high voltage
Hz	Hertz
i.d.	Inner diameter
i.e.	idem est (lat.), that being
ICP	inductively coupled plasma
IMS	ion mobility spectrometry
IP	ionization potential
^{i}PrOH	propan-2-ol
IR	Infrared (spectroscopy)
K	ion mobility
kg	kilogram
KM	Kendrick mass (mass in Kendrick scale)

KMD	Kendrick mass defect
KNM	Kendrick nominal mass
L	liter
LC	liquid chromatography
LDI	laser desorption ionization
LEC	ligand exchange chromatography
LTQ	linear trapping quadrupole
m	mass
m/z	mass-to-charge ratio
max.	maximum
mbar	millibar
mDa	milli-Dalton
mg	milligram
mL	milliliter
mm	millimeter
mmu	milli mass units
MOF	metal-organic framework
MS	mass spectrometry
nm	nanometer
NMR	nuclear magnetic resonance
NP	normal phase

ODS	octadecyl substituted silica
PAH	polycyclic aromaitc hydrocarbons
PAXH	polycyclic aromatic heterocycles, X denoting the heteroatom N, O or S
ppb	parts per billion
ppm	parts per million
Q1/2	quadrupole 1/2
QqQ	triple quadrupole setup
R	reolving power
	Pearson correlation coefficient
RCC	reconstructed class chromatogram
REMPI	Resonance Enhanced MultiPhoton ionization
RF	radio-frequency
RP	reversed phase
s	second
SARA	Saturates, Aromatics, Resins, Asphaltenes
SCD	sulfur chemiluminescence detector
SIM	selected ion monitoring
SRM	single reaction monitoring
SVG	Scalable Vector Graphics
T	Tesla
TEM	transmission electron microscopy

THF	tetrahydrofuran
TIC	total ion chromatogram
TOF MS	time-of-flight mass mpectrometry
TOL	toluene
tot.	total
TWIMS	travelling wave IMS
UV	ultraviolet
V	Volume
v	velocity
V	Volt
VBA	Visual Basic for Applications
vs	versus
VUV	vacuum ultraviolet
w	fraction of weight
W	Watt
WDXRF	Wavelength dispersive x-ray fluorescence
wh.	whole
wt.-%	percentage of weight
XANES	x-ray absorption near edge structure
XML	Extensible Markup Language
XSLT	Extensible Stylesheet Language Transformations

ZDV	zero-dead-volume
Δm	mass deviation
v	frequency
ω	angular frequency

10.2 List of Schemes

10.3 List of Figures

10.4 List of Tables

10.5 Publication list

Reviewed articles

Vetere, Alessandro; Schrader, Wolfgang, *Mass Spectrometric Coverage of Complex Systems: Exploring the Carbon Space of Crude Oil*, *ChemistrySelect* **2017**, *2* (3), 849-853.

Vetere, Alessandro; Schrader, Wolfgang, *1- and 2-Photon Ionization for Online FAIMS-FTMS Coupling Allows New Insights into the Constitution of Crude Oils*, *Anal. Chem.* **2015**, *87* (17), 8874–8879.

Vetere, Alessandro; Pröfrock, Daniel and Schrader, Wolfgang, *Quantitative and qualitative analysis of three classes of sulfur compounds in crude oil*, submitted to *Angewandte Chemie*.

Vetere, Alessandro; Pröfrock, Daniel and Schrader, Wolfgang, *Combining HPLC-FTMS and HPLC-ICP-MS/MS: Qualitative and quantitative analysis of sulfur compounds in heavy crude oil and its fractions*, submitted to *Analytical Chemistry*.

Invited talks

Vetere, Alessandro; Schrader, Wolfgang, *FAIMS-FTMS: A New Approach to Unravelling Crude Oil*, Meeting of the Separation Science Group of The Royal Society of Chemistry, London, UK, 14 November **2014**.

Talks

Vetere, Alessandro; Schrader, Wolfgang, *APPI-FAIMS-FTMS source and electrode optimization for the elucidation of structural features of crude oil constituents*, 50th Annual Meeting of the DGMS, Kiel, Germany, 5-8 March **2017**.

Vetere, Alessandro; Schrader, Wolfgang, *High performance analysis of complex mixtures by high-field FT-Orbitrap MS*, 49th Annual Meeting of the DGMS, Hamburg, Germany, 28 February - 2 March **2016**.

Vetere, Alessandro; Schrader, Wolfgang, *HPLC-FTMS and FAIMS-FTMS hyphenations for the analysis of crude oils*, 26th Ph.D Seminar of the Separation Science Group, Focus group "Analytical Chemistry" of the GDCh, Hohenroda, Germany, 10-12 January **2016**.

Vetere, Alessandro; Schrader, Wolfgang, *FAIMS-HRMS: A novel tool for in-depth analysis of crude oil*, 20th International Mass Spectrometry Conference, Genva, Switzerland, 24-29 August **2014**.

Vetere, Alessandro; Schrader, Wolfgang, *FAIMS-MS as a novel approach for crude oil analysis*, 5th Users Meeting Ion Mobility Spectrometry, Essen, Germany, 25-26 March **2014**.

Vetere, Alessandro; Schrader, Wolfgang, *Using an Orbitrap for characterizing crude oil - A complex challenge for a complex mixture*, Meeting of the focus group "FT-MS and high-resolving Mass Spectrometry" of the DGMS, Heidelberg, Germany, 26-27 September **2013**.

Posters

Vetere, Alessandro; Schrader, Wolfgang, *High-field FT Orbitrap MS: A competitive alternative for the analysis of complex mixtures*, 64th ASMS Conference on Mass Spectrometry and Allied Topics, San Antonio, TX, USA, 5-10 June **2016**.

Vetere, Alessandro; Schrader, Wolfgang, *First application of both APPI- and APLI-FAIMS-FTMS for the analysis of crude oil*, 63rd ASMS Conference on Mass Spectrometry and Allied Topics, St. Louis, MO, USA, 31 May - 4 June **2015**.

Vetere, Alessandro; Schrader, Wolfgang, *Ein Orbitrap-Prototyp zur hochauflösenden Untersuchung von Erdöl*, 48th Annual Meeting of the DGMS, Wuppertal, Germany, 1-4 March **2015**.

Vetere, Alessandro; Schrader, Wolfgang, *High-Resolution online LC/MS for characterizing crude oils – grinding the data*, 62nd ASMS Conference on Mass Spectrometry and Allied Topics, Baltimore, MD, USA, 15-19 June **2014**.

Vetere, Alessandro; Schrader, Wolfgang, *Characterization of crude oil components by ultrahigh resolution online-HPLC/MS*, 47th Annual Meeting of the DGMS, Frankfurt/Main, Germany, 2-5 March **2014**.

10.6 Curriculum Vitae

The curriculum has been removed from the online version for data privacy.

10.7 Acknowledgements

Although only a single name is written on the cover page, a work like this can never be accomplished by one person alone. Many others have had their share in starting, conducting and finalizing this thesis. These people deserve and shall receive their proper credit.

My most obvious thanks go to my supervisor Prof. Dr. Wolfgang Schrader who gave me the opportunity to conduct this piece of work. Thank you also for the freedom you gave me to follow all those little things that, finally, were not included into this thesis, for the ability to not only use but also dig myself into this adult playground called “machine park” and, most of all, for the trust you placed in me.

Many thanks also go to my cooperation partners; Jean-Jaques Dunyach from Thermo Fisher Scientific who lent us the FAIMS unit for the course of this work and Daniel Pröfrock from Helmholtz-Zentrum Geesthacht in whose lab we were allowed to conduct the ICP-MS experiments. Without their help this work would not have been possible.

Thank you also to the members of the institute’s workshops who built several pieces of equipment for me. Special thanks go to Sebastian Plankert for the production of the new FAIMS source block and to Ralf Thomas who helped with all sorts of electronic problems.

My heartfelt thanks go to all members of the mass spectrometry group, explicitly including the technical staff, past and present. Every single day there were problems to be solved, stories to be told and lessons to be learned. You – we – are a silly bunch of people but one thing is for sure: It’s never going to be boring. Thank you all for that!

Thank you also to my parents who, over all these years, supported me in whichever direction I chose to go. Thank you for the possibilities you gave me, for everything I was taught and for all your patience.

Last but not least, very special thanks go to my partner, Stefanie Schilson, who never stopped believing in me, even when I didn’t myself. Without your backup, your support and your love I would not be who I am today. Thank you so much!

Finally, I cannot do anything rather than to repeatedly repeat myself in saying:

Thank you!